

CALIFORNIA INSTITUTE OF TECHNOLOGY

EARTHQUAKE ENGINEERING RESEARCH LABORATORY

**DYNAMIC RESPONSE OF STRUCTURES  
WITH UNCERTAIN PARAMETERS**

By

Hector A. Jensen

Report No. EERL 89-02

A Report on Research Supported by Grants  
from the National Science Foundation,  
and by the Earthquake Research Affiliates  
of the California Institute of Technology

Pasadena, California

1989

**Dynamic Response of Structures  
with Uncertain Parameters**

**Thesis by  
Hector A. Jensen**

**In Partial Fulfillment of the Requirements  
for the Degree of  
Doctor of Philosophy**

**California Institute of Technology  
Pasadena, California**

**1990**

**(Submitted September 28, 1989)**

© 1990

Hector Jensen

All Rights Reserved

## Acknowledgments

I would like to express my sincere appreciation to Professor W. D. Iwan for his guidance and encouragement throughout the course of this investigation. His bright insight and many useful suggestions were a decisive factor in the completion of this thesis.

I would also like to thank the California Institute of Technology for the excellent education that I received and for the financial support that made it possible.

Thanks are extended to the many people at Caltech who have made my stay here a great experience.

The technical assistance of Crista Potter and Cecilia Lin in the preparation of this manuscript is also gratefully acknowledged.

Finally, I wish to express my appreciation to my wife, Maria Ines, for her patience and understanding throughout the preparation of this thesis.

## Abstract

This thesis presents a technique for obtaining the response of linear structural systems with parameter uncertainties subjected to either deterministic or random excitation. The parameter uncertainties are modeled as random variables or random fields, and are assumed to be time-independent. The new method is an extension of the deterministic finite element method to the space of random functions.

First, the general formulation of the method is developed, in the case where the excitation is deterministic in time. Next, the application of this formulation to systems satisfying the one-dimensional wave equation with uncertainty in their physical properties is described. A particular physical conceptualization of this equation is chosen for study, and some engineering applications are discussed in both an earthquake ground motion and a structural context.

Finally, the formulation of the new method is extended to include cases where the excitation is random in time. Application of this formulation to the random response of a primary-secondary system is described. It is found that parameter uncertainties can have a strong effect on the system response characteristics.

## TABLE OF CONTENTS

	<b>Page</b>
<b>Acknowledgments</b>	iii
<b>Abstract</b>	iv
<b>List of Figures</b>	viii
<b>List of Tables</b>	xiv
<b>1 Introduction</b>	<b>1</b>
<b>2 Formulation of the Random Finite Element Method</b>	<b>5</b>
2.1 Introduction	5
2.2 Problem Definition	5
2.3 Random Fields Representation	7
2.4 Strong Form of the Problem	10
2.5 Weak Formulation	12
2.6 Matrix Equations	17
2.7 Discrete Time Solution	22
2.8 Response Uncertainty and Statistics	24
<b>3 Application to One-Dimensional Wave Equation</b>	<b>28</b>
3.1 Introduction	28
3.2 Random Field Discretization	29
3.3 Description of the Physical System	31
3.4 Representation of the Random Field	34
3.5 Performance Evaluation	36

3.5.1	Introduction	36
3.5.2	First Validation Problem	37
3.5.3	Second Validation Problem	41
3.6	Description of the Example Problem	44
3.7	Finite Element Discretization	45
3.8	Results of the Example Problem	47
3.8.1	Case I	47
3.8.2	Application of the Results to Earthquake Engineering	48
3.8.3	Case II	50
3.8.4	Application of the Results to Structural Engineering	51
<b>4</b>	<b>Formulation of the Random Finite Element Method for Stochastic Excitation</b>	<b>81</b>
4.1	Introduction	81
4.2	Development of the Covariance Equation	82
4.3	Response Uncertainty and Statistics	85
4.4	Alternative Formulation for Gaussian White Noise Excitation	87
4.4.1	Weak Formulation and Matrix Equations	87
4.4.2	Development of the Covariance Equation	92
4.4.3	Response Uncertainty and Statistics	95
<b>5</b>	<b>Application to Primary-Secondary Systems</b>	<b>97</b>
5.1	Introduction	97
5.2	Description of the Physical System	98
5.3	Ground Motion Model	100
5.4	Formulation of the Covariance Equation	104

5.5	Description of the Example Problem	108
5.6	Results of the Example Problem	112
5.7	Application of the Results to Reliability Analysis	115
<b>6</b>	<b>Summary and Conclusions</b>	<b>137</b>
	<b>References</b>	<b>143</b>
	<b>Appendix A</b>	<b>149</b>

## List of Figures

- Figure 3.1:** Shear beam under base excitation.
- Figure 3.2:** Finite element model for first validation problem.
- Figure 3.3:** Artificial base excitation for validation calculations.
- Figure 3.4:** Comparison of the mean value of the absolute acceleration response of the proposed method to that obtained by an “exact” solution. First validation problem. (a) 10% Coefficient of variation. (b) 20% Coefficient of variation. (c) 30% Coefficient of variation.
- Figure 3.5:** Comparison of the standard deviation of the absolute acceleration response of the proposed method to that obtained by an “exact” solution. First validation problem. (a) 10% Coefficient of variation. (b) 20% Coefficient of variation. (c) 30% Coefficient of variation.
- Figure 3.6:** Comparison of the mean value and the standard deviation of the absolute acceleration response of the “exact” solution to those obtained by the perturbation method. First validation problem.
- Figure 3.7:** Comparison of the results of the proposed method to those obtained by an “exact” solution and by the perturbation method. Case of a Gaussian distribution of the shear stiffness parameter with a 20% coefficient of variation. First validation problem.
- Figure 3.8:** Finite element model for second validation problem.
- Figure 3.9:** Comparison of the mean value of the absolute acceleration response of the proposed method to that obtained by an “exact” solution. Second validation problem. (a)  $\rho = 0.0$ . (b)  $\rho = 0.5$ . (c)  $\rho = 1.0$ .
- Figure 3.10:** Comparison of the standard deviation of the absolute acceleration response of the proposed method to that obtained by an “exact” solution. Second validation problem. (a)  $\rho = 0.0$ . (b)  $\rho = 0.5$ . (c)  $\rho = 1.0$ .
- Figure 3.11:** Comparison of the mean value and the standard deviation of the absolute acceleration response of the “exact” solution to those obtained by the perturbation method. Second validation problem,  $\rho = 0.5$ .

**Figure 3.12:** Absolute acceleration response as a function of the two random variables that describe the random field. (a) Response at the time in which the mean value response is maximum. (b) Response at the time in which the standard deviation response is maximum.

**Figure 3.13:** Artificial base excitation for Case I of the example problem.

**Figure 3.14:** Covariance functions.

**Figure 3.15:** Gaussian and Ultraspherical distributions with a 40% coefficient of variation.

**Figure 3.16:** Finite element mesh used for the shear beam in example problem.

**Figure 3.17:** Coefficient of variation along the beam axis of the three most significant pairs of eigenvectors-eigenvalues of the random field covariance matrix. Case I of the example problem.

**Figure 3.18:** Coefficient of variation along the beam axis of the three most significant pairs of eigenvectors-eigenvalues of the random field covariance matrix. Case II of the example problem.

**Figure 3.19:** Second moment characterization of the absolute acceleration response. Case I of the example problem,  $\delta = \infty$ .

**Figure 3.20:** Second moment characterization of the absolute acceleration response. Case I of the example problem,  $\delta = 0.5$ .

**Figure 3.21:** Standard deviation of the response due to each one of the three most significant pairs of eigenvectors-eigenvalues of the random field covariance matrix. Case I of the example problem,  $\delta = 0.5$ . (a) First random variable. (b) Second random variable. (c) Third random variable.

**Figure 3.22:** Effects of the uncertainties in the parameters of the soil column on the response of a single-degree-of-freedom system. (1) Maximum mean value of the response. (2) Maximum mean plus one standard deviation value of the response. Case I of the example problem,  $\delta = \infty$ . (a) 2% of critical damping. (b) 5% of critical damping.

**Figure 3.23:** Effects of the uncertainties in the parameters of the soil column on the response of a single-degree-of-freedom system. (1) Maximum mean value of the response. (2) Maximum mean plus one standard deviation value of the response. Case I of the example problem,  $\delta = 0.5$ . (a) 2% of critical damping. (b) 5% of critical damping.

**Figure 3.24:** Second moment characterization of the absolute acceleration response. Case II of the example problem,  $\delta = \infty$ .

**Figure 3.25:** Second moment characterization of the absolute acceleration response. Case II of the example problem,  $\delta = 0.5$ .

**Figure 3.26:** Standard deviation of the response due to each one of the three most significant pairs of eigenvectors-eigenvalues of the random field covariance matrix. Case II of the example problem,  $\delta = 0.5$ . (a) First random variable. (b) Second random variable. (c) Third random variable.

**Figure 3.27:** Effects of the uncertainties in the parameters of the shear beam on the response of a substructure. (1) Maximum mean value of the response. (2) Maximum mean plus one standard deviation value of the response. Case II of the example problem,  $\delta = \infty$ . (a) 2% of critical damping. (b) 5% of critical damping.

**Figure 3.28:** Effects of the uncertainties in the parameters of the shear beam on the response of a substructure. (1) Maximum mean value of the response. (2) Maximum mean plus one standard deviation value of the response. Case II of the example problem,  $\delta = 0.5$ . (a) 2% of critical damping. (b) 5% of critical damping.

**Figure 5.1:** Finite element model for the primary system.

**Figure 5.2:** Ultraspherical probability density functions with coefficients of variation (c.v.) of 15%, 30% and 40%.

**Figure 5.3:** Effect of the uncertainties in the filter parameters on the response variability of the secondary system. Nominal filter parameters:  $\omega_g = 4.0$  Hz,  $\xi_g = 0.3$ . (1) Normalized nominal solution. (2) Normalized mean plus one standard deviation value of the solution when the frequency is uncertain. (3) Normalized mean plus one standard deviation value of the solution when the damping is uncertain. (a)  $\omega_s/\omega_1 = 0.50, \gamma = 0.01$ . (b)  $\omega_s/\omega_1 = 0.75, \gamma = 0.01$ .

**Figure 5.4:** Effect of the uncertainties in the filter parameters on the response variability of the secondary system. Nominal filter parameters:  $\omega_g = 4.0$  Hz,  $\xi_g = 0.3$ . (1) Normalized nominal solution. (2) Normalized mean plus one standard deviation value of the solution when the frequency is uncertain. (3) Normalized mean plus one standard deviation value of the solution when the damping is uncertain. (a)  $\omega_s/\omega_1 = 1.25, \gamma = 0.01$ . (b)  $\omega_s/\omega_1 = 1.50, \gamma = 0.01$ .

**Figure 5.5:** Effect of the uncertainties in the filter parameters on the response variability of the secondary system. Nominal filter parameters:  $\omega_g = 4.0$  Hz,  $\xi_g = 0.3$ . (1) Normalized nominal solution. (2) Normalized mean plus one standard deviation value of the solution when the frequency is uncertain. (3) Normalized mean plus one standard deviation value of the solution when the damping is uncertain. (a)  $\omega_s/\omega_1 = 0.50, \gamma = 0.1$ . (b)  $\omega_s/\omega_1 = 0.75, \gamma = 0.1$ .

**Figure 5.6:** Effect of the uncertainties in the filter parameters on the response variability of the secondary system. Nominal filter parameters:  $\omega_g = 4.0$  Hz,  $\xi_g = 0.3$ . (1) Normalized nominal solution. (2) Normalized mean plus one standard deviation value of the solution when the frequency is uncertain. (3) Normalized mean plus one standard deviation value of the solution when the damping is uncertain. (a)  $\omega_s/\omega_1 = 1.25, \gamma = 0.1$ . (b)  $\omega_s/\omega_1 = 1.50, \gamma = 0.1$ .

**Figure 5.7:** Effect of the uncertainties in the primary system parameters on the response variability of the secondary system. Nominal filter parameters:  $\omega_g = 4.0$  Hz,  $\xi_g = 0.3$ . (1) Normalized nominal solution. (2) Normalized mean plus one standard deviation value of the solution when the stiffness is uncertain. (3) Normalized mean plus one standard deviation value of the solution when the damping is uncertain. (a)  $\omega_s/\omega_1 = 0.50, \gamma = 0.01$ . (b)  $\omega_s/\omega_1 = 0.75, \gamma = 0.01$ .

**Figure 5.8:** Effect of the uncertainties in the primary system parameters on the response variability of the secondary system. Nominal filter parameters:  $\omega_g = 4.0$  Hz,  $\xi_g = 0.3$ . (1) Normalized nominal solution. (2) Normalized mean plus one standard deviation value of the solution when the stiffness is uncertain. (3) Normalized mean plus one standard deviation value of the solution when the damping is uncertain. (a)  $\omega_s/\omega_1 = 1.25, \gamma = 0.01$ . (b)  $\omega_s/\omega_1 = 1.50, \gamma = 0.01$ .

**Figure 5.9:** Effect of the uncertainties in the primary system parameters on the response variability of the secondary system. Nominal filter parameters:  $\omega_g = 4.0$  Hz,  $\xi_g = 0.3$ . (1) Normalized nominal solution. (2) Normalized mean plus one standard deviation value of the solution when the stiffness is uncertain. (3) Normalized mean plus one standard deviation value of the solution when the damping is uncertain. (a)  $\omega_s/\omega_1 = 0.50, \gamma = 0.1$ . (b)  $\omega_s/\omega_1 = 0.75, \gamma = 0.1$ .

**Figure 5.10:** Effect of the uncertainties in the primary system parameters on the response variability of the secondary system. Nominal filter parameters:  $\omega_g = 4.0$  Hz,  $\xi_g = 0.3$ . (1) Normalized nominal solution. (2) Normalized mean plus one standard deviation value of the solution when the stiffness is uncertain. (3) Normalized mean plus one standard deviation value of the solution when the damping is uncertain. (a)  $\omega_s/\omega_1 = 1.25, \gamma = 0.1$ . (b)  $\omega_s/\omega_1 = 1.50, \gamma = 0.1$ .

**Figure 5.11:** Effect of the uncertainties in the secondary system parameters on the response variability of the secondary system. Nominal filter parameters:  $\omega_g = 4.0$  Hz,  $\xi_g = 0.3$ . (1) Normalized nominal solution. (2) Normalized mean plus one standard deviation value of the solution when the stiffness is uncertain. (3) Normalized mean plus one standard deviation value of the solution when the damping is uncertain. (a)  $\omega_s/\omega_1 = 0.50, \gamma = 0.01$ . (b)  $\omega_s/\omega_1 = 0.75, \gamma = 0.01$ .

**Figure 5.12:** Effect of the uncertainties in the secondary system parameters on the response variability of the secondary system. Nominal filter parameters:  $\omega_g = 4.0$  Hz,  $\xi_g = 0.3$ . (1) Normalized nominal solution. (2) Normalized mean plus one standard deviation value of the solution when the stiffness is uncertain. (3) Normalized mean plus one standard deviation value of the solution when the damping is uncertain. (a)  $\omega_s/\omega_1 = 1.25, \gamma = 0.01$ . (b)  $\omega_s/\omega_1 = 1.50, \gamma = 0.01$ .

**Figure 5.13:** Effect of the uncertainties in the secondary system parameters on the response variability of the secondary system. Nominal filter parameters:  $\omega_g = 4.0$  Hz,  $\xi_g = 0.3$ . (1) Normalized nominal solution. (2) Normalized mean plus one standard deviation value of the solution when the stiffness is uncertain. (3) Normalized mean plus one standard deviation value of the solution when the damping is uncertain. (a)  $\omega_s/\omega_1 = 0.50, \gamma = 0.1$ . (b)  $\omega_s/\omega_1 = 0.75, \gamma = 0.1$ .

**Figure 5.14:** Effect of the uncertainties in the secondary system parameters on the response variability of the secondary system. Nominal filter parameters:  $\omega_g = 4.0$  Hz,  $\xi_g = 0.3$ . (1) Normalized nominal solution. (2) Normalized mean plus one standard deviation value of the solution when the stiffness is uncertain. (3) Normalized mean plus one standard deviation value of the solution when the damping is uncertain. (a)  $\omega_s/\omega_1 = 1.25, \gamma = 0.1$ . (b)  $\omega_s/\omega_1 = 1.50, \gamma = 0.1$ .

**Figure 5.15:** Effect of the uncertainties in the filter parameters on the response variability of the secondary system. Nominal filter parameters:  $\omega_g = 1.0$  Hz,  $\xi_g = 0.3$ . (1) Normalized nominal solution. (2) Normalized mean plus one standard deviation value of the solution when the frequency is uncertain. (3) Normalized mean plus one standard deviation value of the solution when the damping is uncertain. (a)  $\omega_s/\omega_1 = 0.75, \gamma = 0.01$ . (b)  $\omega_s/\omega_1 = 0.75, \gamma = 0.1$ .

**Figure 5.16:** Probability of exceeding the threshold level  $\eta$  versus time for the relative displacement of the secondary system. Nominal filter parameters:  $\omega_g = 4.0$  Hz,  $\xi_g = 0.3$ . (1) Probability of exceedance for the nominal system. (2) Probability of exceedance for the system with uncertainty in the stiffness parameter of the primary system.

**Figure 5.17:** Probability of exceeding the threshold level  $\eta$  versus time for the relative displacement of the secondary system. Nominal filter parameters:  $\omega_g = 4.0$  Hz,  $\xi_g = 0.3$ . (1) Probability of exceedance for the nominal system. (2) Probability of exceedance for the system with uncertainty in the stiffness parameter of the secondary system.

## List of Tables

**Table 2.1:** Number of unknowns per node.

**Table 5.1:** Natural frequencies of the primary system.

## Chapter 1

### Introduction

Many real engineering problems have uncertainty in their definition. One common source of this uncertainty is the structural characteristics. Such randomness or uncertainty can arise from several sources. Among these are randomness in material properties because of variations in material composition; manufacturing processes or lack of understanding of the material's constitutive behavior; randomness in structural dimensions due to geometrical variations; randomness in boundary conditions because of assembly procedures; randomness or uncertainties in measurements due to testing errors, etc. Another source of uncertainty in many analyses is in the specification of the external loads. In fact, many structural excitations encountered in practice exhibit a stochastic nature. For example, some random-like excitations are seismic excitations, blast loadings on structures, wind excitations, water wave excitations, aerodynamic turbulences, etc. These excitations are often modeled as stochastic processes.

The uncertainty of structural characteristics has a direct relationship to the reliability of many engineering structures. For example, the response of primary and secondary systems associated with structures such as nuclear power containment, space vehicles, offshore platforms, and industrial structures may be quite sensitive to parameter uncertainties. In these cases, it is necessary to pursue an analysis

that takes into account all the features of a structure and its excitation, including uncertainties. If these uncertainties are not accounted for, then the computed response represents only one result in a spectrum of possibilities. Clearly, the high degree of structural complexity of most modern structural systems requires the use of advanced analytical and numerical techniques, such as the finite element method, to obtain their response behavior. Thus, a challenging task to the analyst is to accurately account for the randomness in a given problem and to obtain the response in the form of statistical quantities.

A number of papers have been published demonstrating the application of probability theory and random field theory in the study of physical systems with random parameters. Early applications used simulation methods to investigate the effects of uncertainty in structural properties [1,2,3,4,5]. Later, first and second order perturbation methods were used to compute second-moment statistics of response quantities in structural and geotechnical applications [6,7,8,9,10,11,12,13,14,15,16,17]. Shinozuka and various co-workers have investigated probabilistic models for the spatial distribution of materials properties [18,19,20,21,22]. They have used simulation and perturbation methods to obtain the statistical properties of the response. Vanmarcke has presented specific models for the description of the spatial correlation of soil properties [23,24]. In general, the spatial correlation is taken into account by assuming an exponentially decaying function of distance for the strength of the correlation.

As mentioned above, both simulation and perturbation methods have been used to investigate the effects of uncertain variability in structural properties. Simulation methods are quite powerful, but in general, are very costly in terms of computational resources. In addition, they provide limited insight into the behavior and sensitivity

of the system under different parameter uncertainties. Perturbation methods are quite general and they are easily integrable into any deterministic solution technique. However, they usually suffer from questions of accuracy and convergence. These questions become more crucial as the degree of uncertainty becomes more pronounced, and when dynamic, particularly transient and wave propagation problems must be considered [25,26].

It is the objective of this thesis to develop an alternative method for the dynamic analysis of linear structural systems with parameter uncertainties subjected to either deterministic or random excitation. The parameter uncertainties are described in a probabilistic sense and are assumed to be time-independent. The new method is an extension of the deterministic finite element method to the space of random functions.

Chapter 2 presents the formulation of the new method for a particular class of partial differential equations with random coefficients. The type of system modeled by this equation is one of significant engineering importance since it contains many common physical systems. The random coefficients, which represent the material properties, are modeled as random variables or random fields. The externally applied load is permitted to have spatial random properties but is assumed to be deterministic in time. Later in Chapter 2, the strong form of the problem and its variational counterpart are presented. Next, the variational formulation is solved using Galerkin's method together with the finite element method for the spatial discretization. A system of linear ordinary differential equations for the unknowns of the problem is derived and then it is integrated in time. Finally, the response variability is computed.

Chapter 3 describes the application of this new procedure to a typical class of problems: systems satisfying the one-dimensional wave equation with uncertainty in their physical properties. Validation calculation results are presented and compared with solutions which are obtainable by other techniques. Engineering applications of the results obtained in this particular example are discussed to highlight the influence of parameter uncertainty.

In Chapter 4, the formulation of the method described in Chapter 2 is extended to include cases where the excitation is random in time. The applied forcing function is modeled as a modulated Gaussian white noise process. Two procedures to derive the random state-space Liapunov equation for the response covariance matrix are presented, and their differences are discussed. The Liapunov equation is then integrated in time and the response variability is computed.

Finally, Chapter 5 describes the application of the solution method, presented in Chapter 4, to the random response of a primary-secondary system. The effects of uncertainty in the system parameters and applied loads on the response of the secondary system and on its reliability are discussed.

## Chapter 2

### Formulation of the Random Finite Element Method

#### 2.1 Introduction

This chapter describes the general linear continuous system with random coefficients which is the subject of this investigation. This is followed by a description of the numerical implementation of the mathematical solution algorithms and by the characterization of the response variability.

#### 2.2 Problem Definition

Consider the continuous linear system described by the partial differential equation

$$\begin{aligned} \nabla \cdot \boldsymbol{\tau}(\mathbf{k}(\mathbf{x}), \mathbf{u}) - \mathbf{Q}(c(\mathbf{x}), \dot{\mathbf{u}}) - m(\mathbf{x})\ddot{\mathbf{u}} + \mathbf{f}(\mathbf{x}, t) = \mathbf{0} \\ \text{on } \Omega \times ]0, T_0[ , \end{aligned} \tag{2.1}$$

where

$\Omega = \Omega(\mathbf{x})$  is the spatial domain,

$]0, T_0[$  is the time interval of length  $T_0 > 0$ ,

$\mathbf{u} = \mathbf{u}(\mathbf{x}, t)$  is the dependent variable representing the displacement field,

$\mathbf{k}(\mathbf{x})$  and  $\mathbf{c}(\mathbf{x})$  are stiffness and damping parameter fields, respectively,

$\mathbf{m}(\mathbf{x})$  is the mass distribution in the system,

$\mathbf{f}(\mathbf{x}, t)$  is the externally applied load,

$\boldsymbol{\tau}$  is the linear stress operator of first order on the displacements  $\mathbf{u}$  and stiffness function  $\mathbf{k}(\mathbf{x})$ ,

$\mathbf{Q}$  is the linear damping operator on the velocities  $\dot{\mathbf{u}}$  and damping function  $\mathbf{c}(\mathbf{x})$ , and

$\nabla \cdot$  is the divergence operator.

The material properties  $\mathbf{k}(\mathbf{x})$  and  $\mathbf{c}(\mathbf{x})$ , as well as the external load  $\mathbf{f}(\mathbf{x}, t)$  are permitted to have spatially random properties, so the stiffness, damping, and the external load are modeled as random fields. On the boundary  $\Gamma$ , the following homogeneous boundary conditions are assumed to hold:

$$\mathbf{B}^{(g)}(\mathbf{u}) = \mathbf{0} \quad \text{on} \quad \Gamma_g \quad (2.2)$$

$$\mathbf{B}^{(n)}(\mathbf{u}) = \mathbf{0} \quad \text{on} \quad \Gamma_n, \quad (2.3)$$

where  $\Gamma_g$  and  $\Gamma_n$  are complimentary sets such that  $\Gamma = \Gamma_g \cup \Gamma_n$ , and  $\mathbf{B}^{(g)}$  and  $\mathbf{B}^{(n)}$  are linear operators representing the geometric and natural boundary conditions, respectively. Finally, let the initial conditions be given by

$$\mathbf{u}(\mathbf{x}, 0) = \mathbf{u}_0(\mathbf{x}) \quad (2.4)$$

$$\dot{\mathbf{u}}(\mathbf{x}, 0) = \dot{\mathbf{u}}_0(\mathbf{x}). \quad (2.5)$$

Note that terms, such as  $\boldsymbol{\tau}$ ,  $\mathbf{u}$  and  $\mathbf{x}$  in equation (2.1) represent indexed sets. These may be scalars, vectors, or tensors, depending on the number of indices required to describe the particular physical quantity under consideration.

Many systems of engineering interest can be modeled in the form of equation (2.1), for example, axial vibration of a rod, torsional vibration of a shaft, vibration of a shear beam, vibration of a string, vibration of a membrane, propagation of plane waves in a continuum, etc. Thus, the general form of equation (2.1) allows treatment of a wide class of engineering problems.

In the next section, the characterization for random fields which will be used to represent the spatial variation of the material properties of the system and the spatial variation of the external load is presented in detail.

### 2.3 Random Fields Representation

Let  $S(\mathbf{x})$  denote a random process, function of the position  $\mathbf{x}$  over the domain  $\Omega$ . Let  $\bar{S}(\mathbf{x})$  denote the expected value of  $S(\mathbf{x})$  over all possible realizations of the process, and  $R(\mathbf{x}, \mathbf{y})$  denote its covariance function associated with locations  $\mathbf{x}$  and  $\mathbf{y}$ , which by definition is symmetric and positive semi-definite. The random process  $S(\mathbf{x})$  can be defined in terms of its mean value plus its deviatoric component as

$$S(\mathbf{x}) = \bar{S}(\mathbf{x}) + Z(\mathbf{x}) , \quad (2.6)$$

where  $Z(\mathbf{x})$  is a process with zero mean and covariance function  $R(\mathbf{x}, \mathbf{y})$ . That is

$$E(Z(\mathbf{x})) = 0 \quad \text{and} \quad (2.7)$$

$$E(Z(\mathbf{x}) Z(\mathbf{y})) = R(\mathbf{x}, \mathbf{y}) , \quad (2.8)$$

where  $E(\cdot)$  is the operator of mathematical expectation.

In practice, the correlation data is defined at a finite set of discrete points in  $\Omega$ . This suggests that the correlation data may be represented as a variance-covariance matrix of the form

$$C_{ij} = E(Z(\mathbf{x}_i) Z(\mathbf{x}_j)) , \quad (2.9)$$

where  $\mathbf{x}_i$  and  $\mathbf{x}_j$  represent points in  $\Omega$  where the correlation data is known. In the same manner, the expected value of the process may be represented as a vector of the form

$$\bar{s}_i = \bar{S}(\mathbf{x}_i) . \quad (2.10)$$

Then, the representation of the random field is defined in terms of a mean value vector and a covariance matrix defined at such set of discrete points. The discretized version of equation (2.6) can now be written as

$$\mathbf{s} = \bar{\mathbf{s}} + \mathbf{z} , \quad (2.11)$$

where  $\mathbf{s}$  is a random vector that represents the spatial variation of  $S(\mathbf{x})$  at the finite set of discrete points,  $\bar{\mathbf{s}}$  is the mean value vector of the process, and  $\mathbf{z}$  is a vector of random variables with zero mean and covariance matrix  $C$ , whose components are defined in equation (2.9). Recall that the covariance matrix is symmetric and positive semi-definite.

By means of the spectral decomposition of the covariance matrix, the random field can now be described in terms of a vector of uncorrelated random variables. It can be shown that equation (2.11) becomes

$$\mathbf{s} = \bar{\mathbf{s}} + \Phi \mathbf{b} , \quad (2.12)$$

where  $\Phi$  is the matrix of eigenvectors of the covariance matrix  $C$ , and  $\mathbf{b}$  is a vector of uncorrelated random variables with zero mean and covariance matrix  $\Lambda$  given by

$$\Lambda = \Phi^T C \Phi . \quad (2.13)$$

Note that the covariance matrix of the new set of variables is diagonal, and their variances are the eigenvalues of the covariance matrix of the original variables.

Also note that if  $S(\mathbf{x})$  is a Gaussian process, the new set of random variables are jointly Gaussian and since they are uncorrelated, they are also independent.

Equation (2.12) gives the discretized representation of the random process  $S(\mathbf{x})$ . In order to define its representation in the entire domain  $\Omega$ , define the following functions of  $\mathbf{x}$ .

$$\hat{S}(\mathbf{x}) = \sum_{i=1}^{NR} s_i \Psi_i(\mathbf{x}) \quad (2.14)$$

$$\hat{\bar{S}}(\mathbf{x}) = \sum_{i=1}^{NR} \bar{s}_i \Psi_i(\mathbf{x}) \quad (2.15)$$

$$\hat{S}_n(\mathbf{x}) = \sum_{i=1}^{NR} \Phi_{in} \Psi_i(\mathbf{x}) \quad (2.16)$$

where  $NR$  is the dimension of the vector of random variables  $\mathbf{z}$  and it is equal to the number of points in  $\Omega$  where the correlation data is known,  $s_i$  is the  $i$ th component of the random vector  $\mathbf{s}$ ,  $\bar{s}_i$  is the  $i$ th component of the mean value vector  $\bar{\mathbf{s}}$ ,  $\Phi_{in}$  is the  $i$ th component of the  $n$ th eigenvector of the covariance matrix, and  $\Psi_i(\mathbf{x})$ ,  $i = 1, \dots, NR$ , are linearly independent known interpolation functions of  $\mathbf{x}$ , satisfying

$$\Psi_i(\mathbf{x}_j) = \delta_{ij} , \quad (2.17)$$

where  $\mathbf{x}_j$  represents the points in  $\Omega$  where the random field is defined, that is, where the correlation data is known.

Equations (2.14) through (2.16) together with equation (2.12) give the following representation for the random process

$$\hat{S}(\mathbf{x}) = \hat{\bar{S}}(\mathbf{x}) + \sum_{n=1}^{NR} \hat{S}_n(\mathbf{x}) b_n , \quad (2.18)$$

where  $b_n$  is the  $n$ th component of the random vector  $\mathbf{b}$ .

The function  $\hat{S}(\mathbf{x})$  represents an approximation of the expected value of the random process  $S(\mathbf{x})$ , while the functions  $\hat{S}_n(\mathbf{x}), n = 1, \dots, NR$ , denote a continuous representation in  $\Omega$  of the eigenvectors of the covariance matrix, that is,  $\hat{S}_n(\mathbf{x}_i) = \Phi_{in}, i = 1, \dots, NR$ . Equation (2.18) is the characterization for random fields which will be used in the present formulation.

An alternative characterization for random fields has been suggested by Spanos et al. [27], based on the Karhunen-Loeve orthogonal expansion of nonstationary random processes. This expansion consists of the projection of the process onto a space of orthogonal random variables and an expansion similar to equation (2.18) can be defined. This characterization, however, requires the solution of an integral eigenvalue-eigenfunction problem instead of a matrix eigenvalue-eigenvector problem.

Finally, it is interesting to note that if the random process is fully correlated, the process reduces to a random variable. Therefore, the characterization of a random variable is a special case of the general characterization of a random field. If the covariance function is other than a constant function, that is, if the process is not fully correlated, the random process  $S(\mathbf{x})$  will be assumed to be Gaussian. For a constant covariance function, the random process which now is a random variable will not be restricted to be Gaussian. In fact, several probability density functions, in addition to Gaussian, are used in the numerical illustrations described in Chapters 3 and 5 when the process is fully correlated.

## 2.4 Strong Form of the Problem

Making use of the characterization given by equation (2.18) for random fields, the material properties  $\mathbf{k}(\mathbf{x})$  and  $\mathbf{c}(\mathbf{x})$ , and the external load  $\mathbf{f}(\mathbf{x}, t)$  can be

represented as

$$\mathbf{k}(\mathbf{x}) = \bar{\mathbf{k}}(\mathbf{x}) + \sum_{n=1}^r \mathbf{k}_n(\mathbf{x})b_n \quad (2.19)$$

$$\mathbf{c}(\mathbf{x}) = \bar{\mathbf{c}}(\mathbf{x}) + \sum_{n=1}^r \mathbf{c}_n(\mathbf{x})b_n \quad (2.20)$$

$$\mathbf{f}(\mathbf{x}, t) = \bar{\mathbf{f}}(\mathbf{x}, t) + \sum_{n=1}^r \mathbf{f}_n(\mathbf{x}, t)b_n, \quad (2.21)$$

where

$r$  is the total number of random variables used for the representation of the random fields,

$\bar{\mathbf{k}}(\mathbf{x})$ ,  $\bar{\mathbf{c}}(\mathbf{x})$ , and  $\bar{\mathbf{f}}(\mathbf{x}, t)$  denote the expected value of the stiffness, damping and external load fields, respectively, and

$\mathbf{k}_n(\mathbf{x})$ ,  $\mathbf{c}_n(\mathbf{x})$ , and  $\mathbf{f}_n(\mathbf{x}, t)$  represent the continuous representation in  $\Omega$  of the eigenvectors of the corresponding covariance matrices.

Considering the linearity of operators  $\tau$  and  $Q$  it follows that

$$\tau(\mathbf{k}(\mathbf{x}), \mathbf{u}) = \tau(\bar{\mathbf{k}}(\mathbf{x}), \mathbf{u}) + \sum_{n=1}^r \tau(\mathbf{k}_n(\mathbf{x}), \mathbf{u})b_n \quad (2.22)$$

$$Q(\mathbf{c}(\mathbf{x}), \dot{\mathbf{u}}) = Q(\bar{\mathbf{c}}(\mathbf{x}), \dot{\mathbf{u}}) + \sum_{n=1}^r Q(\mathbf{c}_n(\mathbf{x}), \dot{\mathbf{u}})b_n. \quad (2.23)$$

Substituting equations (2.21) through (2.23) into the differential equation (2.1) yields

$$\begin{aligned} \nabla \cdot \tau(\bar{\mathbf{k}}(\mathbf{x}), \mathbf{u}) - Q(\bar{\mathbf{c}}(\mathbf{x}), \dot{\mathbf{u}}) + \sum_{n=1}^r \left( \nabla \cdot \tau(\mathbf{k}_n(\mathbf{x}), \mathbf{u}) - Q(\mathbf{c}_n(\mathbf{x}), \dot{\mathbf{u}}) \right) b_n \\ - \mathbf{m}(\mathbf{x})\ddot{\mathbf{u}} + \bar{\mathbf{f}}(\mathbf{x}, t) + \sum_{n=1}^r \mathbf{f}_n(\mathbf{x}, t)b_n = 0. \end{aligned} \quad (2.24)$$

Equation (2.24) is a partial differential equation with random coefficients represented by the random variables  $b_n$ . This equation, together with its initial and boundary conditions, which are defined in Section 2.2, represent the strong or classical form of the initial-boundary-value problem.

In order to obtain an approximate solution of equation (2.24) a variational formulation is first defined. Then, the variational equations are solved using Galerkin's method together with the finite element method for spatial discretization. This procedure will be described in the next section.

To simplify the notation, assume that the dependent variable  $\mathbf{u}(\mathbf{x}, t)$  is just a scalar,  $u(\mathbf{x}, t)$ . Formulations similar to that which follows are easily developed for cases where  $\mathbf{u}$  is a vector.

## 2.5 Weak Formulation

In order to characterize the weak, or variational counterpart of equation (2.24), define the following two sets of functions

$$V = \left\{ v(\cdot, \mathbf{b}, t) \mid \mathbf{B}^{(g)}(v) = 0 \text{ on } \Gamma_g, E\left(\|v(\cdot, \mathbf{b}, t)\|_{H^1(\Omega)}^2\right) < \infty, \right. \\ \left. t \in [0, T_0], \mathbf{b} \in D \right\}, \text{ and}$$

$$W = \left\{ w(\cdot, \mathbf{b}) \mid w \text{ satisfies homogeneous boundary conditions} \right. \\ \left. \text{on } \Gamma_g, E\left(\|w(\cdot, \mathbf{b})\|_{H^1(\Omega)}^2\right) < \infty, \mathbf{b} \in D \right\},$$

where

$D$  is the probability space,

$\mathbf{b}$  is the random vector with components  $b_n$ ,  $n = 1, \dots, r$ , defined on  $D$ ,

$E(\cdot)$  is the expectation operation defined on  $D$ ,

$H^1(\Omega)$  is the Sobolev space of degree 1, which consists of functions that possess square-integrable generalized derivatives through order 1,

$\|\cdot\|_{H^1(\Omega)}$  is the Sobolev norm defined on  $H^1(\Omega)$ ,

and all other terms are as previously defined.

Now, multiplying the partial differential equation (2.24) by a weighting function  $w \in W$ , integrating by parts over the domain  $\Omega$ , and taking the expectation yields the following weak formulation.

Find  $u(\mathbf{x}, \mathbf{b}, t) \in V$ ,  $\mathbf{x} \in \Omega$ ,  $\mathbf{b} \in D$ ,  $t \in [0, T_0]$ , such that for all  $w(\mathbf{x}, \mathbf{b}) \in W$ ,

$$\begin{aligned} & (m\ddot{u}, w)_E + \left( \boldsymbol{\tau}(\bar{\mathbf{k}}(\mathbf{x}), u), \nabla w \right)_E + \left( \mathbf{Q}(\bar{\mathbf{c}}(\mathbf{x}), \dot{u}), w \right)_E \\ & + \sum_{n=1}^r \left\{ \left( \boldsymbol{\tau}(\mathbf{k}_n(\mathbf{x}), u) b_n, \nabla w \right)_E + \left( \mathbf{Q}(\mathbf{c}_n(\mathbf{x}), \dot{u}) b_n, w \right)_E \right\} \\ & = (\bar{f}(\mathbf{x}, t), w)_E + \sum_{n=1}^r (f_n(\mathbf{x}, t) b_n, w)_E, \end{aligned} \quad (2.25)$$

$$(mu(\mathbf{x}, \mathbf{b}, 0), w)_E = (mu_0(\mathbf{x}), w)_E, \quad (2.26)$$

$$(m\dot{u}(\mathbf{x}, \mathbf{b}, 0), w)_E = (m\dot{u}_0(\mathbf{x}), w)_E, \quad (2.27)$$

where  $(\cdot, \cdot)_E$  denotes the expectation of the inner product, that is,

$$(\phi, \psi)_E = E \left( \int_{\Omega} \phi \psi d\Omega \right) , \quad (2.28)$$

where  $\phi$  and  $\psi$  are scalar functions defined on  $\Omega \times D \times [0, T_0]$  and  $\Omega \times D$ , respectively.

In order to define finite-dimensional approximations  $V^h$  and  $W^h$  to  $V$  and  $W$ , respectively, let the domain  $\Omega$  be subdivided into  $NEL$  elements  $\Omega^e$  such that

$$\Omega = \bigcup_{e=1}^{NEL} \Omega^e \quad (2.29)$$

where

$\Omega^e$  is the domain of the  $e^{th}$  element, and

$NEL$  is the number of finite elements in the domain.

Further, let  $u^e(\mathbf{x}, \mathbf{b}, t)$ ,  $\mathbf{x} \in \Omega^e$  denote the restriction of  $u(\mathbf{x}, \mathbf{b}, t)$  to  $\Omega^e$ , so

$$u^e(\mathbf{x}, \mathbf{b}, t) = \begin{cases} u(\mathbf{x}, \mathbf{b}, t) & \forall \mathbf{x} \in \Omega^e \\ 0 & \forall \mathbf{x} \notin \Omega^e . \end{cases} \quad (2.30)$$

Then, from equation (2.29), the solution field is represented as the summation of all these restrictions,

$$u(\mathbf{x}, \mathbf{b}, t) = \sum_{e=1}^{NEL} u^e(\mathbf{x}, \mathbf{b}, t) . \quad (2.31)$$

In the present formulation, the dependent variable  $u^e(\mathbf{x}, \mathbf{b}, t)$  is expanded as a double series over  $\mathbf{x}$  and  $\mathbf{b}$ . The approximation of the solution in the spatial domain is assumed to be given by the finite element shape functions, while an orthogonal set of polynomials with respect to the mean operation is used to approximate the solution in the probability space. Then, the solution takes the form of a double series of space dependent interpolation functions and orthogonal polynomials weighted by time dependent functions. Thus, the dependent variable  $u^e(\mathbf{x}, \mathbf{b}, t)$  is expressed as:

$$u^e(\mathbf{x}, \mathbf{b}, t) = \sum_{j=1}^{NEN} \sum_{0 \leq |\boldsymbol{\ell}| \leq NP} u_{j\ell_1 \dots \ell_r}^e(t) \phi_j^e(\mathbf{x}) \prod_{s=1}^r H_{\ell_s}^{b_s}, \quad (2.32)$$

where

$NP$  is the order of approximation in the probability space,

$NEN$  is the number of nodes per element,

$\phi_j^e(\mathbf{x})$  is the finite element shape function for node  $j$  of element  $e$ ,

$u_{j\ell_1 \dots \ell_r}^e(t)$  is an unknown deterministic function of time,

$\boldsymbol{\ell}$  is a vector with components  $\ell_s$ ,  $s = 1, \dots, r$ ,

$|\boldsymbol{\ell}|$  stand for the norm of  $\boldsymbol{\ell}$  defined by

$$|\boldsymbol{\ell}| = \sum_{s=1}^r \ell_s, \text{ and} \quad (2.33)$$

$\left\{ H_{\ell}^{b_s} \right\}_{\ell=0}^{\infty}$  is an orthogonal set of polynomials with respect to the mean operation, that is,

$$E \left( H_{\ell}^{b_s} H_p^{b_s} \right) = \delta_{\ell p}, \quad (2.34)$$

and with  $H_0^{b_s} = 1$ .

The selection for the set of polynomials depends on the probability density function of the random variable  $b_s$ . For example, the Hermite polynomials satisfy equation (2.34) for Gaussian random variables, the Legendre polynomials do likewise for uniform random variables, the Laguerre polynomials are appropriate for exponential random variables, etc.

It follows from equations (2.31) and (2.32) that the discretization of  $u(\mathbf{x}, \mathbf{b}, t)$  can be expressed as

$$u(\mathbf{x}, \mathbf{b}, t) = \sum_{e=1}^{NEL} \sum_{j=1}^{NEN} \sum_{0 \leq |\boldsymbol{\ell}| \leq NP} u_{j\ell_1 \dots \ell_r}^e(t) \phi_j^e(\mathbf{x}) \prod_{s=1}^r H_{\ell_s}^{b_s} (b_s) \quad (2.35)$$

Note that the unknown nodal values  $u_{j\ell_1 \dots \ell_r}^e(t)$  are deterministic functions of time.

Next, let the set of functions define as

$$\left\{ \phi_j(\mathbf{x}) \prod_{s=1}^r H_{\ell_s}^{b_s} (b_s) \right\}_{\substack{j=1, \dots, NTOT \\ \ell_s=0, 1, \dots}} \quad (2.36)$$

be a base for  $V^h$  and  $W^h$ , where  $NTOT$  is the total number of nodes in the finite element discretization, and  $\phi_j(\mathbf{x})$  is the global shape function for node  $j$ . Then the variational formulation previously defined becomes:

find  $u^h(\mathbf{x}, \mathbf{b}, t) \in V^h$ ,  $\mathbf{x} \in \Omega$ ,  $\mathbf{b} \in D$ ,  $t \in [0, T_0]$ , such that for all  $w^h(\mathbf{x}, \mathbf{b}) \in W^h$ ,

$$\begin{aligned} & (m\ddot{u}^h, w^h)_E + \left( \boldsymbol{\tau}(\bar{\mathbf{k}}(\mathbf{x}), u^h), \nabla w^h \right)_E + \left( \mathbf{Q}(\bar{\mathbf{c}}(\mathbf{x}), \dot{u}^h), w^h \right)_E \\ & + \sum_{n=1}^r \left\{ \left( \boldsymbol{\tau}(\mathbf{k}_n(\mathbf{x}), u^h) b_n, \nabla w^h \right)_E + \left( \mathbf{Q}(\mathbf{c}_n(\mathbf{x}), \dot{u}^h) b_n, w^h \right)_E \right\} \\ & = (\bar{f}(\mathbf{x}, t), w^h)_E + \sum_{n=1}^r (f_n(\mathbf{x}, t) b_n, w^h)_E, \end{aligned} \quad (2.37)$$

$$(m u^h(\mathbf{x}, \mathbf{b}, 0), w^h)_E = (m u_0(\mathbf{x}), w^h)_E, \quad (2.38)$$

$$(m \dot{u}^h(\mathbf{x}, \mathbf{b}, 0), w^h)_E = (m \dot{u}_0(\mathbf{x}), w^h)_E, \quad (2.39)$$

where all terms are as defined previously.

The equations (2.37) through (2.39) represent the semidiscrete Galerkin formulation of the governing equation (2.1) with boundary and initial conditions defined by equations (2.2) through (2.5).

Finally, it is noted that an expansion similar to equation (2.32) has been proposed in reference [28]. A Fourier-series expansion in the probability space was used to compute the mean and variance of the response of a single-degree-of-freedom system with uncertain natural frequency. It was concluded that this expansion works well for one uncertain parameter, but becomes cumbersome if the parameter space is of higher dimension.

## 2.6 Matrix Equations

The semidiscrete Galerkin formulation defined in Section 2.5 leads to a coupled system of linear ordinary differential equations for the unknowns. In order to obtain the set of equations, the following recurrence relation for the orthogonal set of polynomials  $\{H_{\ell}^{b_s}(b_s)\}_{\ell=0}^{\infty}$  [29] will be needed

$$\begin{aligned} b_n H_{\ell_n}^{b_n}(b_n) &= a_{\ell_n-1}^{b_n} H_{\ell_n-1}^{b_n}(b_n) + a_{\ell_n}^{b_n} H_{\ell_n}^{b_n}(b_n) + a_{\ell_n+1}^{b_n} H_{\ell_n+1}^{b_n}(b_n), \\ n &= 1, \dots, r \\ \ell_n &= 0, 1, \dots \end{aligned} \tag{2.40}$$

where the coefficients  $a_{\ell_n}^{b_n}$  depend on the probability density function of the random variable  $b_n$ .

The set of equations for the element  $e$  of the finite element mesh is obtained using the equations (2.37) through (2.39) together with the characterization of  $V^h$  and  $W^h$  described in Section 2.5, the independence property of the random variables

$b_n$ , the orthogonality of the set of polynomials defined in equation (2.34), and the recurrence relation (2.40). This leads to the following set of equations

$$\begin{aligned}
& \sum_{j=1}^{NEN} \left\{ \left[ \int_{\Omega^e} m(\mathbf{x}) \phi_j^e(\mathbf{x}) \phi_i^e(\mathbf{x}) d\Omega \right] \ddot{u}_{j\ell_1 \dots \ell_r}^e(t) + \left[ \int_{\Omega^e} \mathbf{Q}(\bar{\mathbf{c}}(\mathbf{x}), \phi_j^e(\mathbf{x})) \phi_i^e(\mathbf{x}) d\Omega \right] \right. \\
& \quad \ddot{u}_{j\ell_1 \dots \ell_r}^e(t) + \left[ \int_{\Omega^e} \boldsymbol{\tau}(\bar{\mathbf{k}}(\mathbf{x}), \phi_j^e(\mathbf{x})) \nabla \phi_i^e(\mathbf{x}) d\Omega \right] u_{j\ell_1 \dots \ell_r}^e(t) \\
& \quad + \sum_{n=1}^r \left( \left[ \int_{\Omega^e} \mathbf{Q}(\mathbf{c}_n(\mathbf{x}), \phi_j^e(\mathbf{x})) \phi_i^e(\mathbf{x}) d\Omega \right] \right. \\
& \quad \left. \left( a_{\ell_n-1}^{b_n} \dot{u}_{j\ell_1 \dots \ell_n-1 \dots \ell_r}^e(t) + a_{\ell_n}^{b_n} \dot{u}_{j\ell_1 \dots \ell_n \dots \ell_r}^e(t) + a_{\ell_n+1}^{b_n} \dot{u}_{j\ell_1 \dots \ell_n+1 \dots \ell_r}^e(t) \right) \right. \\
& \quad \left. + \left[ \int_{\Omega^e} \boldsymbol{\tau}(\mathbf{k}_n(\mathbf{x}), \phi_j^e(\mathbf{x})) \nabla \phi_i^e(\mathbf{x}) d\Omega \right] \left( a_{\ell_n-1}^{b_n} u_{j\ell_1 \dots \ell_n-1 \dots \ell_r}^e(t) \right. \right. \quad (2.41) \\
& \quad \left. \left. + a_{\ell_n}^{b_n} u_{j\ell_1 \dots \ell_n \dots \ell_r}^e(t) + a_{\ell_n+1}^{b_n} u_{j\ell_1 \dots \ell_n+1 \dots \ell_r}^e(t) \right) \right) \left. \right\} \\
& = \int_{\Omega^e} \bar{f}(\mathbf{x}, t) \phi_i^e(\mathbf{x}) d\Omega \prod_{s=1}^r \delta_{\ell_s, 0} + \sum_{n=1}^r \left[ \int_{\Omega^e} f_n(\mathbf{x}, t) \phi_i^e(\mathbf{x}) d\Omega \right] \\
& \quad \quad \quad i = 1, \dots, NEN, \\
& \quad \left( a_0^{b_n} \prod_{s=1}^r \delta_{\ell_s, 0} + a_1^{b_n} \prod_{\substack{s=1 \\ s \neq n}}^r \delta_{\ell_s, 0} \delta_{\ell_n, 1} \right), \quad \ell_s = 0, 1, \dots \\
& \quad \quad \quad s = 1, \dots, r
\end{aligned}$$

$$\begin{aligned}
& \sum_{j=1}^{NEN} \left[ \int_{\Omega^e} m(\mathbf{x}) \phi_j^e(\mathbf{x}) \phi_i^e(\mathbf{x}) d\Omega \right] u_{j\ell_1 \dots \ell_r}^e(0) \\
& = \left( \int_{\Omega^e} m(\mathbf{x}) u_0(\mathbf{x}) \phi_i^e(\mathbf{x}) d\Omega \right) \prod_{s=1}^r \delta_{\ell_s, 0}, \quad i = 1, \dots, NEN, \quad (2.42) \\
& \quad \quad \quad \ell_s = 0, 1, \dots \\
& \quad \quad \quad s = 1, \dots, r
\end{aligned}$$

$$\begin{aligned}
 & \sum_{j=1}^{NEN} \left[ \int_{\Omega^e} m(\mathbf{x}) \phi_j^e(\mathbf{x}) \phi_i^e(\mathbf{x}) d\Omega \right] \dot{u}_{j\ell_1 \dots \ell_r}^e(0) \\
 & = \left( \int_{\Omega^e} m(\mathbf{x}) \dot{u}_0(\mathbf{x}) \phi_i^e(\mathbf{x}) d\Omega \right) \prod_{s=1}^r \delta_{\ell_s, 0} .
 \end{aligned}
 \quad \begin{array}{l}
 i = 1, \dots, NEN, \\
 \ell_s = 0, 1, \dots \\
 s = 1, \dots, r
 \end{array} \quad (2.43)$$

Equations (2.41), (2.42) and (2.43) can be written now in terms of the components of elemental matrices and vectors as

$$\begin{aligned}
 & \sum_{j=1}^{NEN} \left\{ m_{ij}^e \ddot{u}_{j\ell_1 \dots \ell_r}^e(t) + c_{ij}^e \dot{u}_{j\ell_1 \dots \ell_r}^e(t) + k_{ij}^e u_{j\ell_1 \dots \ell_r}^e(t) \right. \\
 & + \sum_{n=1}^r \left[ c_{nij}^e (a_{\ell_n-1}^{b_n} \dot{u}_{j\ell_1 \dots \ell_n-1 \dots \ell_r}^e(t) + a_{\ell_n}^{b_n} \dot{u}_{j\ell_1 \dots \ell_n \dots \ell_r}^e(t) \right. \\
 & + a_{\ell_n+1}^{b_n} \dot{u}_{j\ell_1 \dots \ell_n+1 \dots \ell_r}^e(t)) + k_{nij}^e (a_{\ell_n-1}^{b_n} u_{j\ell_1 \dots \ell_n-1 \dots \ell_r}^e(t) \\
 & \left. \left. + a_{\ell_n}^{b_n} u_{j\ell_1 \dots \ell_n \dots \ell_r}^e(t) + a_{\ell_n+1}^{b_n} u_{j\ell_1 \dots \ell_n+1 \dots \ell_r}^e(t)) \right] \right\} \\
 & = f_i^e \prod_{s=1}^r \delta_{\ell_s, 0} + \sum_{n=1}^r f_{ni}^e \left( a_0^{b_n} \prod_{s=1}^r \delta_{\ell_s, 0} + a_1^{b_n} \prod_{\substack{s=1 \\ s \neq n}}^r \delta_{\ell_s, 0} \delta_{\ell_n, 1} \right) ,
 \end{aligned}
 \quad \begin{array}{l}
 i = 1, \dots, NEN, \\
 \ell_s = 0, 1, \dots \\
 s = 1, \dots, r
 \end{array} \quad (2.44)$$

$$\sum_{j=1}^{NEN} m_{ij}^e u_{j\ell_1 \dots \ell_r}^e(0) = u_{0i}^e \prod_{s=1}^r \delta_{\ell_s, 0} ,
 \quad \begin{array}{l}
 i = 1, \dots, NEN, \\
 \ell_s = 0, 1, \dots \\
 s = 1, \dots, r
 \end{array} \quad (2.45)$$

$$\sum_{j=1}^{NEN} m_{ij}^e \dot{u}_{j\ell_1 \dots \ell_r}^e(0) = \dot{u}_{0i}^e \prod_{s=1}^r \delta_{\ell_s, 0} ,
 \quad \begin{array}{l}
 i = 1, \dots, NEN, \\
 \ell_s = 0, 1, \dots \\
 s = 1, \dots, r
 \end{array} \quad (2.46)$$

where

$m_{ij}^e = \int_{\Omega^e} m(\mathbf{x}) \phi_i^e(\mathbf{x}) \phi_j^e(\mathbf{x}) d\Omega$ , which defines the element mass matrix,

$c_{ij}^e = \int_{\Omega^e} \mathbf{Q}(\bar{\mathbf{c}}(\mathbf{x}), \phi_j^e(\mathbf{x})) \phi_i^e(\mathbf{x}) d\Omega$ , which defines the nominal element damping matrix,

$k_{ij}^e = \int_{\Omega^e} \tau(\bar{\mathbf{k}}(\mathbf{x}), \phi_j^e(\mathbf{x})) \nabla \phi_i^e(\mathbf{x}) d\Omega$ , which defines the nominal element stiffness matrix,

$c_{nij}^e = \int_{\Omega^e} \mathbf{Q}(\mathbf{c}_n(\mathbf{x}) \phi_j^e(\mathbf{x})) \phi_i^e(\mathbf{x}) d\Omega$ , which defines the element damping matrix that accounts for the uncertainty in damping parameter field,

$k_{nij}^e = \int_{\Omega^e} \tau(\mathbf{k}_n(\mathbf{x}), \phi_j^e(\mathbf{x})) \nabla \phi_i^e(\mathbf{x}) d\Omega$ , which defines the element stiffness matrix that accounts for the uncertainty in stiffness parameter field,

$f_i^e = \int_{\Omega^e} \bar{f}(\mathbf{x}, t) \phi_i^e(\mathbf{x}) d\Omega$ , which defines the nominal element force vector,

$f_{ni}^e = \int_{\Omega^e} f_n(\mathbf{x}, t) \phi_i^e(\mathbf{x}) d\Omega$ , which defines the element force vector that accounts for the uncertainty in force field,

$u_{0i}^e = \int_{\Omega^e} m(\mathbf{x}) u_o(\mathbf{x}) \phi_i^e(\mathbf{x}) d\Omega$ , which defines the element initial condition vector on displacement, and

$\dot{u}_{0i}^e = \int_{\Omega^e} m(\mathbf{x}) \dot{u}_o(\mathbf{x}) \phi_i^e(\mathbf{x}) d\Omega$ , which defines the element initial condition vector on velocity.

The coupled system of linear ordinary differential equations for the unknowns is found by assembling equations (2.44) through (2.46) for all elements, into a set of global equations. This leads to a deterministic equation of the form

$$M\ddot{\mathbf{d}}(t) + C\dot{\mathbf{d}}(t) + K\mathbf{d}(t) = \mathbf{p}(t), \quad (2.47)$$

where  $\mathbf{d}(t)$  is the global vector of unknowns with components  $u_{j\ell_1\dots\ell_r}(t)$ ,  $\mathbf{p}(t)$  is the total effective load vector, and  $M$ ,  $C$  and  $K$  are the mass, damping and stiffness matrices for the system, respectively.

The initial conditions are given by

$$\mathbf{d}(0) = \mathbf{d}_0 \quad \text{and} \quad (2.48)$$

$$\dot{\mathbf{d}}(0) = \dot{\mathbf{d}}_0, \quad (2.49)$$

where  $\mathbf{d}_0$  and  $\dot{\mathbf{d}}_0$  are vectors whose elemental components are defined by the equations (2.42) and (2.43), respectively. Note that homogeneous boundary conditions are satisfied for all nodes on  $\Gamma_g$ .

It is interesting to note that the dimension of the matrices  $M$ ,  $C$  and  $K$  increase very rapidly with both the number of random variables  $b_n$ , and the order of approximation of the finite element solution in the probability space  $D$  (equation (2.35)). Nevertheless, these matrices are thinly populated, that is, there are relatively few nonzero terms.

In order to illustrate the manner in which the dimension of the matrices of the system increase, the number of unknowns per node as a function of the number of random variables and the order of approximation in the probability space is presented in Table 2.1. The same order of approximation is considered for each one of the random variables. In general, however, the approximation of the response in terms of a random variable with a small variance requires lower order of approximation than for a random variable with a large variance. Thus, the number of unknowns per node can be reduced significantly. An example in which different orders of approximation are used for the random variables is presented in Chapter 3.

$NP \backslash r$	1	2	3	4
1	2	3	4	5
2	3	6	10	15
3	4	10	20	35
4	5	15	35	70
5	6	21	56	126

**Table 2.1** Number of unknowns per node.

Finally, it is reiterated that the elemental matrices of the system defined by equation (2.44) are sparse, that is, the number of nonzero terms is relatively small.

## 2.7 Discrete Time Solution

Equation (2.47) can be integrated in time to find the global vector of unknowns  $d(t)$  for all time. Most time integration schemes fall into one of two classes: implicit or explicit. An implicit algorithm requires solution of a matrix equation at every time step to advance the solution. In contrast, explicit algorithms do not demand a simultaneous equation solution, but do require smaller time step to maintain stability and accuracy. As previously pointed out, the size of the matrices  $M$ ,  $C$  and  $K$  may become very large, so the time integration algorithm should be chosen such that computer high-speed memory requirements are minimized. Low order explicit algorithms are very memory efficient, thus allowing solution of large problems in a given memory size.

The modified Euler scheme is an explicit, second order accurate integration procedure which is well suited to solve the first order state space equation corresponding to equation (2.47). This algorithm is conditionally stable, with stability guaranteed for a sufficiently small time step  $\Delta t$  [30,31].

In order to convert the 2nd order differential equation (2.47) to a 1st order state space equation, define the system state vector  $\mathbf{s}(t)$  as

$$\mathbf{s}(t) = \begin{Bmatrix} \mathbf{d} \\ \dot{\mathbf{d}} \end{Bmatrix} . \quad (2.50)$$

Then, using this definition, the governing discrete equation (2.47) can be written

$$\dot{\mathbf{s}}(t) = \mathbf{A}\mathbf{s}(t) + \mathbf{F}(t) , \quad (2.51)$$

where

$$\mathbf{A} = \begin{bmatrix} \mathbf{0} & \mathbf{I} \\ -\mathbf{M}^{-1}\mathbf{K} & -\mathbf{M}^{-1}\mathbf{C} \end{bmatrix} \quad (2.52)$$

is the system matrix, and

$$\mathbf{F}(t) = \begin{Bmatrix} \mathbf{0} \\ \mathbf{M}^{-1}\mathbf{p}(t) \end{Bmatrix} \quad (2.53)$$

is the state space load vector. In the above expression,  $\mathbf{I}$  is the identity matrix of appropriate dimension.

The Euler algorithm begins at step  $k$ , time  $t_k$ , when  $\mathbf{s}(t_k)$  is known, and computes the updated vector  $\mathbf{s}(t_{k+1})$  as follows:

1. Predictor equation: Compute predicted  $\mathbf{s}(t_{k+1})$  and  $\dot{\mathbf{s}}(t_{k+1})$  from

$$\mathbf{s}(t_{k+1}) = \mathbf{s}(t_k) + \Delta t \dot{\mathbf{s}}(t_k) \quad (2.54)$$

$$\dot{\mathbf{s}}(t_{k+1}) = \mathbf{A}\mathbf{s}(t_{k+1}) + \mathbf{F}(t_{k+1}) \quad (2.55)$$

2. Corrector equation: Compute corrected new  $\mathbf{s}(t_{k+1})$  and  $\dot{\mathbf{s}}(t_{k+1})$  from

$$\mathbf{s}(t_{k+1}) = \mathbf{s}(t_k) + \frac{\Delta t}{2} (\dot{\mathbf{s}}(t_k) + \dot{\mathbf{s}}(t_{k+1})) \quad (2.56)$$

$$\dot{\mathbf{s}}(t_{k+1}) = \mathbf{A}\mathbf{s}(t_{k+1}) + \mathbf{F}(t_{k+1}) \quad (2.57)$$

Note that only the nonzero terms of  $A$  need to be stored for computer implementation to produce a more memory efficient scheme. In addition, since no matrix decompositions are involved, the scheme is efficiently implemented in a vector processing computer environment. Also note that if a diagonal or “lumped” mass matrix is employed for the element mass matrix in the finite element formulation, then the mass matrix  $M$  will be diagonal and the construction of the system matrix  $A$  will be immediate.

This completes the specification of the solution procedure. The next section describes the probabilistic characterization of the response process.

## 2.8 Response Uncertainty and Statistics

Once the unknowns  $u_{j_{\ell_1 \dots \ell_r}}^e(t)$  have been determined, an analytical approximation to the solution in the spatial and probability space is completely defined by equation (2.35). The response, which is random, will be described by its probability density or cumulative probability function, or by its statistical moments. Of particular importance is the second moment representation defined by the mean or

expected response of all possible outcomes, and by the variance and covariance of the response.

Using equation (2.32), the mean value, variance and covariance response for the element  $e$  are given by

$$E(u^e(\mathbf{x}, \mathbf{b}, t)) = \sum_{j=1}^{NEN} \sum_{0 \leq |\boldsymbol{\ell}| \leq NP} u_{j\ell_1 \dots \ell_r}^e(t) \phi_j^e(\mathbf{x}) E \left( \prod_{s=1}^r H_{\ell_s}^{b_s}(b_s) \right), \quad (2.58)$$

$$e = 1, \dots, NEL,$$

$$Var(u^e(\mathbf{x}, \mathbf{b}, t)) = \sum_{i=1}^{NEN} \sum_{j=1}^{NEN} \sum_{0 \leq |\boldsymbol{\ell}| \leq NP} \sum_{0 \leq |\mathbf{k}| \leq NP} u_{i\ell_1 \dots \ell_r}^e(t) u_{jk_1 \dots k_r}^e(t) \phi_i^e(\mathbf{x}) \phi_j^e(\mathbf{x}) E \left( \prod_{s=1}^r H_{\ell_s}^{b_s}(b_s) \prod_{s=1}^r H_{k_s}^{b_s}(b_s) \right) \quad (2.59)$$

$$- \sum_{i=1}^{NEN} \sum_{j=1}^{NEN} \sum_{0 \leq |\boldsymbol{\ell}| \leq NP} \sum_{0 \leq |\mathbf{k}| \leq NP} u_{i\ell_1 \dots \ell_r}^e(t) u_{jk_1 \dots k_r}^e(t) \phi_i^e(\mathbf{x}) \phi_j^e(\mathbf{x})$$

$$E \left( \prod_{s=1}^r H_{\ell_s}^{b_s}(b_s) \right) E \left( \prod_{s=1}^r H_{k_s}^{b_s}(b_s) \right), \quad e = 1, \dots, NEL,$$

$$\begin{aligned}
C_{ov}(u^{e_1}(\mathbf{x}, \mathbf{b}, t_1), u^{e_2}(\mathbf{y}, \mathbf{b}, t_2)) = & \\
& \sum_{i=1}^{NEN} \sum_{j=1}^{NEN} \sum_{0 \leq |\boldsymbol{\ell}| \leq NP} \sum_{0 \leq |\mathbf{k}| \leq NP} u_{i\ell_1 \dots \ell_r}^{e_1}(t_1) u_{jk_1 \dots k_r}^{e_2}(t_2) \phi_i^{e_1}(\mathbf{x}) \phi_j^{e_2}(\mathbf{y}) \\
& E \left( \prod_{s=1}^r H_{\ell_s}^{b_s}(b_s) \prod_{s=1}^r H_{k_s}^{b_s}(b_s) \right) - \sum_{i=1}^{NEN} \sum_{j=1}^{NEN} \sum_{0 \leq |\boldsymbol{\ell}| \leq NP} \sum_{0 \leq |\mathbf{k}| \leq NP} \\
& u_{i\ell_1 \dots \ell_r}^{e_1}(t_1) u_{jk_1 \dots k_r}^{e_2}(t_2) \phi_i^{e_1}(\mathbf{x}) \phi_j^{e_2}(\mathbf{y}) E \left( \prod_{s=1}^r H_{\ell_s}^{b_s}(b_s) \right) E \left( \prod_{s=1}^r H_{k_s}^{b_s}(b_s) \right), \\
& e_1, e_2 = 1, \dots, NEL.
\end{aligned} \tag{2.60}$$

Finally, using the orthogonality of the set of polynomials as defined in equation (2.34), the second moment representation for the element response is given by

$$E(u^e(\mathbf{x}, \mathbf{b}, t)) = \sum_{j=1}^{NEN} u_{j_0 \dots 0}^e(t) \phi_j^e(\mathbf{x}), \quad e = 1, \dots, NEL \tag{2.61}$$

$$\begin{aligned}
V_{ar}(u^e(\mathbf{x}, \mathbf{b}, t)) = & \sum_{i=1}^{NEN} \sum_{j=1}^{NEN} \sum_{1 \leq |\boldsymbol{\ell}| \leq NP} u_{i\ell_1 \dots \ell_r}^e(t) u_{j\ell_1 \dots \ell_r}^e(t) \phi_i^e(\mathbf{x}) \phi_j^e(\mathbf{x}), \\
& e = 1, \dots, NEL
\end{aligned} \tag{2.62}$$

and

$$\begin{aligned}
C_{ov}(u^{e_1}(\mathbf{x}, \mathbf{b}, t_1), u^{e_2}(\mathbf{y}, \mathbf{b}, t_2)) & \\
= & \sum_{i=1}^{NEN} \sum_{j=1}^{NEN} \sum_{1 \leq |\boldsymbol{\ell}| \leq NP} u_{i\ell_1 \dots \ell_r}^{e_1}(t_1) u_{j\ell_1 \dots \ell_r}^{e_2}(t_2) \phi_i^{e_1}(\mathbf{x}) \phi_j^{e_2}(\mathbf{y}), \\
& e_1, e_2 = 1, \dots, NEL
\end{aligned} \tag{2.63}$$

where equations (2.61), (2.62) and (2.63) represent the mean value, variance and covariance response, respectively.

This characterization of the response is completely defined by the nodal unknowns  $u_{j\ell_1\dots\ell_r}^e(t)$ , and does not require the solution of a multiple integral in the probability space. A similar characterization can also be defined for the velocity, acceleration, strain and stress response fields. Finally, it is noted that using the analytical approximation for the response, given by equation (2.35), higher statistical moments can be computed as well as the probability function. These higher statistical moments can be computed using higher order recurrence relations for the orthogonal set of polynomials, while the probability function can be computed by numerical integration.

This completes the formulation of the random finite element method for the governing second order partial differential equation described in Section 2.2. The next chapter describes the application of this technique to the solution of one specific system of engineering interest.

## Chapter 3

### Application to One-Dimensional Wave Equation

#### 3.1 Introduction

This chapter describes the application of the newly developed solution method to one specific problem. Before beginning discussion of the particular problem to be studied, it is appropriate to consider the objectives of such a numerical investigation.

The numerical illustrations described in this chapter are chosen with the following goals in mind. The first motive is to exercise the new technique and acquire facility in its application. The second, is that it is important to validate the accuracy of the new method by comparing it against other available solution techniques. Finally, it is of engineering interest to assess the influence of uncertainties in structural properties on the structural response of an example system.

The system chosen for study in this chapter is a one-dimensional continuum described by the wave equation in which the physical properties exhibit a one-dimensional spatial random variation. This spatial variability is modeled as an homogeneous Gaussian random field, or random process [32]. The class of systems modeled by the wave equation is one of significant engineering importance since it contains many common physical systems, such as axial vibration of a rod, propagation of plane waves in a continuum, and vibration of a shear beam. The particular

problem chosen for study will be described later. In what follows, the discretization of the random field will be discussed in detail.

### 3.2 Random Field Discretization

The finite element analysis involves the discretization of the parameter-space of a random field of material properties into a random vector representation. Two methods of discretization have generally been used. In one method, the field values are defined at a finite set of discrete points, which typically corresponds to either: the mesh nodes, the midpoint of the elements, or the integration points. Then, the representation of the random field is defined in terms of a mean value vector and a covariance matrix defined at such points. These two statistical moments are obtained in terms of the mean and covariance functions of the process from well known results in random field theory [32].

In the second method, the field values are defined at a finite set of elements, called random field elements. Their values are represented by the spatial average of the process over the element, as originally suggested by Vanmarcke et al. [32]. A key component of this approach is the treatment of the correlation structure of the random material property in terms of the variance function and its principal parameter, the scale of fluctuation. In this context, the variance function represents the dependence of the variance of spatial averages on the size of the averaging element, while the scale of fluctuation measures the distance within which the random process shows relatively strong correlation from point to point. Similar to the first method, the representation of the random field is defined in terms of a mean value vector and a matrix of covariances between local spatial averages associated with pairs of random field elements. One of the advantages of this formulation is that

detailed knowledge about the correlation structure of the process, which in practice is seldom available, is unnecessary.

Both methods of discretization of the random field imply that its representation will consist of a vector of random variables with a jointly Gaussian probability density function. As indicated in Section 2.3, the random field can be described in terms of a vector of independent random variables by using the spectral decomposition of the covariance matrix. To show this result in detail, let  $\mathbf{z}$  be the vector of random variables that describe the random field, and let  $C$  be its covariance matrix with components  $C_{ij}$ . Depending on which method of discretization has been used,  $i$  and  $j$  represent either points or random field elements in the spatial domain. By the spectral decomposition theorem, the covariance matrix can be represented as a summation of the form

$$C = \sum_{\ell=1}^N \phi_{\ell} \phi_{\ell}^T \lambda_{\ell}, \quad (3.1)$$

where  $N$  is the dimension of the vector of random variables  $\mathbf{z}$ ,  $\lambda_{\ell}$  are the eigenvalues of the covariance matrix ordered in a decreasing manner, and  $\phi_{\ell}$  are the corresponding eigenvectors, normalized such that

$$\phi_{\ell}^T \phi_s = \delta_{\ell s}. \quad (3.2)$$

To obtain an uncorrelated set of random variables, the random vector  $\mathbf{z}$  is transformed into a new vector of random variables  $\mathbf{b}$ , defined by

$$\mathbf{b} = \Phi^T \mathbf{z}, \quad (3.3)$$

where  $\Phi$  is the matrix of eigenvectors of the covariance matrix.

The orthogonality property of the eigenvectors (3.2) together with the uniqueness of the spectral decomposition (3.1), imply that the covariance matrix of the

new set of variables is diagonal, and their variances are simply the eigenvalues of the covariance matrix of the original variables. So, the new random variables are uncorrelated and since they are Gaussian, they are also independent.

The contribution of each successive eigenvalue-eigenvector pair to the total correlation (equation (3.1)) is observed to decrease steadily for many problems of interest [14,33,34]. Consequently, there is the possibility of truncating the series in (3.1) at some value  $n < N$  without significant loss of accuracy. This reduction of variables is particularly important in the representation of strongly correlated fields, allowing their description by a proper set of uncorrelated random variables.

Another important issue related with finite element analysis and the discretization of the random field is the selection of the mesh size. When the material properties exhibit spatial variability two separate factors should be considered for this selection. One is the expected gradient of the stress field [30], and the other is the expected rate of fluctuation of the random field, as measured, for example, by the corresponding strength of correlation [15,19,22]. The two requirements do not necessarily coincide in each region of the structure and, hence, it is usually necessary to consider two or more separate meshes. In the present application, the finite element mesh is selected such that both sets of requirements in each region of the structure are satisfied. Then for a given random field, a separate mesh is considered which is equal to or coarser than the finite element mesh, such that each random field element is a block of one or more finite elements.

### 3.3 Description of the Physical System

The particular problem chosen for study is a shear beam whose rigidity varies randomly along its axis. As shown in Figure 3.1, the beam lies along the  $x$  axis.

The transverse displacement in an inertial coordinate frame is denoted by  $v(x, t)$ , while the displacement relative to the base of any point  $x$  at time  $t$  is denoted by  $u(x, t)$ . The beam is assumed to have constant mass,  $m$ , per unit of length. The base acceleration  $\ddot{q}(t)$  is taken to be an earthquake-like excitation.

The equation of motion for this system is easily shown to be

$$\frac{\partial \tau}{\partial x} = m\ddot{v}, \quad (3.4)$$

or in terms of relative displacement

$$\frac{\partial \tau}{\partial x} = m\ddot{u} + m\ddot{q}, \quad (3.5)$$

where  $\tau$  is the shear stress, and all other terms are as defined above. The shear stress is related to the relative displacement by the equation

$$\tau = k(x) \frac{\partial u}{\partial x}, \quad (3.6)$$

where  $k(x)$  is the shear stiffness defined by

$$k(x) = G(x) A(x), \quad (3.7)$$

where  $G(x)$  is the elastic shear modulus and  $A(x)$  is the cross-sectional area.

Substitution of equations (3.6) and (3.7) into equation (3.5) yields the equation of motion in terms of displacement relative to the base as

$$\frac{\partial}{\partial x} \left( k(x) \frac{\partial u}{\partial x} \right) = m\ddot{u} + m\ddot{q}. \quad (3.8)$$

This system is cast into the general form, described in Chapter 2 (equation 2.1), by letting the stiffness parameter  $k(x)$  represent the shear stiffness, the divergence operator  $\nabla$  represent the derivative with respect to the variable  $x$ , and the external

load  $f$  represent the load due to the base excitation, with the operator  $\tau(\cdot)$  defined as

$$\tau(k(x), u) = k(x) \frac{\partial u}{\partial x} . \quad (3.9)$$

To complete the formulation of the system, it is necessary to add some amount of damping to the mathematical model. Often the physical mechanisms producing damping in a given system are not well understood, and the addition of damping is based on experience or experimental data rather than rigorous derivation. One form of damping widely used in structural calculations is Rayleigh damping, where the damping matrix is constructed as a linear combination of the stiffness and mass matrices. This form of damping is achieved in the model by defining the operators  $\tau(\cdot)$  and  $Q(\cdot)$ , which are described in equation (2.1), as

$$\tau(k(x), u) = k(x) \left( \frac{\partial u}{\partial x} + c_1 \frac{\partial^2 u}{\partial x \partial t} \right) \quad (3.10)$$

$$Q(c(x), \dot{u}) = c(x) \dot{u} , \quad (3.11)$$

where

$$c(x) = c_2 m , \quad (3.12)$$

and  $c_1$  and  $c_2$  are constant parameters reflecting the participation of damping proportional to stiffness and mass, respectively. All other terms are as previously defined. Frequently, mass proportional damping is referred to as external damping, and stiffness proportional damping is also known as internal damping. It is emphasized that the new method of analysis is not restricted to Rayleigh damping in any way, and that many other techniques could equally well be used to incorporate damping into the model.

### 3.4 Representation of the Random Field

In order to consider the uncertainty in the beam rigidity along its axis, the spatial variation of the shear stiffness  $k(x)$ , is assumed to be a one-dimensional homogeneous Gaussian random field. It is defined in terms of a mean value plus a deviatoric component, that is

$$k(x) = \bar{k}(x) + Z(x) , \quad (3.13)$$

where  $\bar{k}(x)$  is the shear stiffness mean value and  $Z(x)$  represents its fluctuating or deviatoric component.

The fluctuating component is assumed to have zero mean, that is

$$E(Z(x)) = 0 , \quad (3.14)$$

and covariance function defined by

$$R(x, x + \zeta) = E(Z(x) Z(x + \zeta)) , \quad (3.15)$$

where  $x$  and  $x + \zeta$  are points along the  $x$  axis.

Since the random field is assumed to be homogeneous, the covariance function of the spatial variation is a function only of the distance between the two points. While the new method of analysis is not restricted to any particular form of the covariance function, the following exponential function is considered in the present analysis:

$$R(\zeta) = \sigma^2 e^{-(\zeta/\delta L)^2} , \quad (3.16)$$

where  $\sigma$  is the standard deviation of the random process,  $\zeta$  is the distance between two points along the  $x$  axis,  $L$  is the length of the shear beam, and  $\delta$  is a dimensionless parameter. The parameter  $\delta$  is a measure of the correlation length and the

product  $\delta L$  is usually defined as the scale or strength of correlation [22,32]. Note that  $\delta = \infty$  corresponds to a fully correlated random field and the process reduces to a random variable. In contrast, the random field is completely uncorrelated and becomes white noise when  $\delta = 0$ .

Next, the random field is discretized in accordance with a suitable finite element mesh. This suitable mesh should satisfy the requirements pointed out in Section 3.2. Then, the discretized version of equation (3.13) is given by

$$\mathbf{k} = \bar{\mathbf{k}} + \mathbf{z} , \quad (3.17)$$

where  $\mathbf{k}$  is the random vector that represents the spatial variation of the shear stiffness at a set of discrete points,  $\bar{\mathbf{k}}$  is the mean value vector of the process, and  $\mathbf{z}$  is a vector of Gaussian random variables with zero mean and covariance matrix  $C$ , whose  $(i, j)$  component is given by

$$C_{ij} = E(z_i z_j) , \quad (3.18)$$

where  $z_i$  and  $z_j$  are the  $i$ -th and  $j$ -th components of the random vector  $\mathbf{z}$ , respectively. The  $C_{ij}$  components are obtained in terms of the covariance function defined in equation (3.16).

Finally, by means of the transformation defined in equation (3.3), the representation of the discretized random field can be written in terms of a vector of uncorrelated and independent random variables. Then, multiplying equation (3.3) by the matrix of eigenvectors of the covariance matrix  $\Phi$ , and substituting into (3.17) yields

$$\mathbf{k} = \bar{\mathbf{k}} + \Phi \mathbf{b} , \quad (3.19)$$

where  $\mathbf{b}$  is a vector of independent Gaussian random variables with zero mean. As mentioned in the previous section, there is the possibility of considering only a few of these random variables to represent the random field without significant loss of accuracy. The actual number of random variables that are retained in the analysis depends on the correlation length parameter of the random field. A particular example will be considered in Section 3.6.

This completes the description of the physical system and the representation of the random field, which have been cast into the general formulation described in Chapter 2. The next two sections describe the comparison of the new method against other techniques and the application of the method to the solution of some particular examples of the physical system considered in Section 3.3.

## **3.5 Performance Evaluation**

### **3.5.1 Introduction**

In order to evaluate the performance of the newly developed method on problems involving uncertainty in physical properties, two examples are solved and their solutions are compared with solutions which are obtainable by other techniques.

Early applications used the Monte Carlo simulation method to investigate the effect of uncertain variability in structural properties. Later, first and second-order Taylor series or perturbation methods were used to compute second-moment statistics of response quantities in structural and geotechnical applications. In Monte Carlo simulation, the computer is used to generate a particular realization of the structural properties, and the deterministic solution is found using classical analysis techniques. This process is repeated until the ensemble of realizations of the structural properties represent the statistical distribution to a desired degree of accuracy.

Then, statistics are computed across the ensemble of responses obtained from these particular properties. Although this method is very powerful, it is very costly in terms of computational resources and may become prohibitively expensive.

In perturbation methods, parameter uncertainties are assumed to be “small,” and the expressions for the response are expanded by perturbation about the mean values to obtain the second-moment statistics. These methods are quite general and they are easily integrable into any deterministic solution technique. However, perturbation methods usually suffer from questions on their accuracy and convergence. These questions become more crucial as higher order solutions are sought, as the degree of the material property variability becomes more pronounced, and when dynamic, particularly transient and wave propagation problems must be considered. In fact, when perturbation methods are applied to transient analysis secular terms result in the higher order solution and hence, in all statistical results [14,26]. Consequently, the solution is valid only for a short duration and the accuracy deteriorates rapidly thereafter. Although some methods have been proposed to numerically eliminate secular terms in probabilistic finite element methods [26], their effectiveness is still under investigation.

### **3.5.2 First Validation Problem**

As a first check on the accuracy of the newly developed method, a problem with only one degree-of-freedom is solved. The finite element model corresponding to this problem is shown in Figure 3.2. Note that this model represents a single degree-of-freedom system. For this one element model, a constant mass per unit of length and uniform mean value properties throughout its length are used. The natural frequency of the system is 2 Hz and a damping corresponding to 5% of

critical is added. The variability of the shear stiffness is modeled as a fully correlated random field, that is, as a random variable. As previously discussed in Chapter 2, the probability density function of this random variable is not restricted to be Gaussian. In fact, a uniform probability density function is assumed in this example. The effect of the particular choice for the probability function on the accuracy of the method will be discussed later. The model is subjected to a base excitation, and the variability of the response is studied. In particular, the absolute acceleration response at the free node of the element is considered.

The base excitation is taken to be an earthquake-like excitation. It is generated using the procedure described in reference [35]. In brief, a sample function is generated to represent stationary Gaussian white noise. The sample function is constructed from a sequence of independent normally distributed numbers with zero mean and unit variance. These numbers are used as ordinates of the function at equally spaced time intervals,  $\Delta t$ . The function is assumed to vary linearly over each interval. The numerically generated unit variance sample function is multiplied by a scaling factor to give a process with a power spectral density approaching to a constant. Next, the sample function is multiplied by a shaping function in time  $\theta(t)$ , to produce a single sample of a nonstationary process. In the present example, the shape function chosen is

$$\theta(t) = te^{-\nu t} , \tag{3.20}$$

where  $\nu$  is a free parameter which may be interpreted physically as the reciprocal of the time required for the excitation to build up to its maximum intensity. Finally, the excitation chosen to represent the base excitation is obtained by passing the nonstationary process through a filter with prescribed transfer function. The

resultant base excitation is therefore a sample of a filtered, modulated white noise process. Figure 3.3 shows the base excitation for the present validation problem.

Figures 3.4 and 3.5 show a comparison of the results of the proposed method to those obtained by an "exact" solution for both the mean value and the standard deviation responses of the absolute acceleration of the system. In the "exact" solution, the first two statistical moments are computed numerically. The numerical integration is performed using 200 equally spaced points over the range of shear stiffness values. Three values for the coefficient of variation of the shear stiffness are considered: 10%, 20% and 30%. Recall that the coefficient of variation is the ratio between the standard deviation and the mean value of the random variable. These figures show that the agreement between the proposed method and the "exact" solution is excellent. The two solutions are coincident in every place. Note that the response variability increases with increasing coefficient of variation of the shear stiffness.

In the case of the proposed method, different orders of approximation in the probability space are used as the shear stiffness variability becomes more pronounced. A third order approximation is used for a coefficient of variation of 10%, and a fourth and a fifth order approximation are used for coefficients of variation of 20% and 30%, respectively. The need to use such a high order of approximation clearly shows the high degree of nonlinearity of the response as a function of the shear stiffness parameter. It also indicates that a low order approximation is not adequate to approximate such a nonlinearity.

At this point, it is interesting to compare the relative amounts of computational effort required to obtain the results by the proposed method versus that for the Monte Carlo simulation method. The computer time required by the proposed

method is equivalent to the time required to perform approximately 15 simulations. This number is much less than the number of simulations usually required to obtain dependable results from a simulation study. In fact, more than 100 simulations are needed to obtain the same accuracy that is obtained by the proposed method. Therefore, it is concluded that for this test problem, the new formulation is more efficient than simulation.

In order to illustrate the difficulties of the second-order perturbation method in probabilistic finite elements, the comparison of the results of the “exact” solution to those obtained by the perturbation method are presented in Figure 3.6. A coefficient of variation of 20% is considered in this case. This figure shows that the perturbation method does not give acceptable results. For higher coefficients of variation, it can be shown that the inaccuracy of the perturbation method is even more dramatic. As mentioned before, one of the factors that affects the accuracy of the perturbation method is the existence of secular terms in the higher order solutions. At the same time, the second-order perturbation method is not adequate to approximate the high nonlinearity of the response as a function of the uncertain system parameters.

Finally, an investigation of the effect of different probability density functions for the shear stiffness parameter on the accuracy of the proposed method is performed. In addition to a uniform distribution, three different types of probability density functions are applied in this example, including: Gaussian, Parabolic, and Ultraspherical. The mathematical expressions for these distributions are given in reference [29]. The analysis shows that for all these distributions, the results are

qualitatively similar to those of the corresponding uniform case. That is, the proposed method gives excellent agreement with the "exact" solution, while the performance of the second-order perturbation method is poor. To graphically illustrate these results, the case of a Gaussian distribution of the shear stiffness parameter with a 20% coefficient of variation is presented in Figure 3.7. The results are self-evident.

### 3.5.3 Second Validation Problem

A second validation problem presented considers the variability of the response of a two element model. As before, the absolute acceleration response at the free end of the model is considered. A diagram of the finite element mesh is shown in Figure 3.8. Here, as in the first validation problem, a constant mass per unit of length and uniform mean value properties throughout its length are assumed. The nominal or mean value system is assumed to have 5% of critical damping in both modes, and a fundamental frequency of 2 Hz. Once again, the model is subjected to the base excitation described previously.

The variability of the shear stiffness in space is modeled as a Gaussian random field, which is discretized into two random field elements. Their correlational characteristic is assumed to be specified in terms of the following covariance matrix

$$C = \sigma^2 \begin{pmatrix} 1.0 & \rho \\ \rho & 1.0 \end{pmatrix}, \quad (3.21)$$

where  $\sigma$  is the standard deviation of the process, and  $\rho$  is the coefficient of correlation between the two random field elements. Three values of  $\rho$  are considered:  $\rho = 1.0, 0.5$ , and  $0.0$ . In the first case, the random field elements are fully correlated, while they are completely uncorrelated in the third case. In the second case,

the random field elements can be considered as medially correlated. Note that the covariance matrix corresponding to these three cases can be generated by the covariance function defined in equation (3.16). In fact, if the field value over an element is represented by its value at the midpoint of the element, then the evaluation of the covariance function at  $\zeta = 1.0$ , with parameter  $\delta$  equal to  $\infty$ , 0.6 and 0.0. gives the off-diagonal terms of the covariance matrix for the three cases, respectively. Note that  $\zeta = 1.0$  corresponds to the distance between the midpoints of elements 1 and 2.

Figures 3.9 and 3.10 show a comparison of the results of the proposed method to those obtained by an “exact” solution for both the mean value and the standard deviation responses of the absolute acceleration at the free end of the model. A 20% coefficient of variation of the shear stiffness is considered. In the “exact” solution, the mean value and the standard deviation responses are computed by numerical integration over the range of shear stiffness values. The agreement between the proposed method and the “exact” solution is excellent. These figures also show that the fully correlated case produces the largest response variability. That is, the uncertainty in the absolute acceleration response tend to decrease as the two random field elements become uncorrelated. In the case of the proposed method, the following orders of approximation in the probability space are used: A fifth order approximation is used for a coefficient of correlation of 1.0, and a fourth order approximation is used for coefficients of correlation of 0.5 and 0.0.

Figure 3.11 shows the inadequacy of the second-order perturbation method in this second validation problem. A coefficient of correlation of 0.5 between the random field elements and a coefficient of variation of 20% of the shear stiffness are considered in this case. Once again, the perturbation method does not give

acceptable results. As stated previously, some of the factors that affect the accuracy of the perturbation method are the existence of secular terms in the higher order solutions and the inability of approximating the high nonlinearity of the response as a function of the uncertain system parameters.

In order to illustrate the high nonlinearity of the response as a function of the shear stiffness parameter, the absolute acceleration response at the free end of the model is presented in Figure 3.12 as a function of the two random variables that describe the random field under consideration. This figure depicts the response of the system in the neighborhood of the response of the nominal system at two specific times. The response is plotted for values of the random variables less or equal than one standard deviation about their mean values. The selected times are the time in which the mean value response is maximum and the time in which the standard deviation response is maximum. It is clear from this figure that the response as a function of the two random variables is highly nonlinear. Thus, low order approximations are not appropriate to approximate such a nonlinearity.

Finally, it is interesting to note that the computer time required by the proposed method is equivalent to the time to perform approximately 8 simulations in each one of the two random variables that describe the random field. On the other hand, the total number of simulations needed to obtain the same accuracy that is obtained by the proposed method is more than 400. Thus, once again, the new formulation is more economical than simulation.

Based on the results of the above two validation calculations, the proposed method is judged to produce accurate results for the response variability of the system under consideration.

### 3.6 Description of the Example Problem

In Section 3.3, the physical system chosen for study was described. The efforts of this section together with the following sections are directed toward gaining physical insight into the response of a continuous shear beam whose rigidity varies randomly along its axis. To this end, two sets of calculations are performed to illustrate the influence of uncertain stiffness on the response of the beam. In particular, the absolute acceleration response at the top of the beam is considered. The continuous system is taken to have uniform mean value properties throughout its length, with a fundamental frequency of 2 Hz.

In the first set of calculations, the system is assumed to have a 20% of critical damping in the first two modes. The random field that describes the spatial variation of the shear stiffness is assumed to have a 40% coefficient of variation. The system is subjected to a single sample of a modulated white noise process, which is generated using the procedure described in reference [35]. Figure 3.13 shows the base excitation for this set of calculations. For convenience, this first set of calculations will be referred as Case I of the example problem. One specific engineering application of the results of these calculations will be discussed in Section 3.8.

In the second set of calculations, the system is assumed to have a 5% of critical damping in the first two modes. A coefficient of variation of 20% of the random field that describes the spatial variation of the shear stiffness is considered in this case. The system is subjected to the same base excitation that was used for the validation calculations in Section 3.5. The application of the results of these calculations in a structural engineering context will be discussed in Section 3.8. Finally, this set of calculations will be referred as Case II of the example problem.

In both sets of calculations, two values of correlation length parameter  $\delta$  are considered:  $\delta = \infty$ , and  $\delta = 0.5$ . As it was indicated before,  $\delta = \infty$  corresponds to a fully correlated random field, while  $\delta = 0.5$  corresponds to a random field which may be considered as medially correlated. The covariance functions corresponding to the above correlation length parameters are shown in Figure 3.14.

The assumption of a Gaussian distribution for the components of the random vector  $\mathbf{b}$  (equation 3.19) implies a probability of generating negative values of shear stiffness. This probability is not negligible for high coefficients of variation, such as 40%. Consequently, when high levels of uncertainty are considered, a new probability density function is introduced to avoid the mathematical complications that would arise if the shear stiffness indeed becomes negative. The newly introduced probability density function is of the so-called Ultraspherical type. This name arises from the fact that the set of Ultraspherical polynomials is orthogonal with respect to the mean operation defined by this distribution [29].

Figure 3.15 shows a Gaussian and an Ultraspherical distribution with a coefficient of variation of 40%. It is clear from this figure that the assumption of a Gaussian distribution implies that the probability of generating negative values for the random variable is not zero. On the other hand, it can be shown that this probability is negligible for smaller coefficients of variation, such as 20%. Therefore, an Ultraspherical distribution is assumed in Case I of the example problem, while a Gaussian distribution is used in Case II.

### 3.7 Finite Element Discretization

As discussed in Section 3.2, one of the factors that should be considered in the selection of the mesh size for the finite element analysis is the expected rate of

fluctuation of the random field. Therefore, in order to assure that the mesh used for this example problem adequately represents the physical behavior of the system, a parametric study of mesh size is conducted. For the given range of the correlation length parameter, the response variability of the absolute acceleration at the top of the beam is analyzed using uniform meshes of 10, 15, 20, and 25 elements.

For the uniform mesh of 20 elements, shown in Figure 3.16, it is found that the statistical fluctuations of the random field with correlation length parameter  $\delta = 0.5$  is very small within each element. That is, the random field is almost fully correlated within each element. Note that the random field with correlation length parameter  $\delta = \infty$  is fully correlated in the entire beam, and therefore is also fully correlated within each element. At the same time, it is found that the response is nearly invariant to a finer mesh, such as the 25 element mesh. Hence, the mesh shown in Figure 3.16 satisfies the two sets of requirements discussed in Section 3.2. Based on these results, the uniform 20 element mesh is judged adequate for the current problem. The results for Cases I and II of the example problem, using this uniform mesh of 20 elements, are presented in the next section.

The finite element mesh introduced above implies that the discretized random field is represented by 20 independent random variables (equation 3.19). However, the two values of the correlation length parameter that are considered in the example problem allow truncation of the eigenvectors-eigenvalues of the random field covariance matrix. Thus the number of eigenvectors, and hence the number of random variables in equation 3.19 can be reduced. It is clear that for  $\delta = \infty$ , the number of random variables can be reduced to one, since the process is fully correlated. For  $\delta = 0.5$ , the number of variables that are retained in the analysis is three. The influence of lower eigenvector-eigenvalue pairs is found to have little effect on

the response variability of the system. Figures 3.17 and 3.18 show the three most significant pairs of eigenvectors-eigenvalues of the random field covariance matrix for Case I and Case II of the example problem, respectively.

### 3.8 Results of the Example Problem

#### 3.8.1 Case I

The response variability of the absolute acceleration at the free end of the shear beam, for the 40% coefficient of variation random field, is presented in Figures 3.19 and 3.20. Figure 3.19 shows the second moment characterization of the response for the fully correlated random field case, and Figure 3.20 shows the second moment characterization of the response for the random field with correlation length parameter  $\delta = 0.5$ . The top graph of these figures shows the mean value response, the middle one shows the standard deviation response, and the bottom graph shows the variability parameter defined as the ratio between the standard deviation and the maximum mean value. The maximum values of the variability parameter are about 0.58 and 0.50, that is, 58% and 50% of the maximum mean value. These values illustrate the relatively high variability of the response. At the same time, comparison between the bottom graphs in Figures 3.19 and 3.20 shows the influence of the correlation length parameter on the variability of the absolute acceleration response at the top of the beam. The fully correlated case produces the largest response variability. That is, the uncertainty in the response tend to decrease as the random field become medially correlated.

As mentioned previously, the number of random variables that are retained in the analysis for the random field with correlation length parameter  $\delta = 0.5$  is three. Figure 3.21 shows the uncertainty in the response due to each one of the three most

significant pairs of eigenvectors-eigenvalues of the random field covariance matrix. It is clear that the contribution of each successive eigenvector-eigenvalue pair to the response variability decreases steadily. The first three random variables capture the major characteristics of the random field. Therefore, the contribution of lower eigenvector-eigenvalue pairs of the random field covariance matrix to the response variability is negligible.

Finally, it is noted that a fourth order approximation in the probability space is used for the fully correlated random field case. In the case of the medially correlated random field, different orders of approximation of the response in the probability space are used for three random variables that are retained in the analysis. A third order approximation is used for the first random variable, and a second and a first order approximation are used for the second and third random variables, respectively. The influence of higher order approximation is found to have negligible effect on the response.

### **3.8.2 Application of the Results to Earthquake Engineering**

One specific engineering application of the above results is in the area of geotechnical and earthquake engineering. In this context, one might conceptualize the shear beam as a column of soil excited by motions of underlying bedrock during an earthquake. Then, the surface motions are represented by the free end of the shear beam, and the uncertainty of such motions is represented by the response variability at the top of the beam. In this case, the coefficient of variation of the random field reflects uncertainty in the knowledge of soil properties but assuming that the soil behaves linearly.

The effects of the uncertainty of the surface motions on the response of a simple single-degree-of-freedom system located at the top of the soil column are presented in Figures 3.22 and 3.23. Two values of critical damping for the simple system are considered: 2% and 5%. It is noted that the single-degree-of-freedom system can be represented by a finite element model consisting of one element with linear shape functions (Figure 3.2). Therefore, this simple system can be cast into the general formulation described in Chapter 2, where the physical properties of the system are deterministic, and the externally applied load is random. Note that the external load is characterized by an expression similar to equation (2.35).

Figures 3.22 and 3.23 depict the maximum mean value and the maximum mean plus one standard deviation value of the absolute acceleration response of this simple system for a range of values of periods. Figure 3.22 corresponds to the fully correlated random field case. It is noted that for some periods of the simple system, the maximum mean plus one standard deviation value of the response is more than 50% of the maximum mean value of the response. For the medially correlated random field case (Figure 3.23), similar differences between the maximum mean plus one standard deviation value of response and the maximum mean value of the response are observed. These values clearly illustrate the high variability of the response of this simple system. The peaks of the curves in Figures 3.22 and 3.23 correspond to the first two fundamental frequencies of the soil column and to some of the predominant frequencies of the base excitation.

Note that the curve that represents the maximum mean value of the response may be interpreted as the mean acceleration response spectrum of the simple system, while the curve that represents the maximum mean plus one standard deviation

value of the response may be interpreted as the probabilistic (one standard deviation) acceleration response spectrum of the system. Also note that these figures suggest that the maximum mean value response may be considered unconservative for design as a consequence of the high variability of the response about its mean.

### 3.8.3 Case II

The response variability of the absolute acceleration at the top of the shear beam, for the 20% coefficient of variation random field, is presented in Figures 3.24 and 3.25. Figure 3.24 shows the second moment characterization of the response for the fully correlated random field case, and Figure 3.25 shows the second moment characterization of the response for the medially correlated random field case. The analysis shows that the results are qualitatively similar to those reported for Case I. That is, the relatively high variability of the response and the increase of the response uncertainty with increasing correlation length parameter. The maximum values of the variability parameter are about 0.57 and 0.51 for correlation length parameters equal to  $\infty$ , and 0.5, respectively.

It is noted that a similar level of response uncertainty is obtained for the lightly damped shear beam system (Case II) and for the more heavily damped shear beam system (Case I), even though the coefficient of variation of the random field in Case II (20%) is much smaller than that of the random field in Case I (40%). This result suggests that for lightly damped systems great caution must be exercised when interpreting calculated response if the physical properties are not precisely known.

Figure 3.26 shows the uncertainty in the response due to each one of the three most significant pairs of eigenvectors-eigenvalues of the random field covariance matrix. As before, the contribution of each successive eigenvector-eigenvalue pair

to the response variability decreases steadily, and the major characteristics of the random field are captured by the first three random variables.

Finally, it is noted that a fifth order approximation in the probability space is used for the fully correlated random field case. In the case of the medially correlated random field, different orders of approximation of the response in the probability space are used for the three random variables that are retained in the analysis. A fourth order approximation is used for the first random variable, and a second and a first order approximation are used for the second and third random variables, respectively. The influence of higher order approximation is found to have negligible effect on the response.

#### **3.8.4 Application of the Results to Structural Engineering**

From a structural engineering point of view, one might consider the shear beam to be a shear structure, like a shear building. Then, the response uncertainty at the free end of the shear beam represents the last floor response variability. The effects of this response variability on the response of a substructure located at the top of the building are presented in Figures 3.27 and 3.28. The substructure, which may represent a piece of equipment or a secondary system, is idealized as a single-degree-of-freedom system. Recall that this simple system can be cast into the general formulation described in Chapter 2. Two values of critical damping for the secondary system are considered: 2% and 5%. Additionally, the mass ratio between the equipment and the structure is assumed to be small such that the equipment-structure interaction can be neglected.

Figures 3.27 and 3.28 depict the maximum mean value and the maximum mean plus one standard deviation value of the absolute acceleration response of the

secondary system for a given range of periods. Figure 3.27 corresponds to the fully correlated random field case. For some periods of the substructure, the maximum mean plus one standard deviation value of the response is more than 50% of the maximum mean value of the response. For the medially correlated random field case (Figure 3.28), similar results are obtained. These levels of response uncertainty clearly indicates that the presence of uncertainties in the superstructure physical properties can markedly alter the substructure response characteristics, and in many cases these effects render a deterministic analysis unconservative for design. Finally, it is noted that the peaks of the curves in these figures correspond to the fundamental frequency of the shear beam and to some of the predominant frequencies of the base excitation.

In summary, this example problem has shown that the variability of physical properties of a system can have a strong effect on its response characteristics. Therefore, these uncertainties should be properly accounted for in the analysis of such systems.

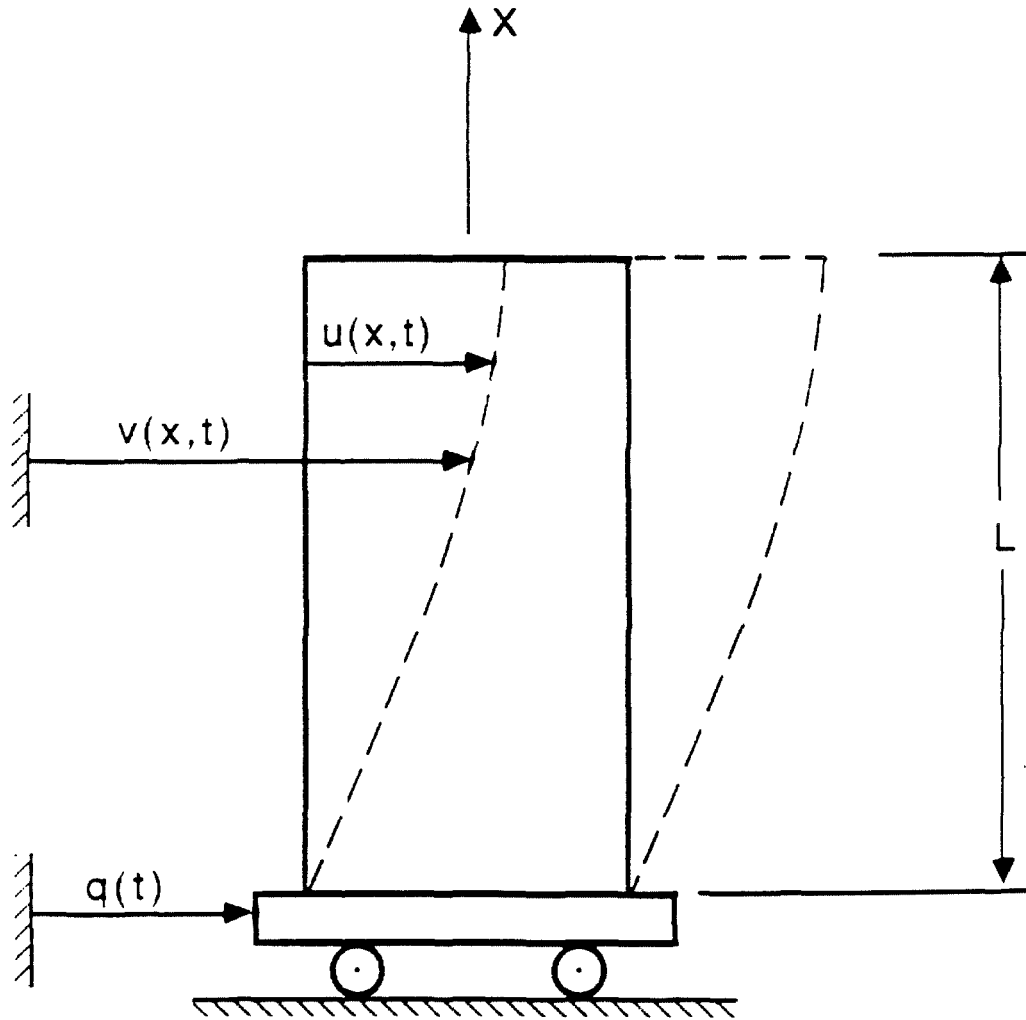


Figure 3.1: Shear beam under base excitation.

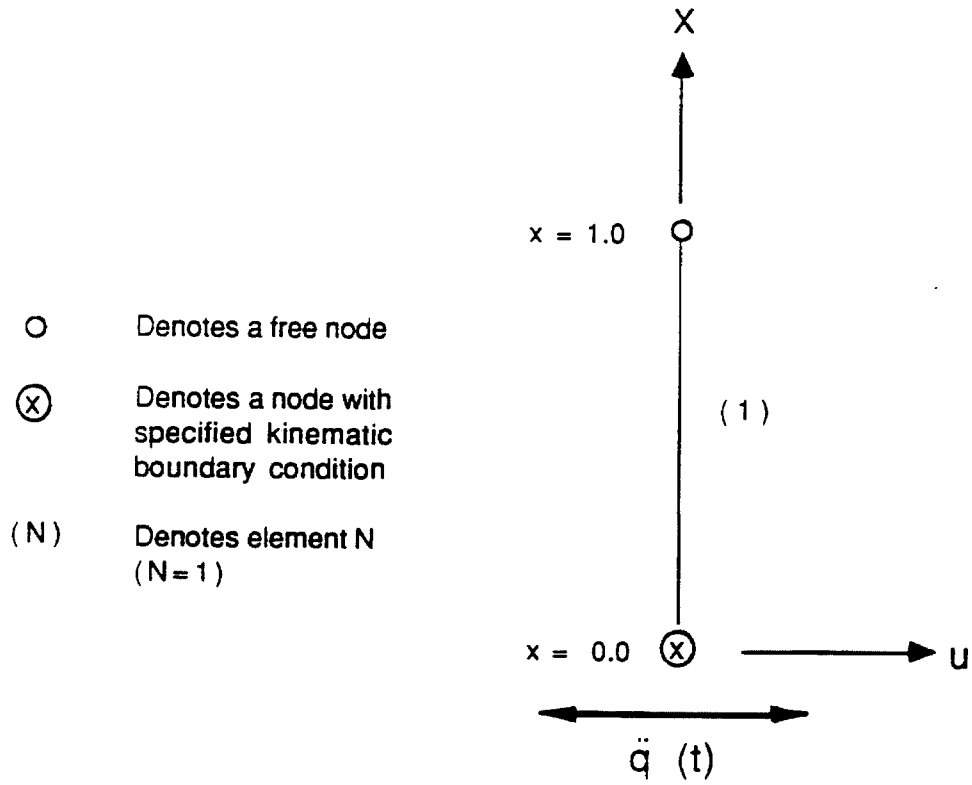
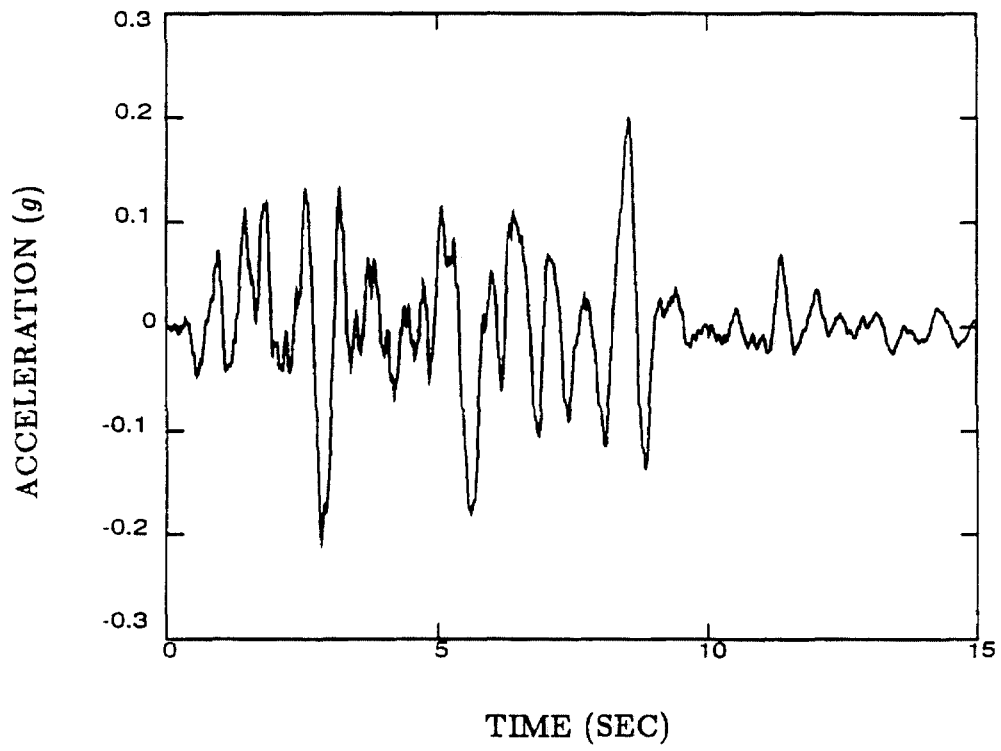
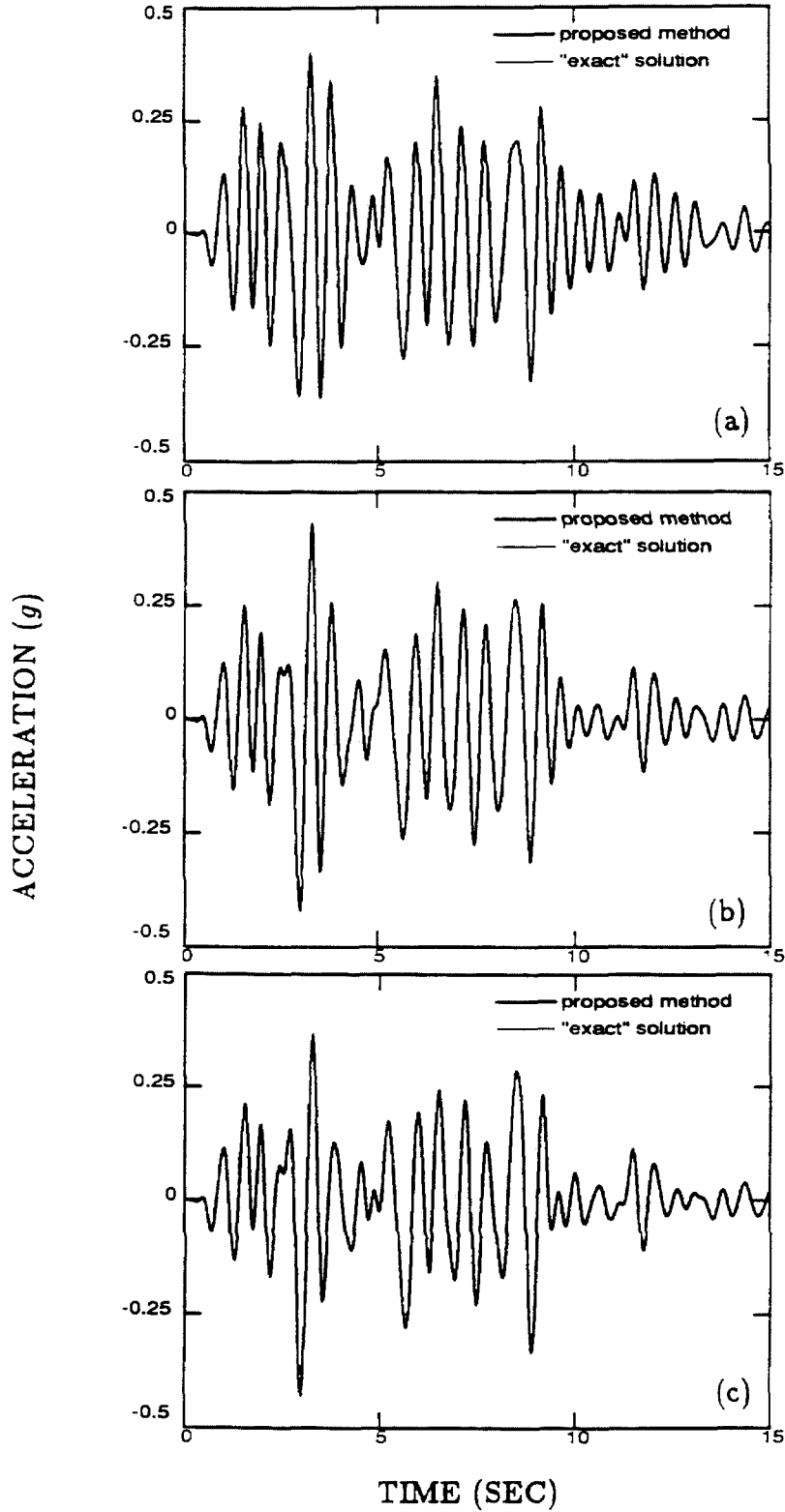


Figure 3.2: Finite element model for first validation problem.



**Figure 3.3:** Artificial base excitation for validation calculations.



**Figure 3.4:** Comparison of the mean value of the absolute acceleration response of the proposed method to that obtained by an “exact” solution. First validation problem. (a) 10% Coefficient of variation. (b) 20% Coefficient of variation. (c) 30% Coefficient of variation.

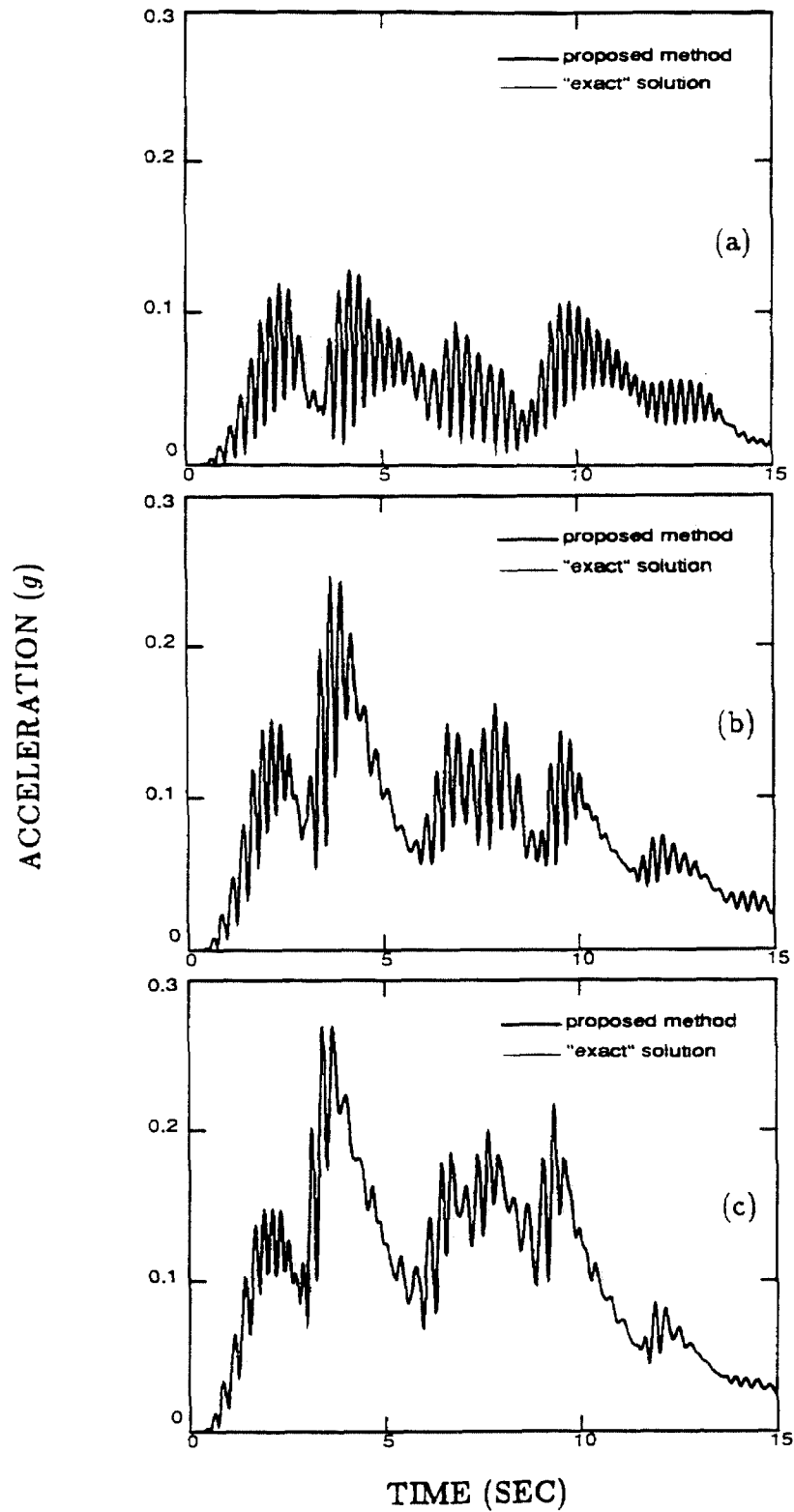
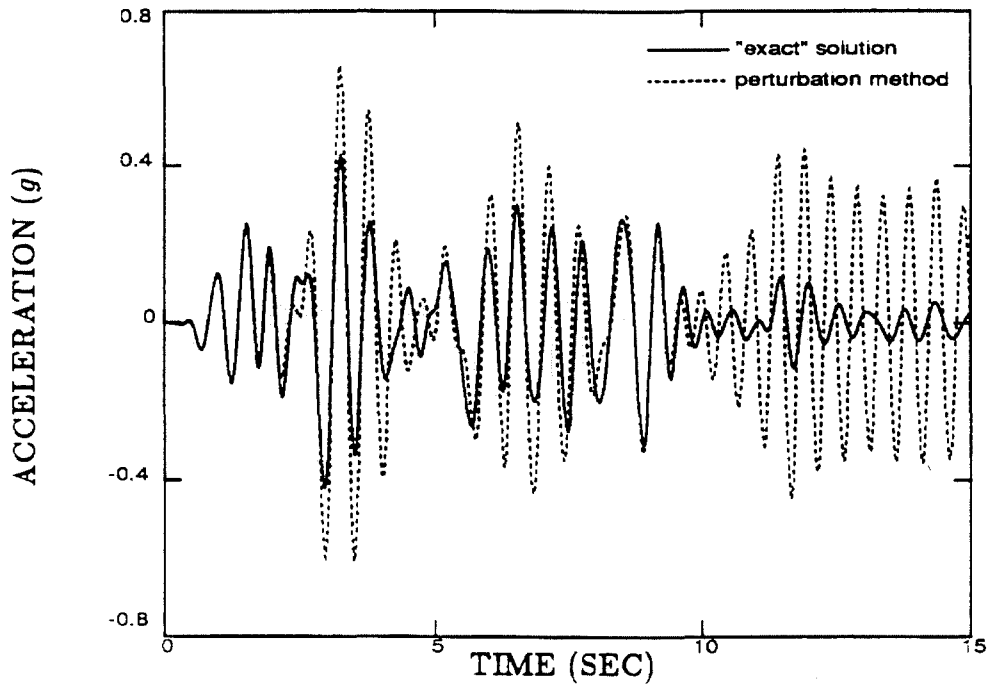


**Figure 3.5:** Comparison of the standard deviation of the absolute acceleration response of the proposed method to that obtained by an “exact” solution. First validation problem. (a) 10% Coefficient of variation. (b) 20% Coefficient of variation. (c) 30% Coefficient of variation.

MEAN VALUE



STANDARD DEVIATION

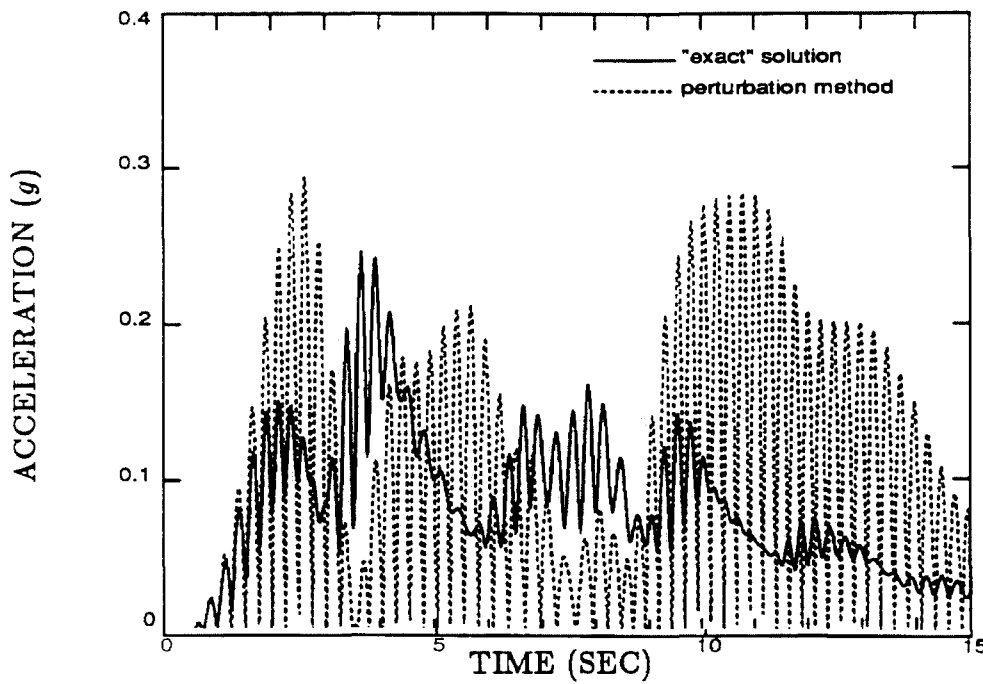
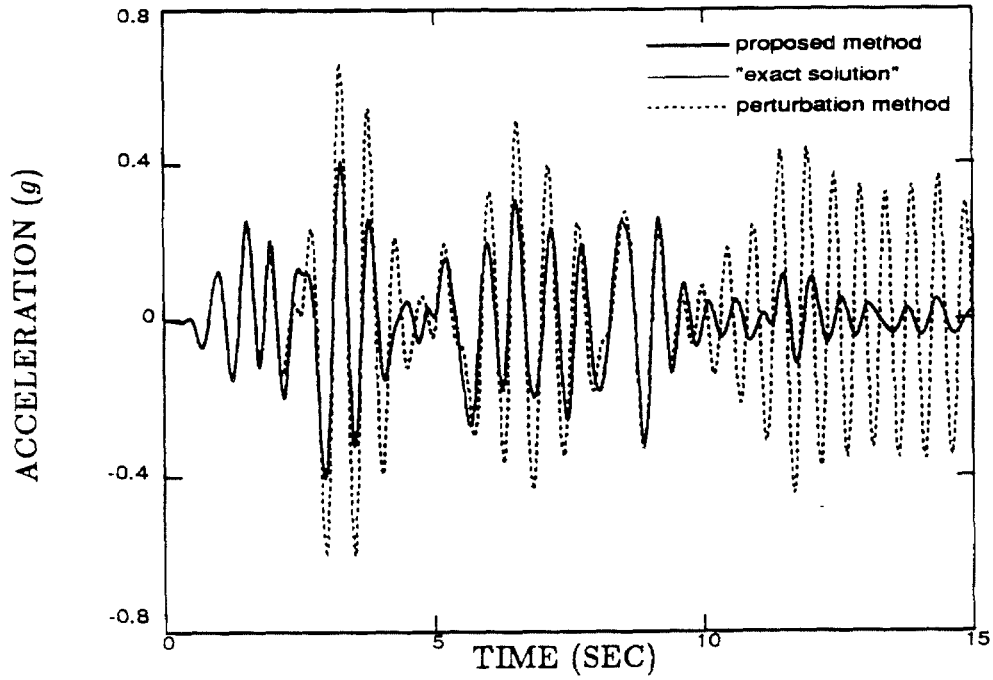


Figure 3.6: Comparison of the mean value and the standard deviation of the absolute acceleration response of the "exact" solution to those obtained by the perturbation method. First validation problem.

MEAN VALUE



STANDARD DEVIATION

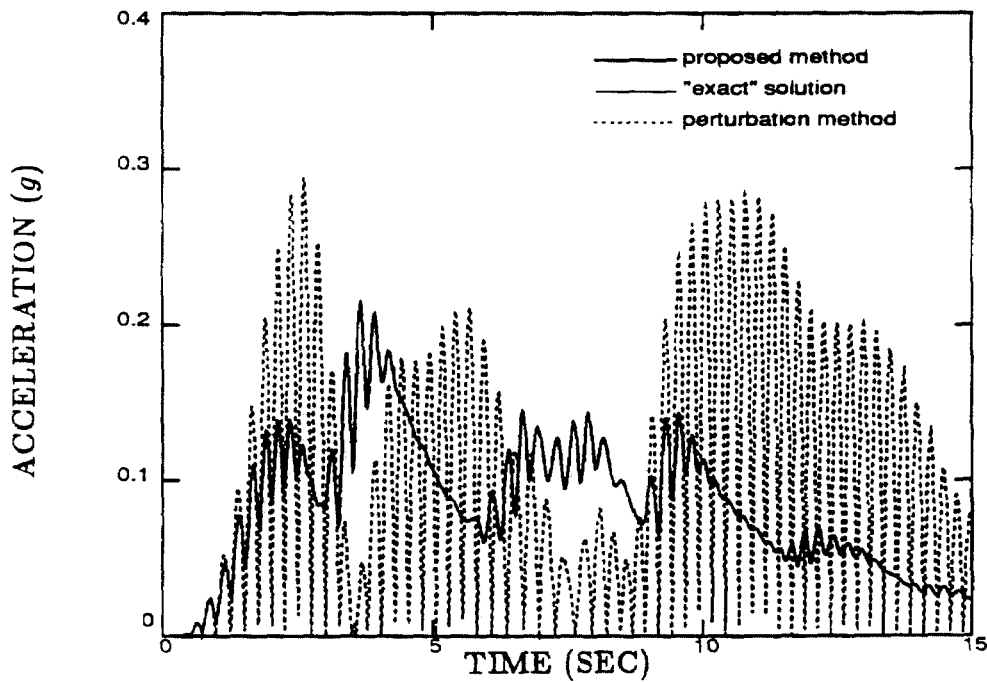


Figure 3.7: Comparison of the results of the proposed method to those obtained by an "exact" solution and by the perturbation method. Case of a Gaussian distribution of the shear stiffness parameter with a 20% coefficient of variation. First validation problem.

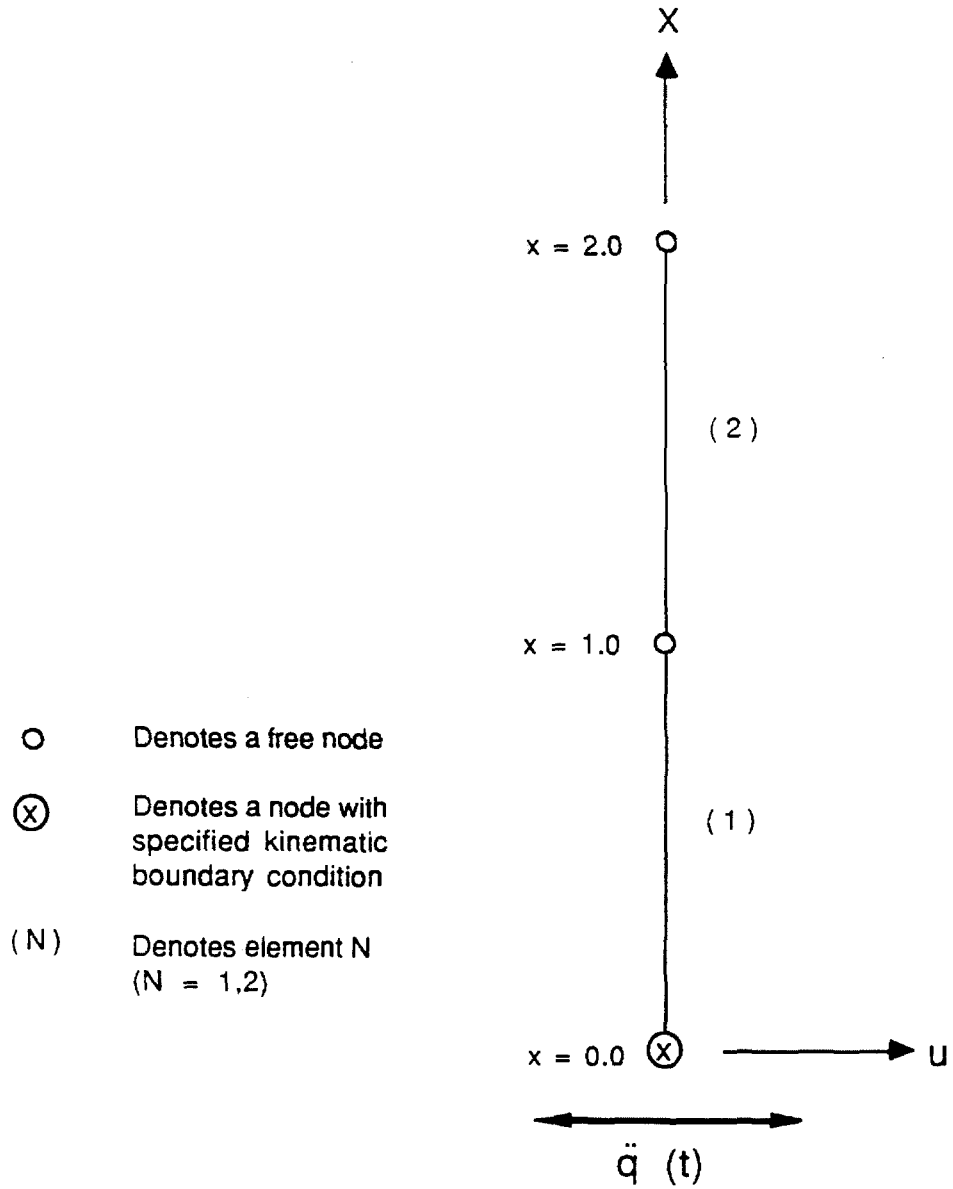


Figure 3.8: Finite element model for second validation problem.

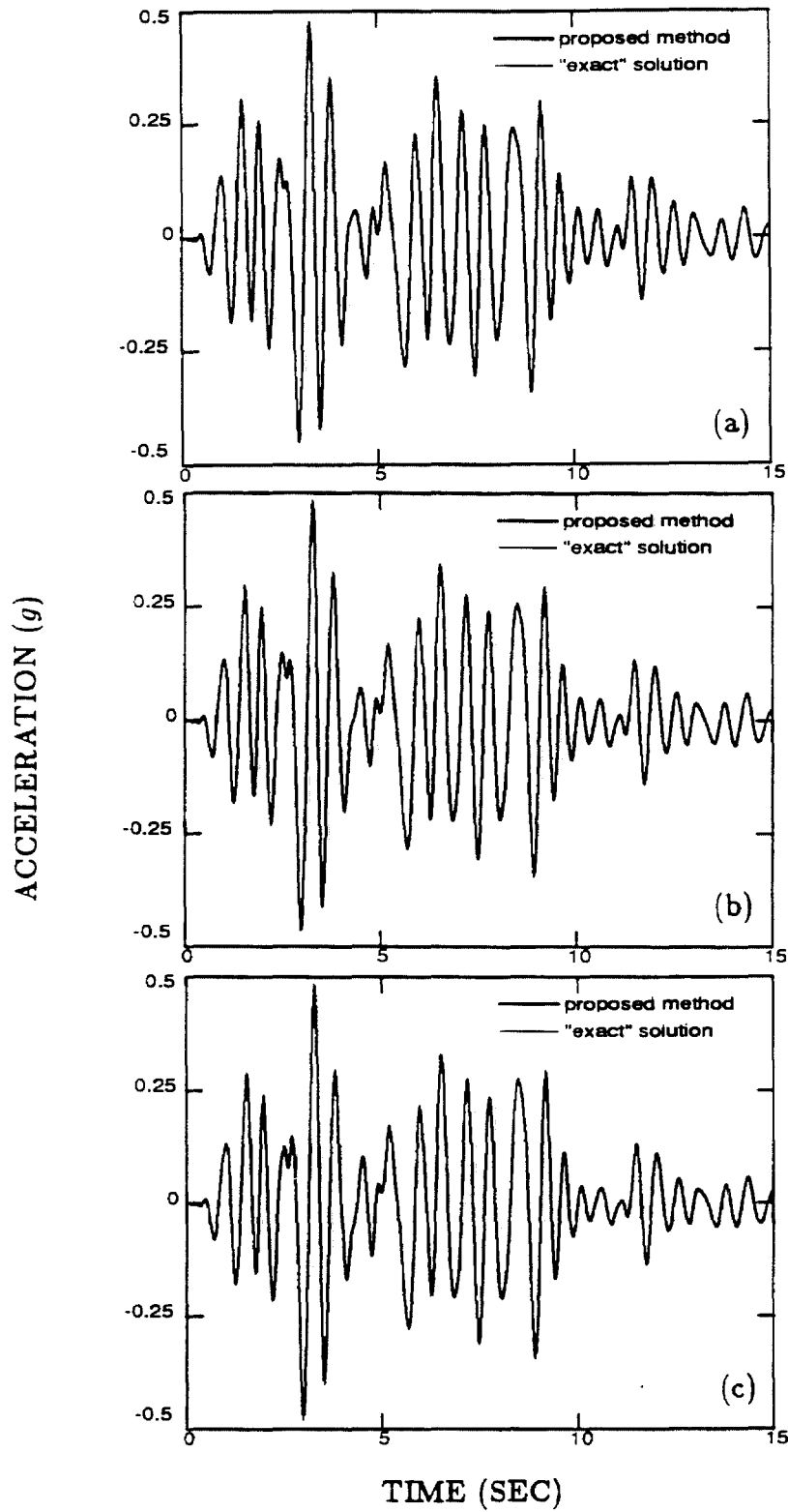
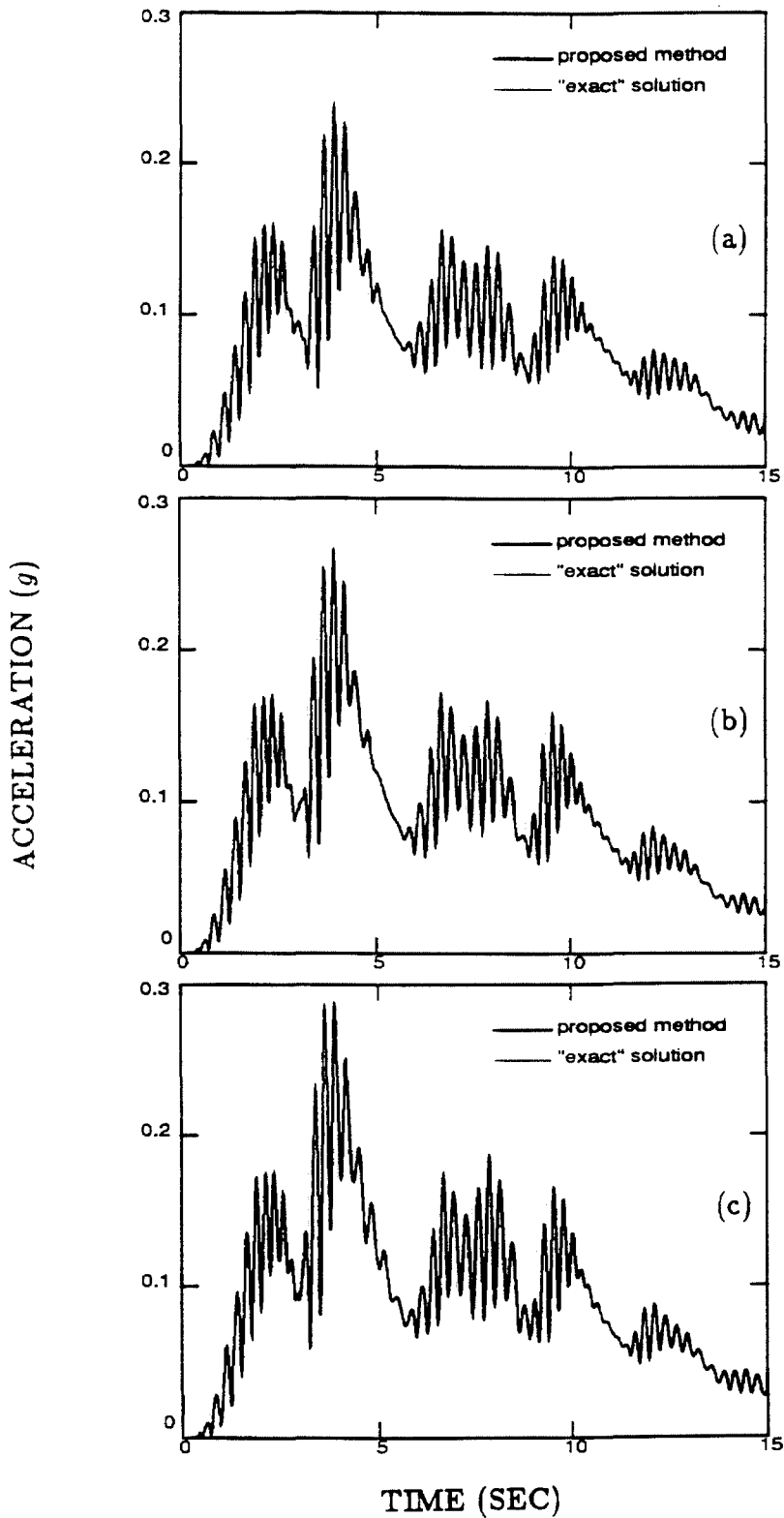


Figure 3.9: Comparison of the mean value of the absolute acceleration response of the proposed method to that obtained by an "exact" solution. Second validation problem. (a)  $\rho = 0.0$ . (b)  $\rho = 0.5$ . (c)  $\rho = 1.0$ .



**Figure 3.10:** Comparison of the standard deviation of the absolute acceleration response of the proposed method to that obtained by an "exact" solution. Second validation problem. (a)  $\rho = 0.0$ . (b)  $\rho = 0.5$ . (c)  $\rho = 1.0$ .

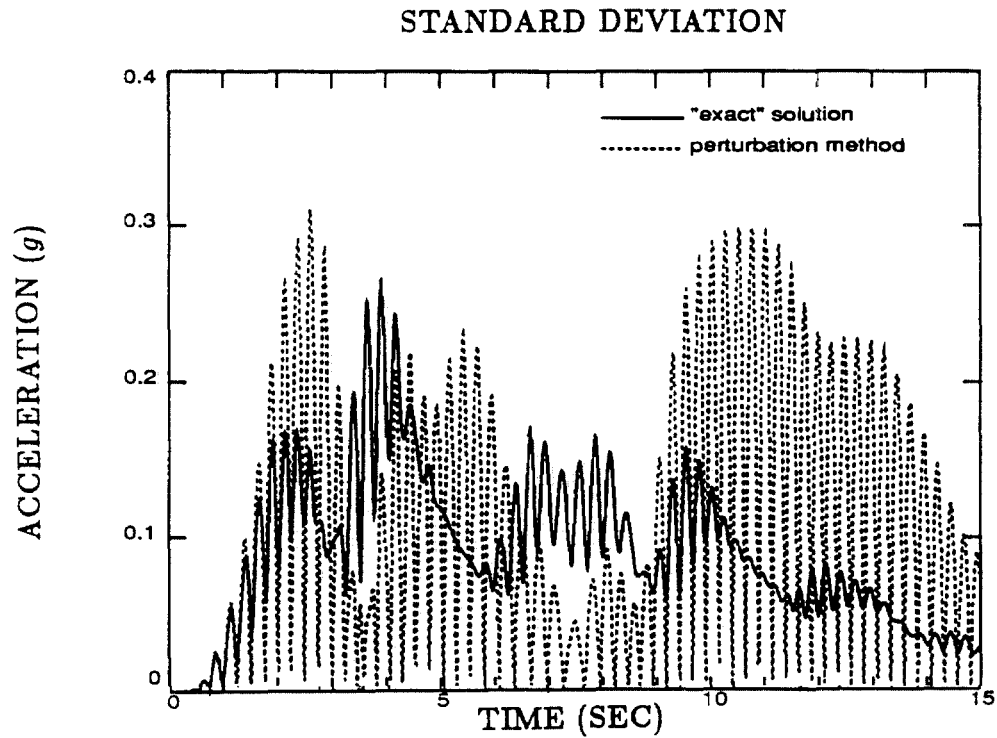
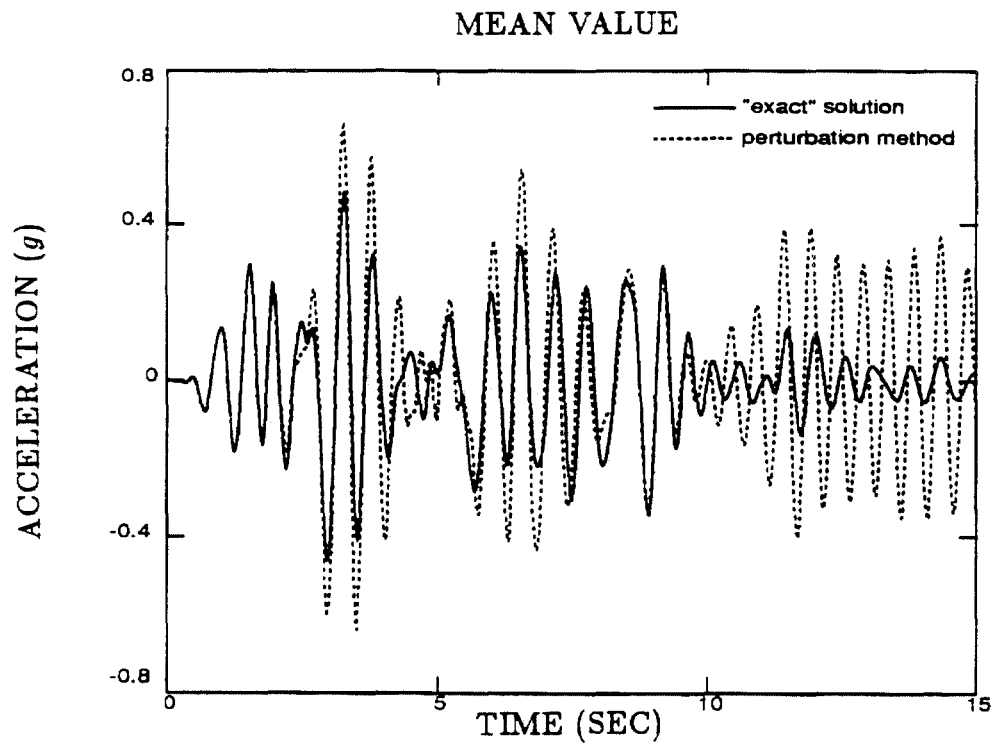
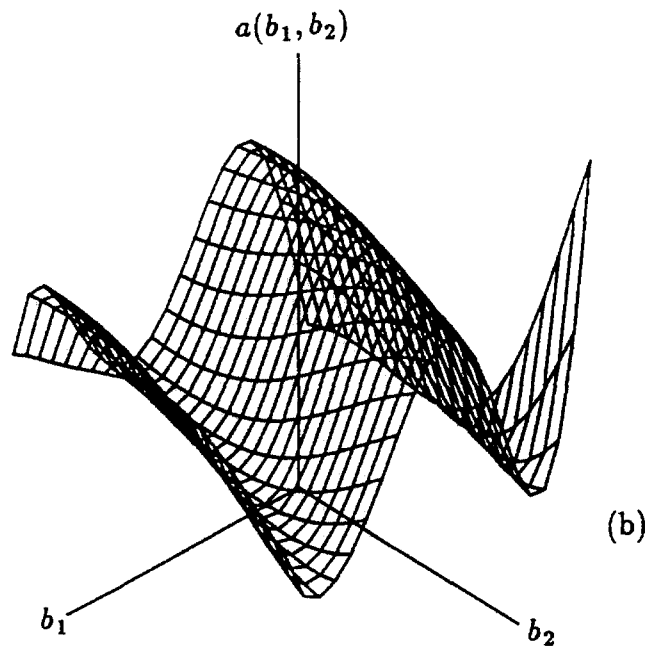
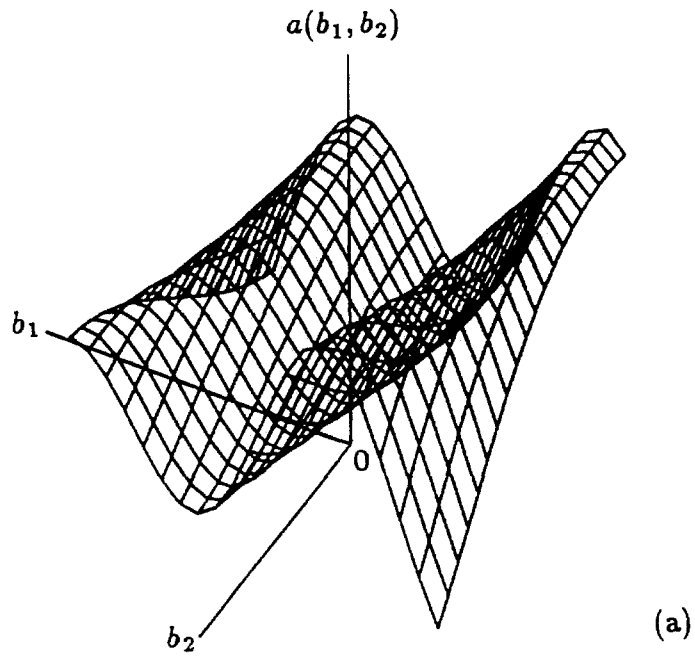


Figure 3.11: Comparison of the mean value and the standard deviation of the absolute acceleration response of the "exact" solution to those obtained by the perturbation method. Second validation problem,  $\rho = 0.5$ .

Absolute acceleration response as a function of the random variables  $b_1$  and  $b_2$



**Figure 3.12:** Absolute acceleration response as a function of the two random variables that describe the random field. (a) Response at the time in which the mean value response is maximum. (b) Response at the time in which the standard deviation response is maximum.

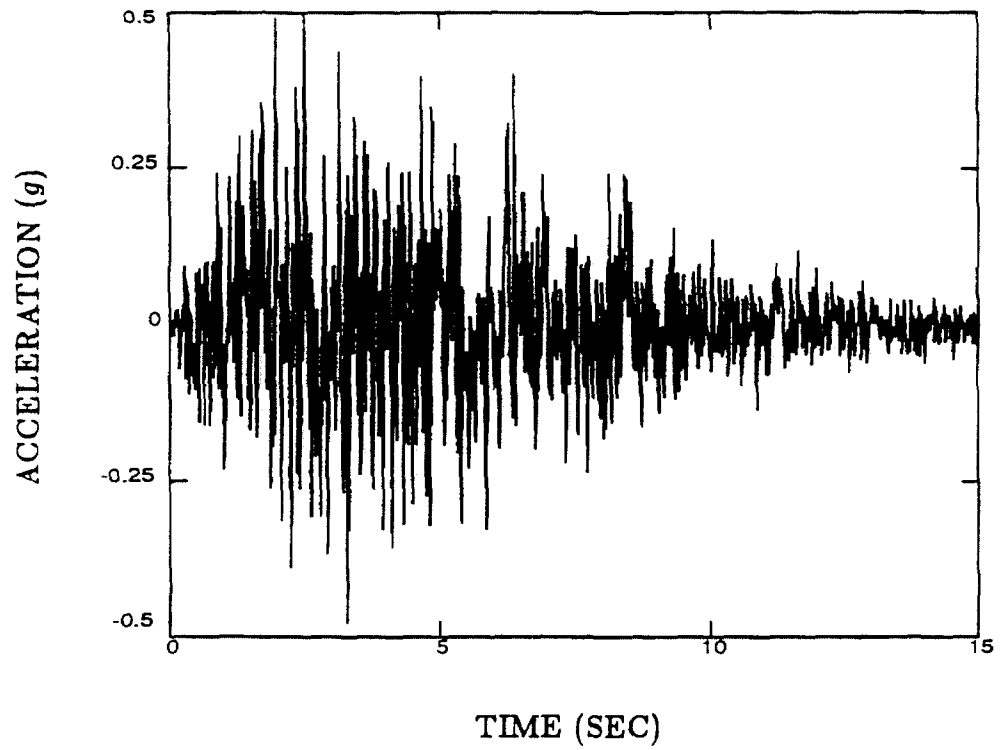


Figure 3.13: Artificial base excitation for Case I of the example problem.

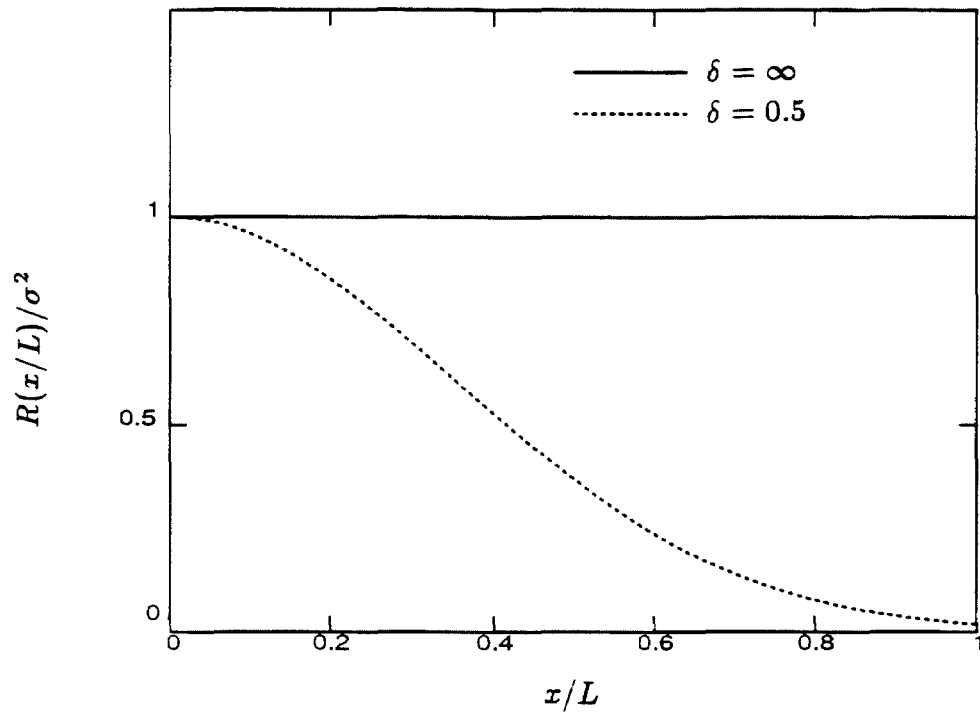
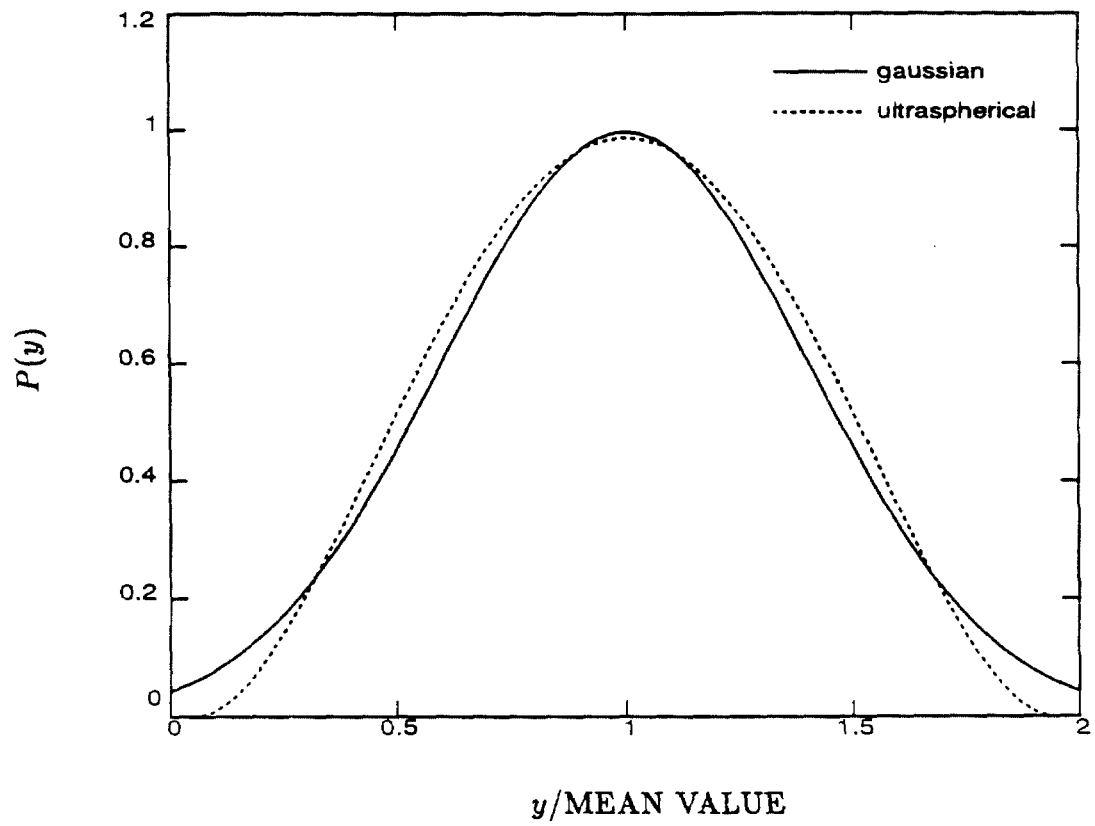


Figure 3.14: Covariance functions.



**Figure 3.15:** Gaussian and Ultraspherical distributions with a 40% coefficient of variation.

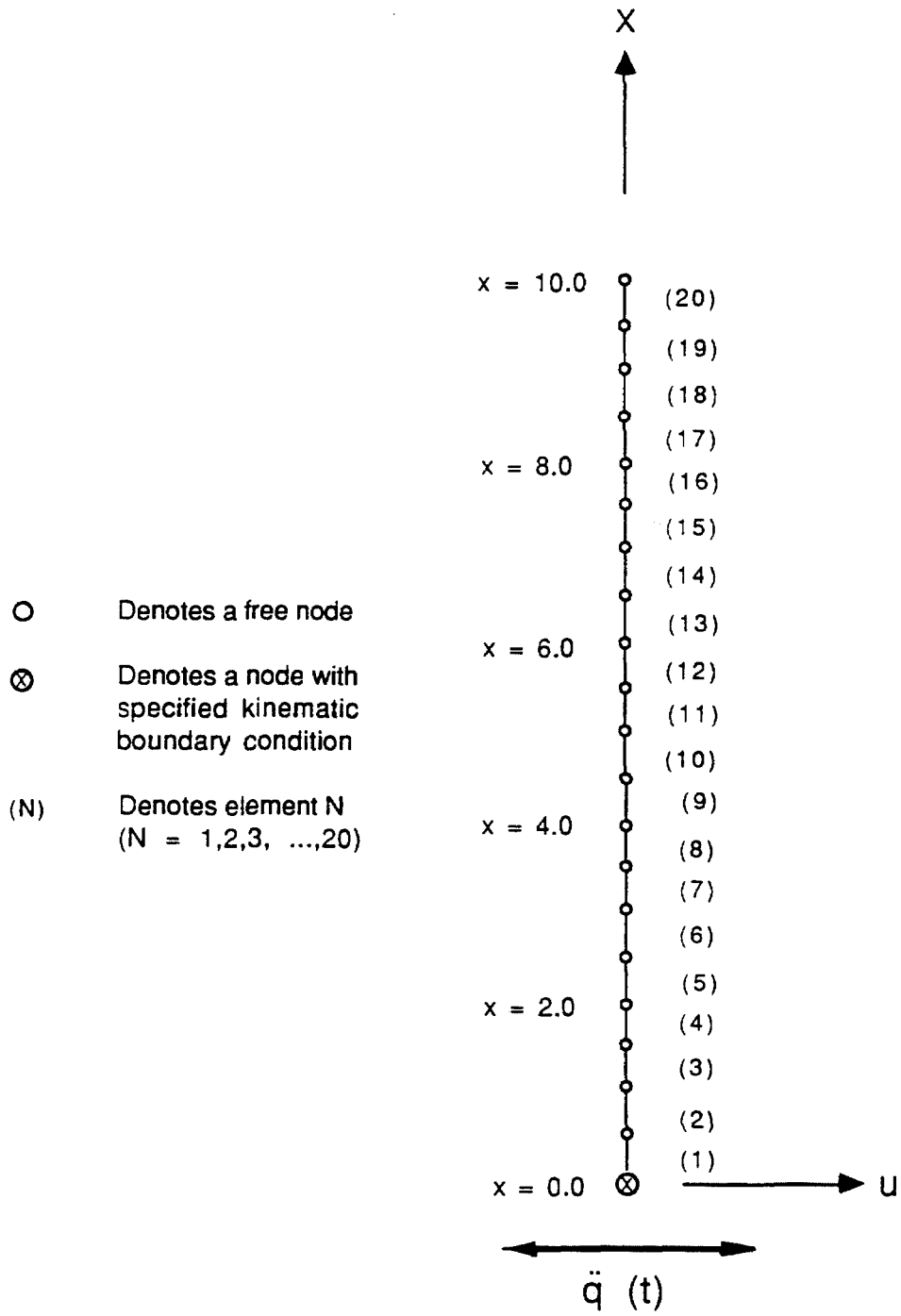
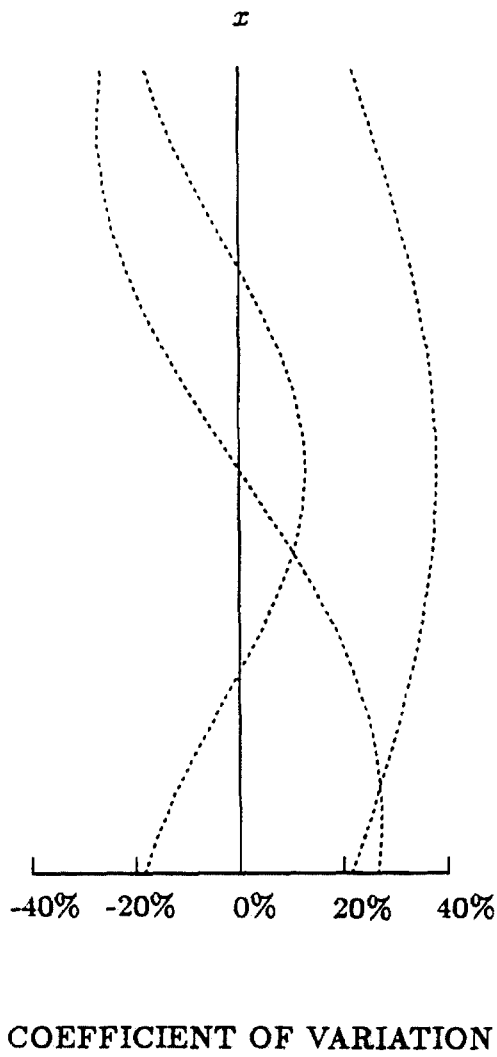
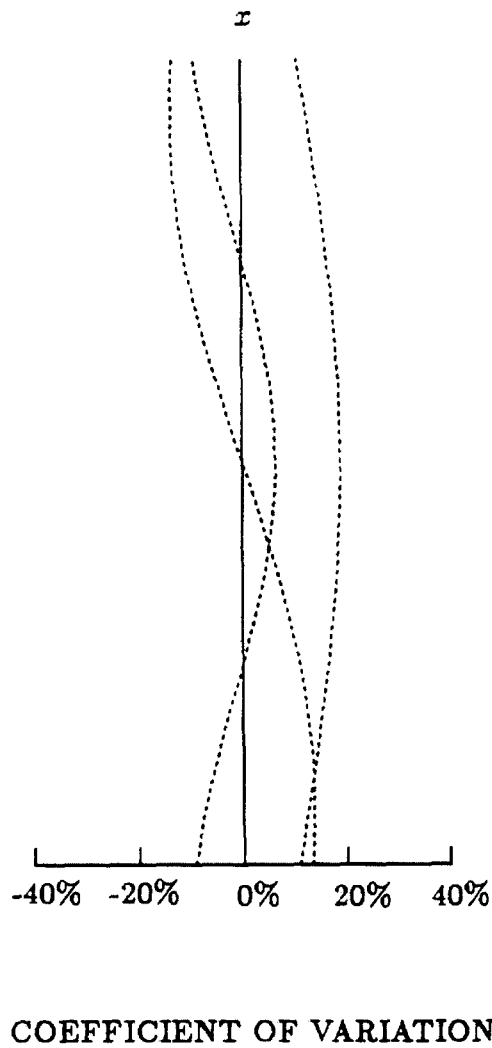


Figure 3.16: Finite element mesh used for the shear beam in example problem.



**Figure 3.17:** Coefficient of variation along the beam axis of the three most significant pairs of eigenvectors-eigenvalues of the random field covariance matrix. Case I of the example problem.



**Figure 3.18:** Coefficient of variation along the beam axis of the three most significant pairs of eigenvectors-eigenvalues of the random field covariance matrix. Case II of the example problem.

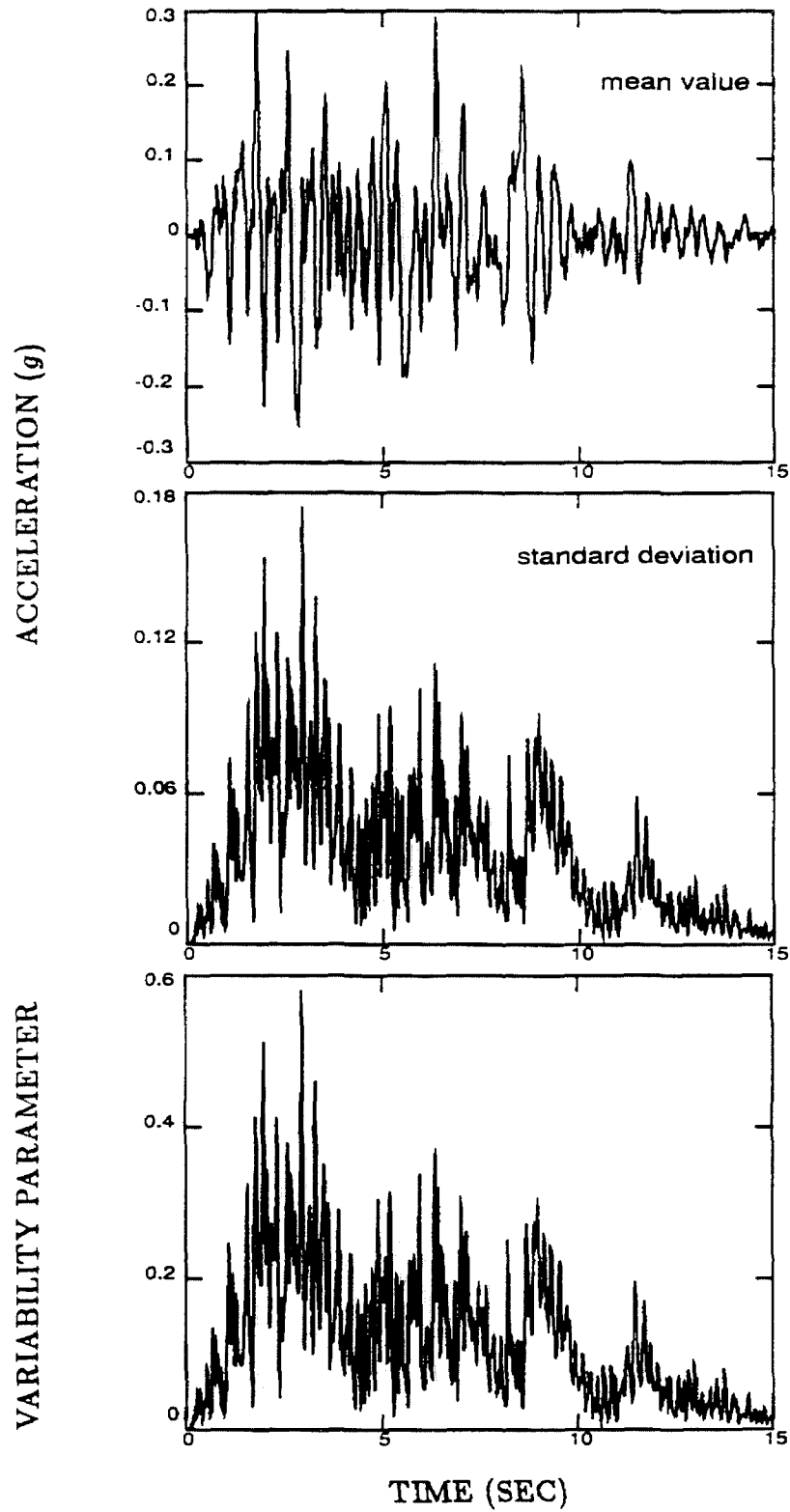


Figure 3.19: Second moment characterization of the absolute acceleration response. Case I of the example problem,  $\delta = \infty$ .

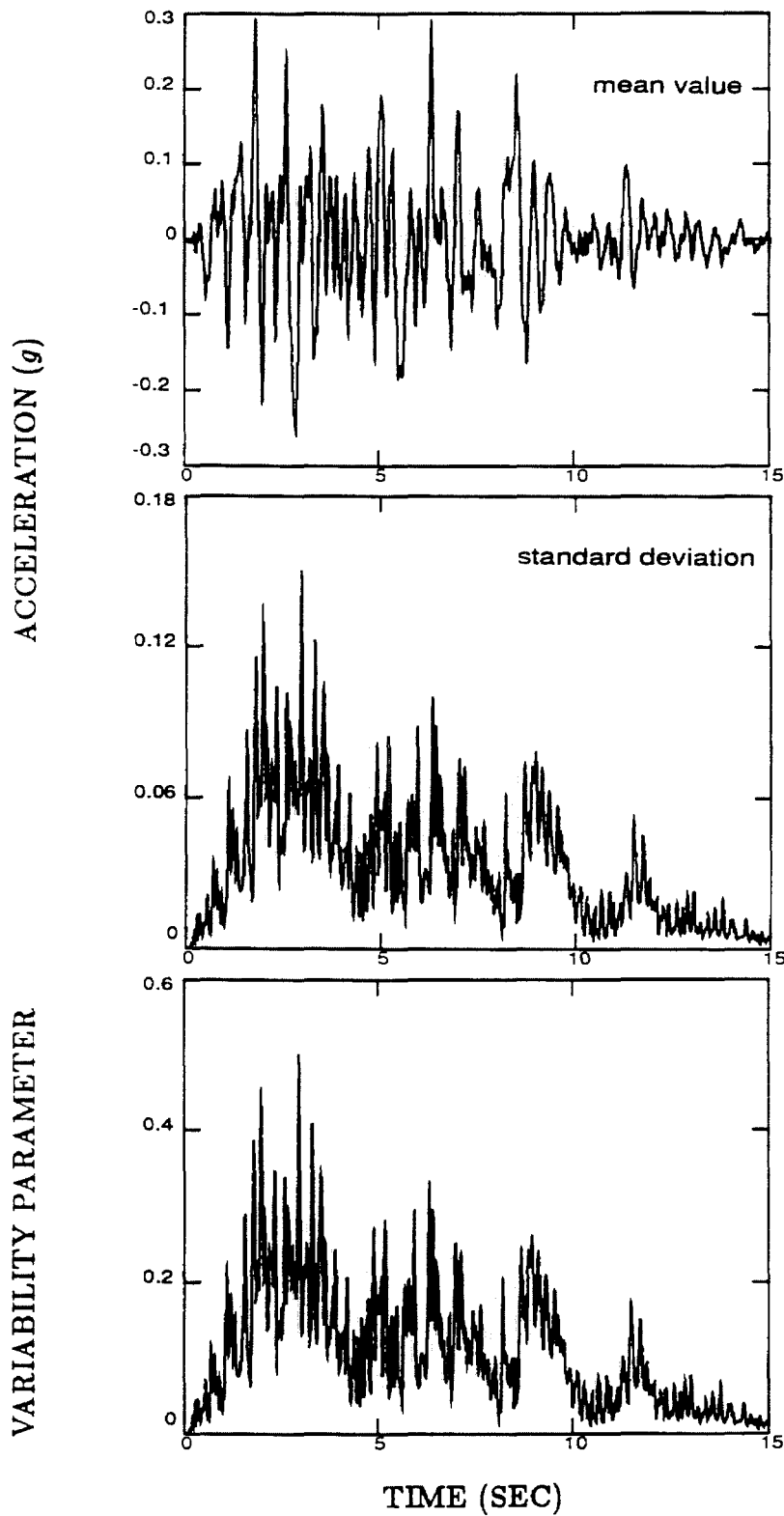
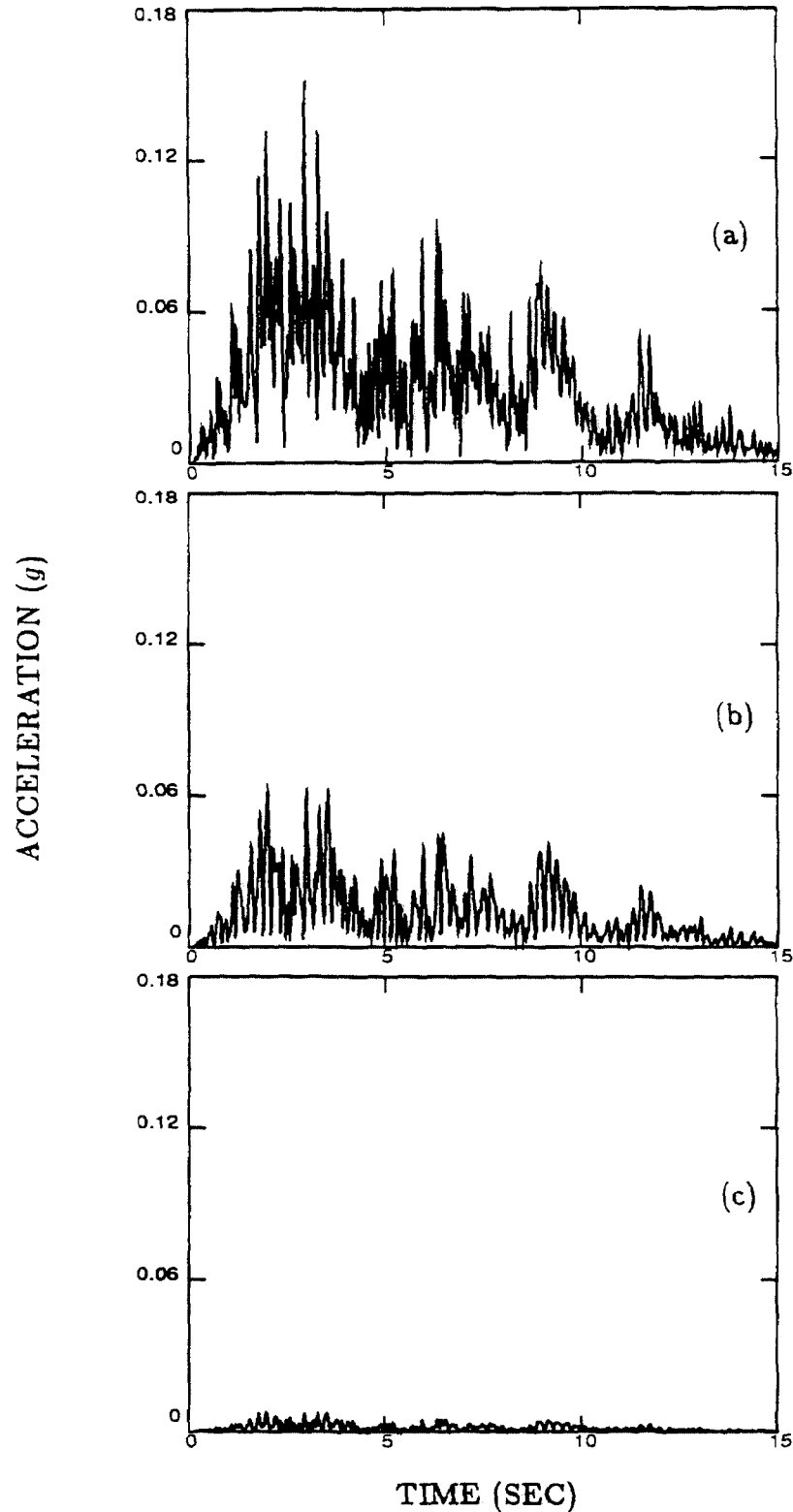
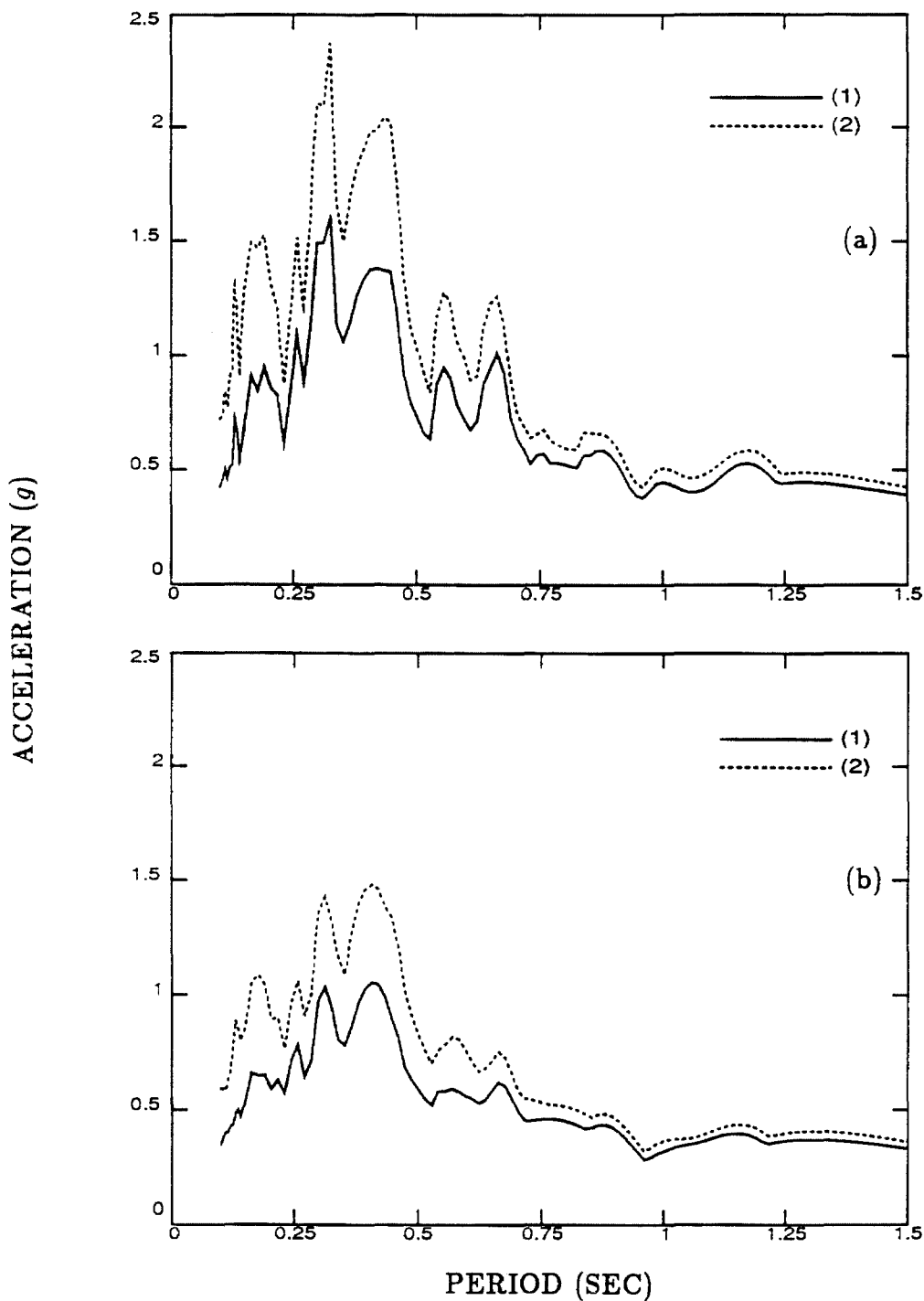


Figure 3.20: Second moment characterization of the absolute acceleration response. Case I of the example problem,  $\delta = 0.5$ .



**Figure 3.21:** Standard deviation of the response due to each one of the three most significant pairs of eigenvectors-eigenvalues of the random field covariance matrix. Case I of the example problem,  $\delta = 0.5$ . (a) First random variable. (b) Second random variable. (c) Third random variable.



**Figure 3.22:** Effects of the uncertainties in the parameters of the soil column on the response of a single-degree-of-freedom system. (1) Maximum mean value of the response . (2) Maximum mean plus one standard deviation value of the response. Case I of the example problem,  $\delta = \infty$ . (a) 2% of critical damping. (b) 5% of critical damping.

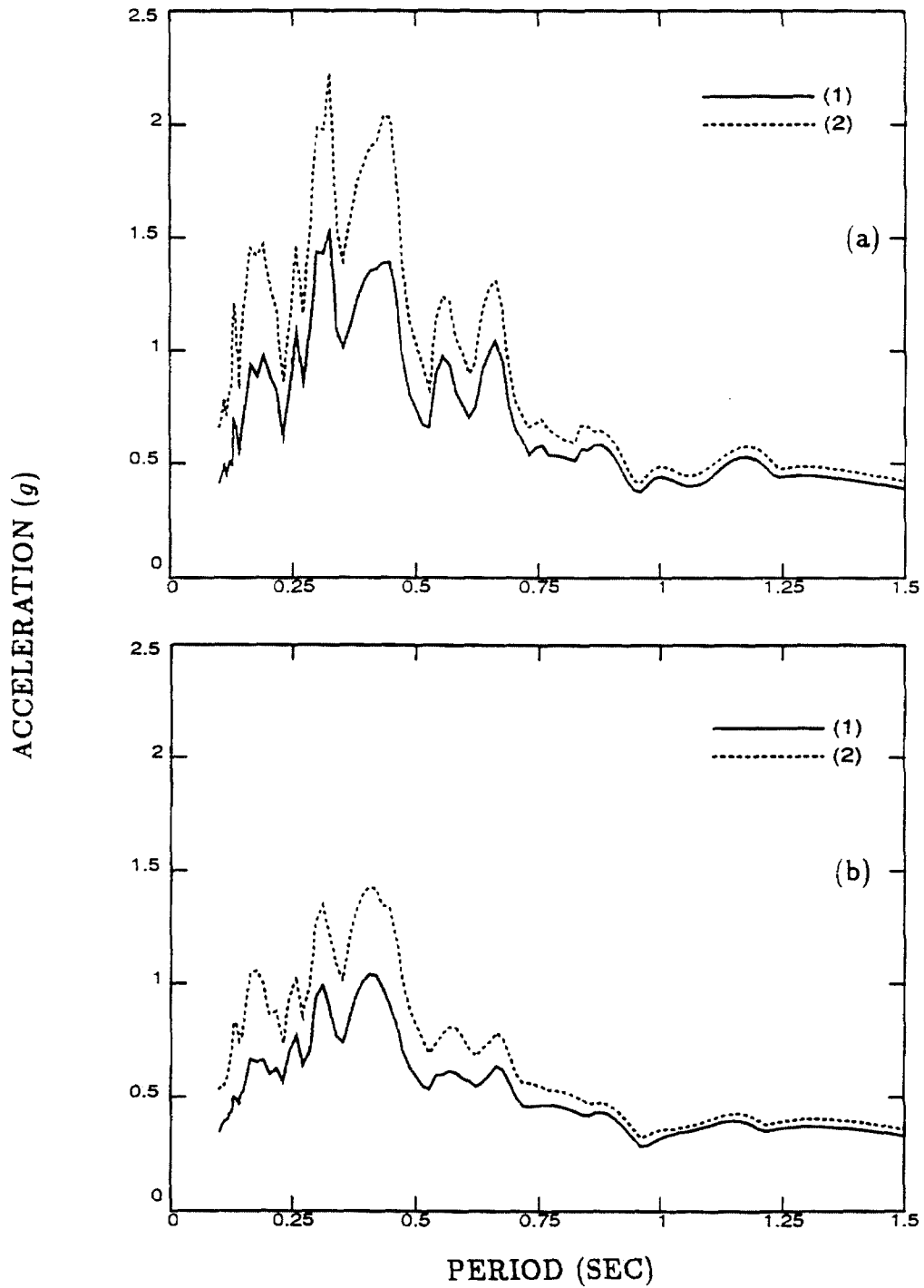


**Figure 3.23:** Effects of the uncertainties in the parameters of the soil column on the response of a single-degree-of-freedom system. (1) Maximum mean value of the response. (2) Maximum mean plus one standard deviation value of the response. Case I of the example problem,  $\delta = 0.5$ . (a) 2% of critical damping. (b) 5% of critical damping.

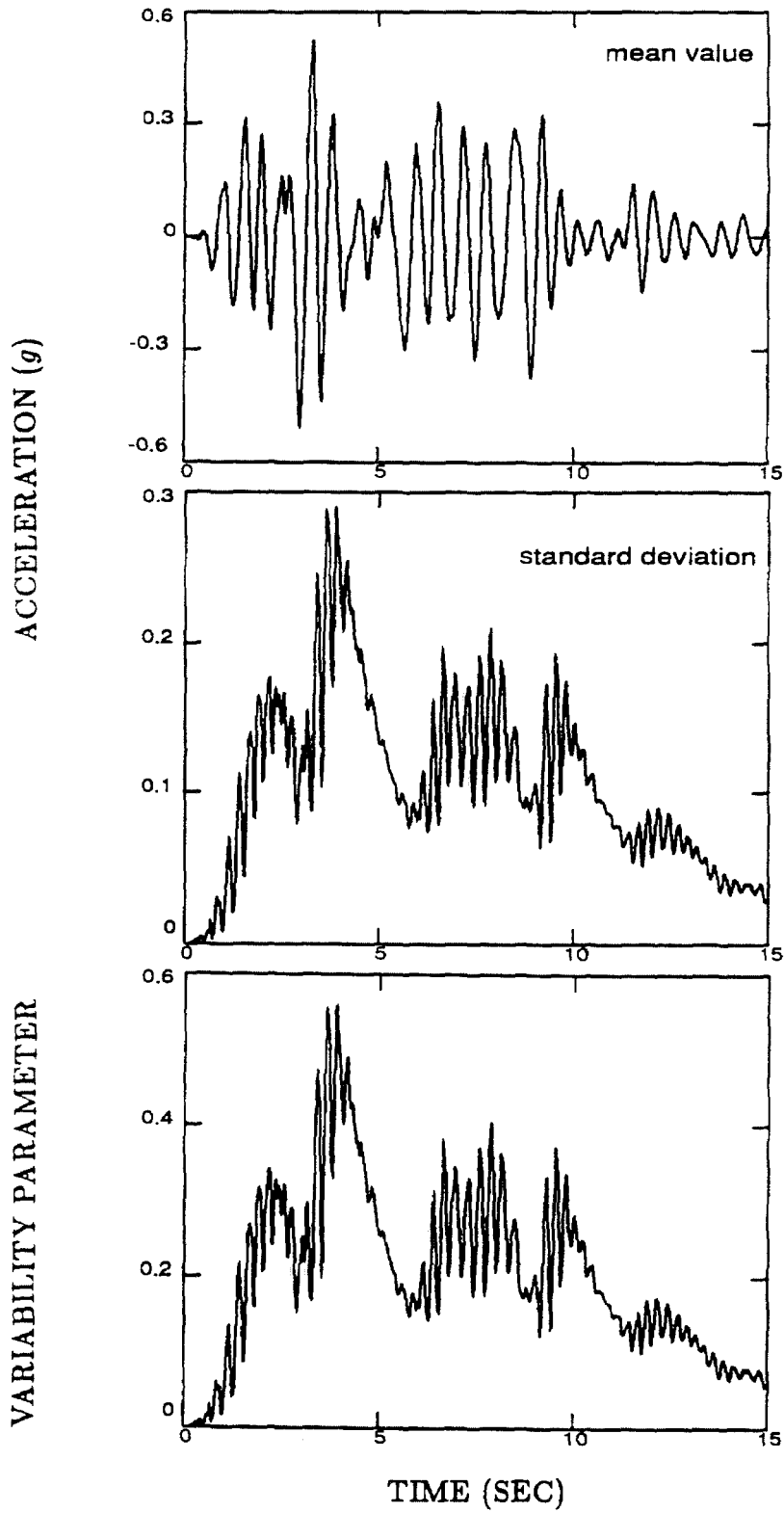


Figure 3.24: Second moment characterization of the absolute acceleration response. Case II of the example problem,  $\delta = \infty$ .

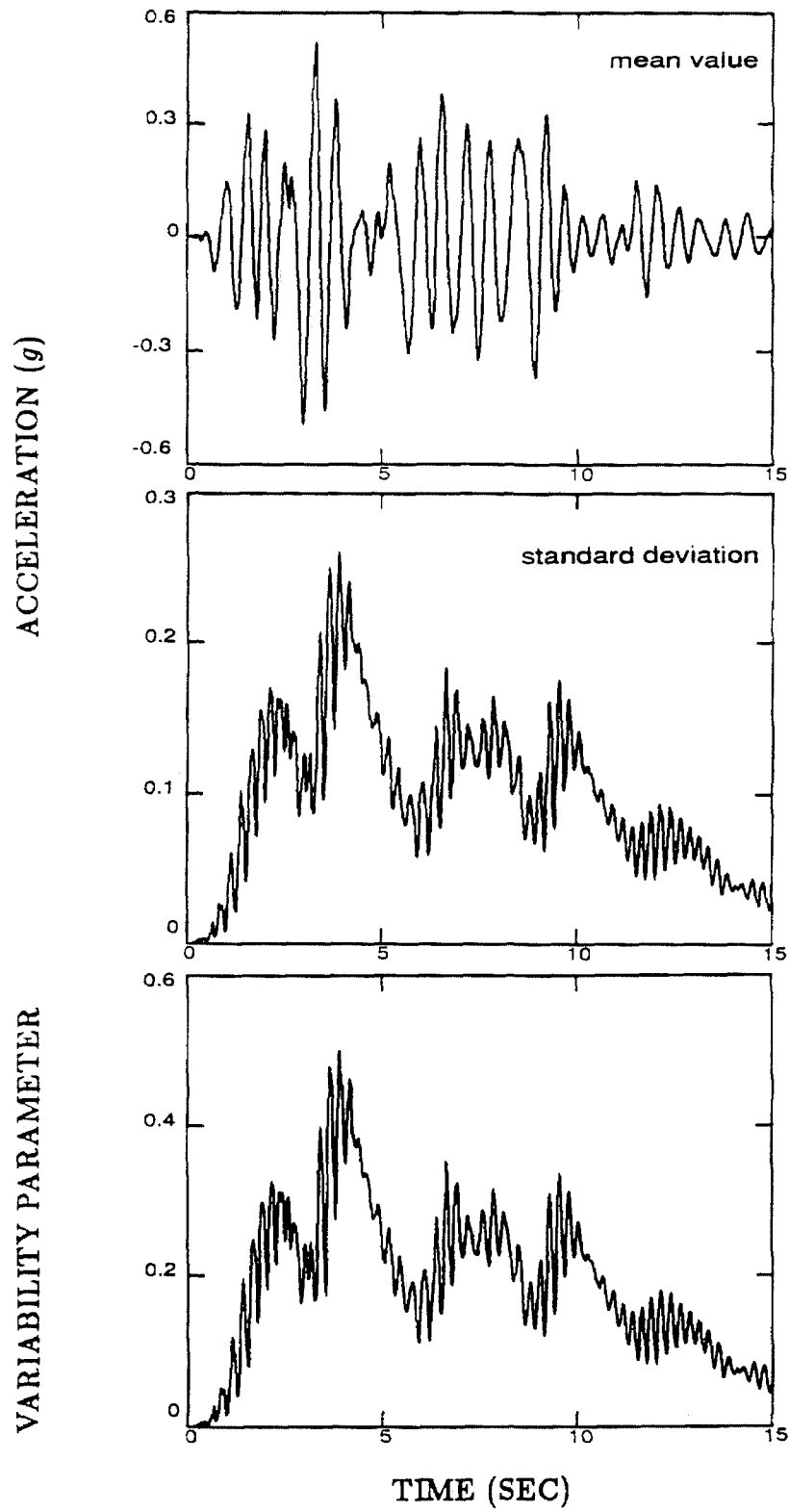
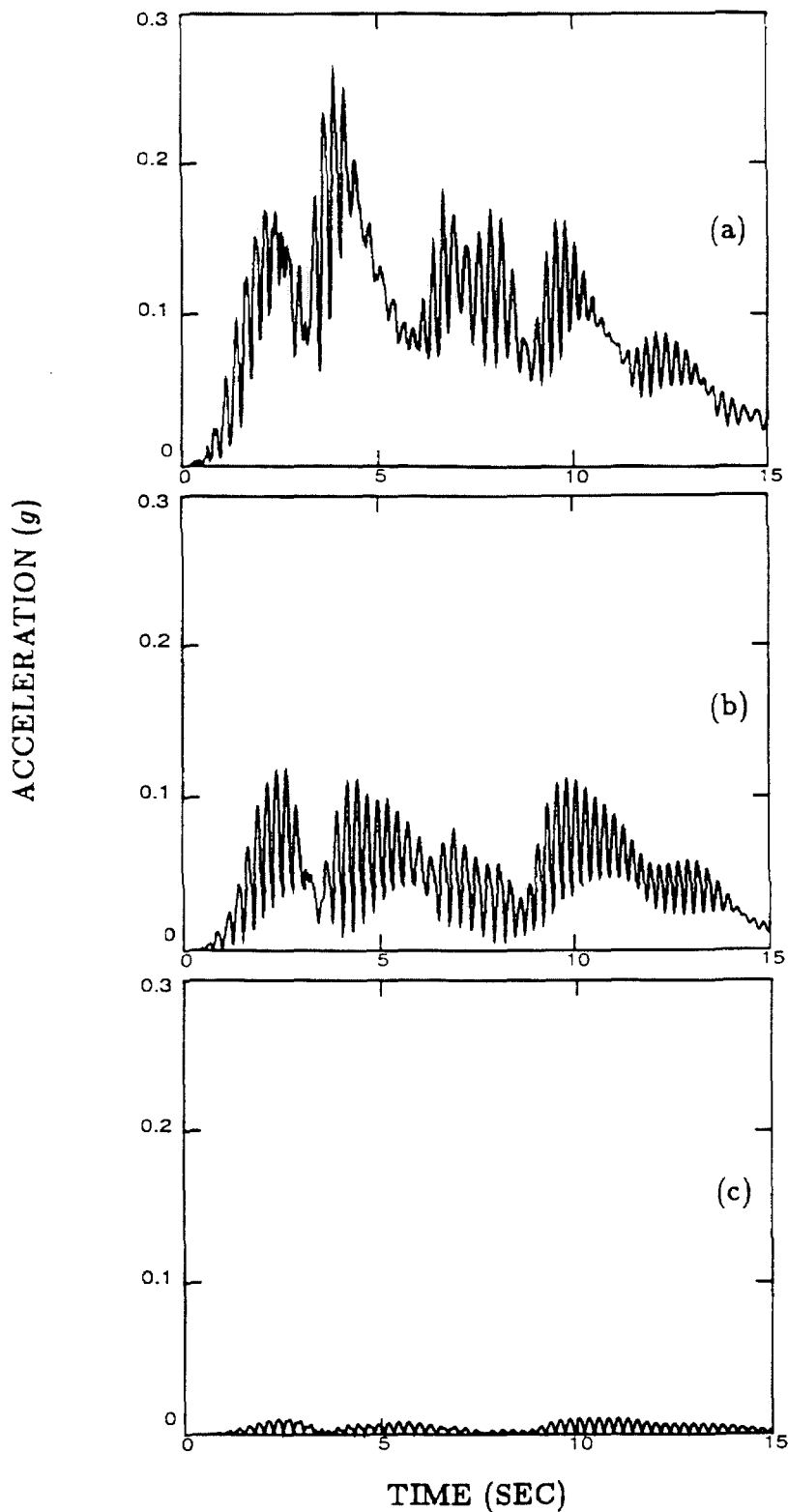
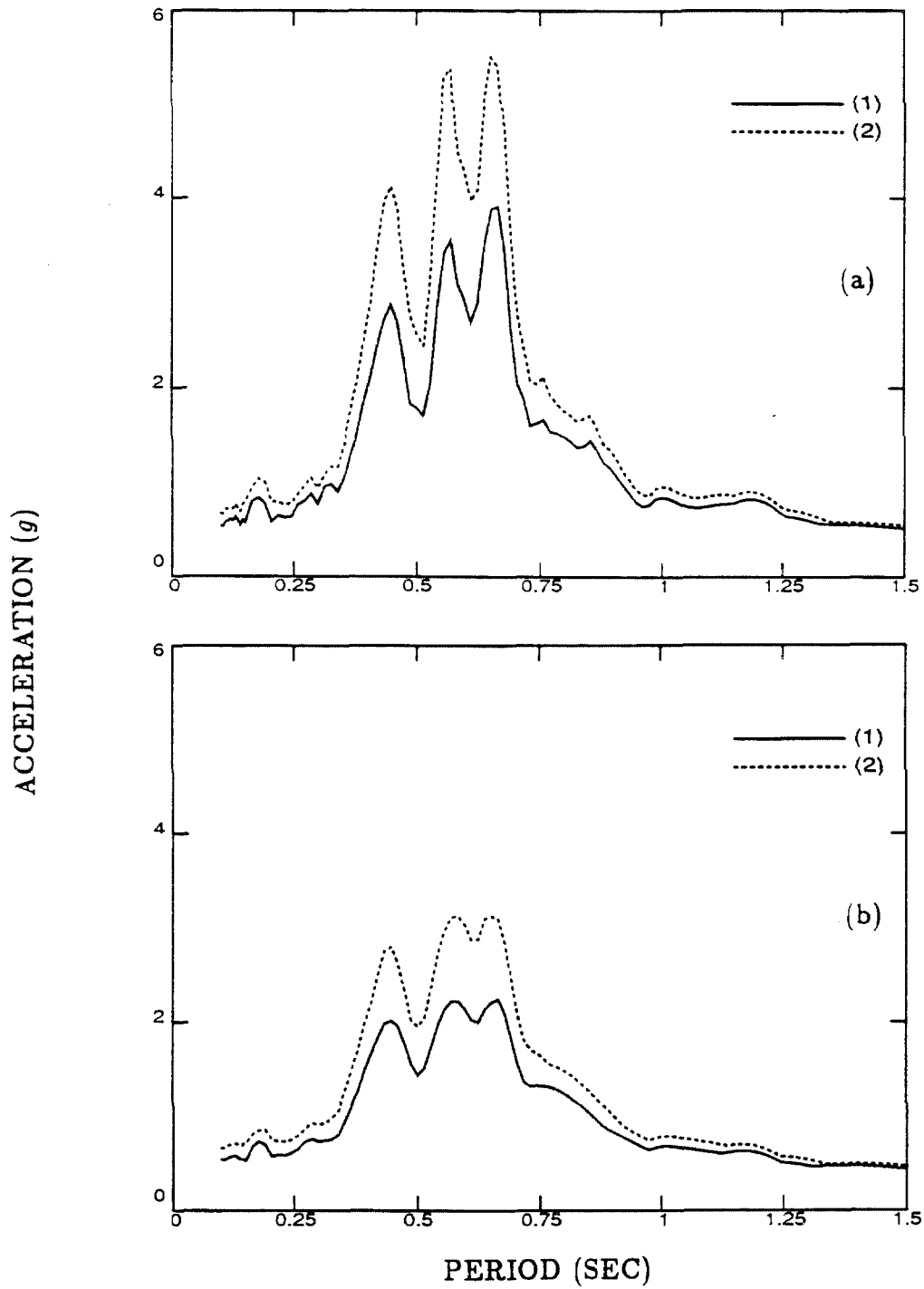


Figure 3.25: Second moment characterization of the absolute acceleration response. Case II of the example problem,  $\delta = 0.5$ .



**Figure 3.26:** Standard deviation of the response due to each one of the three most significant pairs of eigenvectors-eigenvalues of the random field covariance matrix. Case II of the example problem,  $\delta = 0.5$ . (a) First random variable. (b) Second random variable. (c) Third random variable.



**Figure 3.27:** Effects of the uncertainties in the parameters of the shear beam on the response of a substructure. (1) Maximum mean value of the response. (2) Maximum mean plus one standard deviation value of the response. Case II of the example problem,  $\delta = \infty$ . (a) 2% of critical damping. (b) 5% of critical damping.

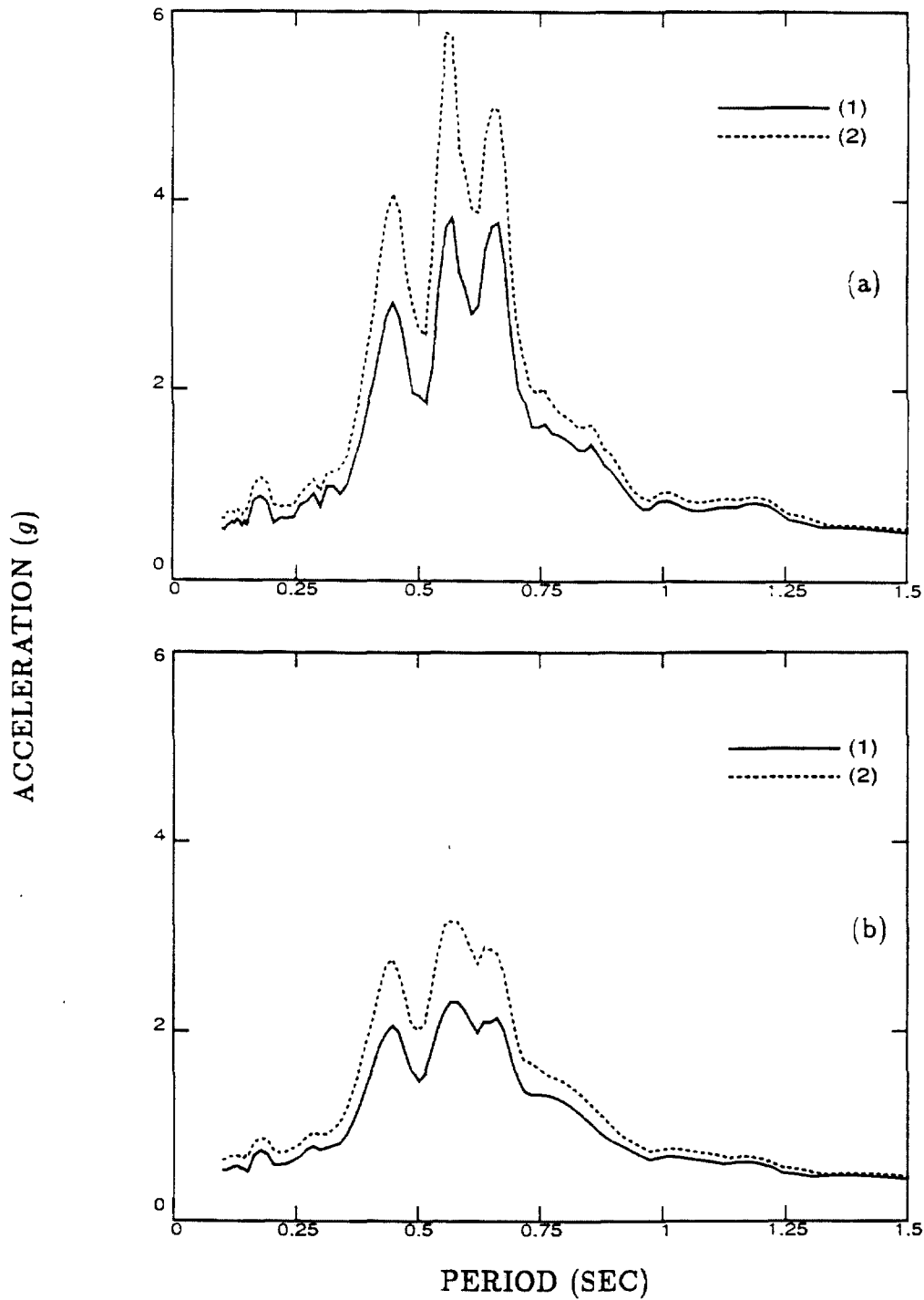


**Figure 3.28:** Effects of the uncertainties in the parameters of the shear beam on the response of a substructure. (1) Maximum mean value of the response. (2) Maximum mean plus one standard deviation value of the response. Case II of the example problem,  $\delta = 0.5$ . (a) 2% of critical damping. (b) 5% of critical damping.

## Chapter 4

### Formulation of the Random Finite Element Method for Stochastic Excitation

#### 4.1 Introduction

In this chapter, the formulation of the random finite element method described in Chapter 2 is extended to include cases where the excitation is random in time. In the previous formulation, the external load was permitted to have spatial random properties but was assumed to be deterministic in time. An additional source of uncertainty is the specification of the external load in time. This uncertainty often arises when the loads result from a physical mechanism so complex that it is best modeled as a random process in time, or a stochastic process.

The classical deterministic approach to deal with stochastic excitation is to assume some average or best estimate functions of time for use in the analysis. At best, a parameter study is conducted to examine the sensitivity of the analysis results to variations in the time history of the applied loading. In contrast, a random vibration analysis acknowledges and quantifies these uncertainties, and thereby provides more useful information to the engineer. The analysis can provide not just one solution, but a spectrum of solutions and their relative likelihoods of occurrence.

Many real excitations result from the combination of a number of different physical processes. According to the central limit theorem of probability theory, under

certain conditions, the sum of a large number of independent statistical distributions converges to a Gaussian distribution. Hence, a Gaussian time dependence for the loading seems like a good first approximation. In addition, for many engineering problems, particularly those where the response is narrow banded, a reasonable starting point is to consider the case of white noise excitation with zero mean, where the power spectrum is uniform across the entire frequency band.

Finally, many processes of engineering relevance are of sufficiently short duration that they must be considered transient, or nonstationary. In order to consider the transient nature of the excitation, the Gaussian white noise process is modulated by a deterministic function of time. Therefore, the applied forcing function will be modeled as a modulated Gaussian white noise process.

## 4.2 Development of the Covariance Equation

Under present assumptions, the external load,  $f(\mathbf{x}, t)$  is characterized by

$$f(\mathbf{x}, t) = \theta(t) n(t) g(\mathbf{x}) , \quad (4.1)$$

where

$\theta(t)$  is a deterministic modulating time function,

$n(t)$  is stationary Gaussian white noise with zero mean and constant power spectral density  $S_0$ , and

$g(\mathbf{x})$  is a spatial random field.

The response uncertainty is now caused by the spatial randomness in material properties and external loads as well as the time history uncertainty of the forcing function. For a given set of deterministic spatial properties, the system described in

Chapter 2 becomes a deterministic linear system subjected to a zero mean Gaussian input. Consequently, the displacement and velocity vectors of the discrete linear system (equation 2.47) are zero mean jointly Gaussian processes. A Gaussian process is completely described by its mean vector and covariance matrix, but due to the uncertainties in spatial properties this description is itself random, that is, the coefficients of the covariance matrix are random variables. This covariance matrix contains the variance of the displacement and velocity for all degrees of freedom, plus all of the cross-covariances as well. A procedure to derive the random response covariance matrix is described below.

First, equation (2.47) becomes a stochastic matrix equation of the form

$$M\ddot{\mathbf{d}}(t) + C\dot{\mathbf{d}}(t) + K\mathbf{d}(t) = \theta(t) n(t) \mathbf{p} , \quad (4.2)$$

where  $\mathbf{p}$  is a time-invariant vector which depends on the spatial distribution of the loads.

Next, equation (4.2) is converted to a 1st order state space equation of higher dimension as follows

$$\mathbf{s}(t) = A\mathbf{s}(t) + \mathbf{F}(t) , \quad (4.3)$$

where  $\mathbf{s}(t)$  is the system state vector defined in (2.50),  $A$  is the system matrix defined in (2.52), and

$$\mathbf{F}(t) = \left\{ \begin{array}{c} \mathbf{0} \\ M^{-1}\mathbf{p} \end{array} \right\} \theta(t) n(t) \quad (4.4)$$

is the state space load vector.

Multiplying equation (4.3) by  $\mathbf{s}^T$ , adding the result to its transpose and taking expected value with respect to randomness in the time domain, gives the Liapunov

equation for the covariance response as

$$\begin{aligned} \dot{Q}_{ss}(t) = & A Q_{ss}(t) + Q_{ss}(t) A^T \\ & + \theta(t) E_t(\mathbf{s}(t) \mathbf{n}(t)) \langle \mathbf{0} \ M^{-1} \mathbf{p} \rangle \end{aligned} \quad (4.5)$$

$$+ \theta(t) \left\{ \begin{array}{c} \mathbf{0} \\ M^{-1} \mathbf{p} \end{array} \right\} E_t(\mathbf{s}^T(t) \mathbf{n}(t)),$$

where  $\langle \cdot \rangle$  denotes a row vector,  $E_t(\cdot)$  is the conditional expectation with respect to uncertainty in the time domain, and

$$Q_{ss}(t) = E_t(\mathbf{s} \mathbf{s}^T) \quad (4.6)$$

is the state space covariance matrix.

Equation (4.5) is a first order ordinary differential equation for the evolution of the nonstationary covariance matrix with time.

The 3rd term on the right-hand-side of the covariance equation can be simplified recalling that  $\mathbf{s}(t)$  satisfies equation (4.3). Then, using the principal matrix solution  $\Phi(t)$ ,  $\mathbf{s}(t)$  can be written as

$$\mathbf{s}(t) = \Phi(t) \mathbf{s}(0) + \Phi(t) \int_0^t \Phi^{-1}(\tau) \mathbf{F}(\tau) d\tau, \quad (4.7)$$

where  $\Phi(t)$  satisfies

$$\dot{\Phi}(t) = A \Phi(t) \quad (4.8)$$

$$\Phi(0) = I. \quad (4.9)$$

Using the expression for the load vector (4.4) in this equation yields

$$\mathbf{s}(t) = \Phi(t) \mathbf{s}(0) + \Phi(t) \int_0^t \theta(\tau) \Phi^{-1}(\tau) \left\{ \begin{array}{c} \mathbf{0} \\ M^{-1} \mathbf{p} \end{array} \right\} \mathbf{n}(\tau) d\tau, \quad (4.10)$$

Multiplying by  $n(t)$  and taking expectation gives

$$E_t(\mathbf{s}(t) n(t)) = \Phi(t) \int_0^t \theta(\tau) \Phi^{-1}(\tau) \left\{ \begin{array}{c} \mathbf{0} \\ M^{-1}\mathbf{p} \end{array} \right\} E_t(n(t) n(\tau)) d\tau . \quad (4.11)$$

For stationary random Gaussian white noise with zero mean, the autocorrelation function takes the form

$$E_t(n(t) n(\tau)) = 2\pi S_0 \delta(t - \tau) , \quad (4.12)$$

and thus equation (4.11) reduces to

$$E_t(\mathbf{s}(t) n(t)) = 2\pi S_0 \theta(t) \left\{ \begin{array}{c} \mathbf{0} \\ M^{-1}\mathbf{p} \end{array} \right\} . \quad (4.13)$$

Observing that the 4th term on the right-hand-side of the covariance equation is simply the transpose of the 3rd term, it follows immediately that

$$E_t(\mathbf{s}^T(t) n(t)) = 2\pi S_0 \theta(t) \langle \mathbf{0} M^{-1}\mathbf{p} \rangle . \quad (4.14)$$

Finally, using the simplified expressions (4.13) and (4.14) in the general covariance equation (4.5) gives

$$\begin{aligned} \dot{Q}_{\mathbf{ss}}(t) &= A Q_{\mathbf{ss}}(t) + Q_{\mathbf{ss}}(t) A^T \\ &+ 4\pi S_0 \theta^2(t) \left\{ \begin{array}{c} \mathbf{0} \\ M^{-1}\mathbf{p} \end{array} \right\} \langle \mathbf{0} M^{-1}\mathbf{p} \rangle . \end{aligned} \quad (4.15)$$

This equation is a first order ordinary differential equation for the evolution of the nonstationary covariance matrix with time.

### 4.3 Response Uncertainty and Statistics

The Liapunov equation (4.15) for the evolution of the system covariance matrix  $Q_{\mathbf{ss}}(t)$  can now be integrated in time. The modified Euler algorithm described in

Section 2.7 will be used herein. The same observation mentioned in Section 2.6 and 2.7 regarding the size and sparseness of the system matrix involved in the differential equation, and the remarks made about the simplicity and efficiency of this numerical scheme are still valid for the Liapunov equation.

Once equation (4.15) has been solved, the characterization for the Gaussian response process can be stated. Using equation (2.32), it follows that the mean value and variance, in the time domain, for the element response are given by

$$\begin{aligned}
 E_t(u^e(\mathbf{x}, \mathbf{b}, t)) &= \sum_{j=1}^{NEN} \sum_{0 \leq |\boldsymbol{\ell}| \leq NP} E_t(u_{j\ell_1 \dots \ell_r}^e(t)) \phi_j^e(\mathbf{x}) \prod_{s=1}^r H_{\ell_s}^{b_s}(b_s) \\
 &= 0, \quad e = 1, \dots, NEL,
 \end{aligned} \tag{4.16}$$

$$\begin{aligned}
 E_t(u^{e^2}(\mathbf{x}, \mathbf{b}, t)) &= \sum_{i=1}^{NEN} \sum_{j=1}^{NEN} \sum_{0 \leq |\boldsymbol{\ell}| \leq NP} \sum_{0 \leq |\mathbf{k}| \leq NP} \\
 &E_t(u_{i\ell_1 \dots \ell_r}^e(t) u_{jk_1 \dots k_r}^e(t)) \phi_i^e(\mathbf{x}) \phi_j^e(\mathbf{x}) \prod_{s=1}^r H_{\ell_s}^{b_s}(b_s) \prod_{s=1}^r H_{k_s}^{b_s}(b_s), \\
 &e = 1, \dots, NEL,
 \end{aligned} \tag{4.17}$$

where the coefficients  $E_t(u_{i\ell_1 \dots \ell_r}^e(t) u_{jk_1 \dots k_r}^e(t))$  are the components of the covariance matrix  $Q_{\mathbf{ss}}(t)$ . Equation (4.16) shows that the mean for the Gaussian response process is zero.

The second moment representation for the Gaussian response process is defined by the first two statistical moments of the variance. The first moment, which corresponds to the expected value is computed directly from equation (4.17). Taking

conditional expectation with respect to uncertainty in spatial properties and using the orthogonality of the set of polynomials  $\left\{H_{\ell}^{b_s}\right\}_{\ell=0}^{\infty}$ , equation (4.17) becomes

$$E\left(E_t\left(u^{e^2}(\mathbf{x}, \mathbf{b}, t)\right)\right) = \sum_{i=1}^{NEN} \sum_{j=1}^{NEN} \sum_{0 \leq |\boldsymbol{\ell}| \leq N_P} E_t\left(u_{i\ell_1 \dots \ell_r}^e(t) u_{j\ell_1 \dots \ell_r}^e(t)\right) \quad (4.18)$$

$$\phi_i^e(\mathbf{x}) \phi_j^e(\mathbf{x}), \quad e = 1, \dots, NEL,$$

where  $E(\cdot)$  is the conditional expectation with respect to uncertainty in spatial space.

As mentioned before, equation (4.18) expresses the expected value of the Gaussian response process variance due to randomness in spatial properties. The second statistical moment of the variance can not be derived directly from equation (4.17), and the use of higher order recurrence relations for the orthogonal set of polynomials is required.

An alternative formulation for Gaussian white noise excitation is described in the following section, where the characterization of the second moment representation for the Gaussian response process is completely defined by the components of the covariance matrix.

## 4.4 Alternative Formulation for Gaussian White Noise Excitation

### 4.4.1 Weak Formulation and Matrix Equations

In order to derive an alternative formulation for Gaussian white noise excitation, consider equation (2.24) and assume for the moment that the random variables  $b_n$  are constant coefficients. Then, the characterization of the variational

counterpart of this equation is obtained by redefining the set of weighting functions  $W$ , defined in Section 2.5, as follows

$$W = \left\{ w(\cdot) \mid w \text{ satisfies homogeneous boundary conditions on } \Gamma_g, \quad \|w(\cdot)\|_{H^1(\Omega)} < \infty \right\}.$$

Note that in the present definition, functions in  $W$  do not depend on the set of random variables  $b_n$ . Multiplying the partial differential equation (2.24) by a weighting function  $w$  and integrating by parts over the domain  $\Omega$  gives the weak form of the governing equation as:

find  $u(\mathbf{x}, \mathbf{b}, t) \in V$ ,  $\mathbf{x} \in \Omega$ ,  $\mathbf{b} \in D$ ,  $t \in [0, T_0]$ , such that for all  $w(\mathbf{x}) \in W$

$$\begin{aligned} & (m\ddot{u}, w) + \left( \tau(\bar{\mathbf{k}}(\mathbf{x}), u), \nabla w \right) + \left( \mathbf{Q}(\bar{\mathbf{c}}(\mathbf{x}), \dot{u}), w \right) \\ & + \sum_{n=1}^r \left\{ \left( \tau(\mathbf{k}_n(\mathbf{x}), u) b_n, \nabla w \right) + \left( \mathbf{Q}(\mathbf{c}_n(\mathbf{x}), \dot{u}) b_n, w \right) \right\} \\ & = (\bar{f}(\mathbf{x}, t), w) + \sum_{n=1}^r (f_n(\mathbf{x}, t) b_n, w), \end{aligned} \quad (4.19)$$

$$(mu(\mathbf{x}, \mathbf{b}, 0), w) = (mu_0(\mathbf{x}), w), \quad (4.20)$$

$$(m\dot{u}(\mathbf{x}, \mathbf{b}, 0), w) = (m\dot{u}_0(\mathbf{x}), w), \quad (4.21)$$

where  $(\cdot, \cdot)$  denotes the inner product, that is,

$$(\phi, \psi) = \int_{\Omega} \phi \psi \, d\Omega, \quad (4.22)$$

where  $\phi$  and  $\psi$  are scalar functions defined on  $\Omega \times D \times [0, T_0]$  and  $\Omega$ , respectively. All other terms in equations (4.19) through (4.21) are as previously defined in Chapter 2.

The semidiscrete Galerkin formulation corresponding to equations (4.19), (4.20) and (4.21) is now achieved using the following finite element approximation within the element  $\Omega^e$

$$u^e(\mathbf{x}, \mathbf{b}, t) = \sum_{j=1}^{NEN} u_j^e(\mathbf{b}, t) \phi_j^e(\mathbf{x}) , \quad (4.23)$$

where  $NEN$  and  $\phi_j^e(\mathbf{x})$  are as defined in Section 2.5, and  $u_j^e(\mathbf{b}, t)$  is the unknown random function of time for node  $j$ . Then, the base for the finite-dimensional approximations  $V^h$  and  $W^h$  to  $V$  and  $W$ , respectively (equation (2.36)), becomes

$$\{\phi_j(\mathbf{x})\}_{j=1, \dots, NTOT} , \quad (4.24)$$

where  $NTOT$  is the total number of nodes in the finite element discretization, and  $\phi_j(\mathbf{x})$  is the global shape function for node  $j$ . Then, the variational formulation previously defined becomes:

find  $u^h(\mathbf{x}, \mathbf{b}, t) \in V^h$ ,  $\mathbf{x} \in \Omega$ ,  $\mathbf{b} \in D$ ,  $t \in [0, T_0]$ , such that for all  $w^h(\mathbf{x}) \in W^h$

$$\begin{aligned} & (m\ddot{u}^h, w^h) + (\boldsymbol{\tau}(\bar{\mathbf{k}}(\mathbf{x}), u^h), \nabla w^h) + (\mathbf{Q}(\bar{\mathbf{c}}(\mathbf{x}), \dot{u}^h), w^h) \\ & + \sum_{n=1}^r \left\{ (\boldsymbol{\tau}(\mathbf{k}_n(\mathbf{x}), u^h) b_n, \nabla w^h) + (\mathbf{Q}(\mathbf{c}_n(\mathbf{x}), \dot{u}^h) b_n, w^h) \right\} \\ & = (\bar{f}(\mathbf{x}, t), w^h) + \sum_{n=1}^r (f_n(\mathbf{x}, t) b_n, w^h) , \end{aligned} \quad (4.25)$$

$$(m u^h(\mathbf{x}, \mathbf{b}, 0), w^h) = (m u_0(\mathbf{x}), w^h) , \quad (4.26)$$

$$(m \dot{u}^h(\mathbf{x}, \mathbf{b}, 0), w^h) = (m \dot{u}_0(\mathbf{x}), w^h) . \quad (4.27)$$

This variational formulation, together with the characterization of  $V^h$  and  $W^h$ , leads to the following set of equations for element  $e$

$$\begin{aligned}
 & \sum_{j=1}^{NEN} \left\{ \left[ \int_{\Omega^e} m(\mathbf{x}) \phi_j^e(\mathbf{x}) \phi_i^e(\mathbf{x}) d\Omega \right] \ddot{u}_j^e(\mathbf{b}, t) \right. \\
 & + \left[ \int_{\Omega^e} Q(\bar{\mathbf{c}}(\mathbf{x}), \phi_j^e(\mathbf{x})) \phi_i^e(\mathbf{x}) d\Omega \right] \dot{u}_j^e(\mathbf{b}, t) \\
 & + \left[ \int_{\Omega^e} \boldsymbol{\tau}(\bar{\mathbf{k}}(\mathbf{x}), \phi_j^e(\mathbf{x})) \nabla \phi_i^e(\mathbf{x}) d\Omega \right] u_j^e(\mathbf{b}, t) \\
 & + \sum_{n=1}^r \left( \left[ \int_{\Omega^e} Q(\mathbf{c}_n(\mathbf{x}), \phi_j^e(\mathbf{x})) \phi_i^e(\mathbf{x}) d\Omega \right] \dot{u}_j^e(\mathbf{b}, t) \right. \\
 & \left. + \left[ \int_{\Omega^e} \boldsymbol{\tau}(\mathbf{k}_n(\mathbf{x}), \phi_j^e(\mathbf{x})) \nabla \phi_i^e(\mathbf{x}) d\Omega \right] u_j^e(\mathbf{b}, t) \right) b_n \left. \right\} = \int_{\Omega^e} \bar{f}(\mathbf{x}, t) \phi_i^e(\mathbf{x}) d\Omega \\
 & + \sum_{n=1}^r \left[ \int_{\Omega^e} f_n(\mathbf{x}, t) \phi_i^e(\mathbf{x}) d\Omega \right] b_n, \quad i = 1, \dots, NEN,
 \end{aligned} \tag{4.28}$$

$$\sum_{j=1}^{NEN} \left[ \int_{\Omega^e} m(\mathbf{x}) \phi_j^e(\mathbf{x}) \phi_i^e(\mathbf{x}) d\Omega \right] u_j^e(\mathbf{b}, 0) = \int_{\Omega^e} m(\mathbf{x}) u_0(\mathbf{x}) \phi_i^e(\mathbf{x}) d\Omega, \tag{4.29}$$

$$i = 1, \dots, NEN,$$

$$\sum_{j=1}^{NEN} \left[ \int_{\Omega^e} m(\mathbf{x}) \phi_j^e(\mathbf{x}) \phi_i^e(\mathbf{x}) d\Omega \right] \dot{u}_j^e(\mathbf{b}, 0) = \int_{\Omega^e} m(\mathbf{x}) \dot{u}_0(\mathbf{x}) \phi_i^e(\mathbf{x}) d\Omega, \tag{4.30}$$

$$i = 1, \dots, NEN.$$

Assembling equations (4.28) through (4.30) for all elements into a set of global equations, gives a random matrix equation of the form

$$M\ddot{\mathbf{d}}(\mathbf{b}, t) + C(\mathbf{b})\dot{\mathbf{d}}(\mathbf{b}, t) + K(\mathbf{b})\mathbf{d}(\mathbf{b}, t) = \mathbf{p}(\mathbf{b}, t), \tag{4.31}$$

where

$\mathbf{d}(\mathbf{b}, t)$  is the global random vector of unknowns with components  $u_j(\mathbf{b}, t)$ ,

$\mathbf{p}(\mathbf{b}, t)$  is the total effective random load vector,

$M$  is the mass matrix,

$C(\mathbf{b})$  is the random damping matrix, and

$K(\mathbf{b})$  is the random stiffness matrix.

The initial conditions of the system are given by

$$\mathbf{d}(\mathbf{b}, 0) = \mathbf{d}_0 \quad \text{and} \quad (4.32)$$

$$\dot{\mathbf{d}}(\mathbf{b}, 0) = \dot{\mathbf{d}}_0, \quad (4.33)$$

where  $\mathbf{d}_0$  and  $\dot{\mathbf{d}}_0$  are vectors whose elemental components are defined by the equations (4.29) and (4.30), respectively.

Note that equation (4.28) allows the following representation for the damping matrix, stiffness matrix, and load vector

$$C(\mathbf{b}) = \bar{C} + \sum_{n=1}^r C_n b_n, \quad (4.34)$$

$$K(\mathbf{b}) = \bar{K} + \sum_{n=1}^r K_n b_n, \quad (4.35)$$

$$\mathbf{p}(\mathbf{b}, t) = \bar{\mathbf{p}}(t) + \sum_{n=1}^r \mathbf{p}_n(t) b_n, \quad (4.36)$$

where  $\bar{C}$ ,  $C_n$ ,  $\bar{K}$  and  $K_n$  are deterministic matrices and  $\bar{\mathbf{p}}(t)$  and  $\mathbf{p}_n(t)$  are time dependent vectors, independent of the random variables  $b_n$ .

Further, under white noise excitation, equation (4.36) becomes

$$\mathbf{p}(\mathbf{b}, t) = \left( \bar{\mathbf{p}} + \sum_{n=1}^r \mathbf{p}_n b_n \right) \theta(t) n(t) \quad (4.37)$$

where  $\bar{\mathbf{p}}$  and  $\mathbf{p}_n$  are deterministic vectors, and  $\theta(t)$  and  $n(t)$  are as defined in Section 4.2.

#### 4.4.2 Development of the Covariance Equation

Once the set of global equations (4.31) has been established, the Liapunov equation for the covariance response may be defined as in Section 4.2, and equation (4.15) takes the form

$$\begin{aligned} \dot{Q}_{ss}(\mathbf{b}, t) = & A(\mathbf{b})Q_{ss}(\mathbf{b}, t) + Q_{ss}(\mathbf{b}, t)A^T(\mathbf{b}) \\ & + 4\pi S_0 \theta^2(t) \left\{ \begin{array}{c} \mathbf{0} \\ M^{-1}\mathbf{p}(\mathbf{b}) \end{array} \right\} \langle \mathbf{0} M^{-1}\mathbf{p}(\mathbf{b}) \rangle, \end{aligned} \quad (4.38)$$

where

$$A(\mathbf{b}) = \begin{bmatrix} \mathbf{0} & I \\ -M^{-1}K(\mathbf{b}) & -M^{-1}C(\mathbf{b}) \end{bmatrix} \quad (4.39)$$

is the random system matrix,

$Q_{ss}(\mathbf{b}, t)$  is the random state space covariance matrix, and

$\mathbf{p}(\mathbf{b})$  is a random time-invariant vector which depends on the spatial distribution of the loads, and defined by

$$\mathbf{p}(\mathbf{b}) = \bar{\mathbf{p}} + \sum_{n=1}^r \mathbf{p}_n b_n, \quad (4.40)$$

where  $\bar{\mathbf{p}}$  and  $\mathbf{p}_n$  are defined in equation (4.37).

It follows from equations (4.34) and (4.35) that the system matrix may now be expressed as:

$$A(\mathbf{b}) = \bar{A} + \sum_{n=1}^r A_n b_n, \quad (4.41)$$

where  $\bar{A}$  and  $A_n$  are deterministic matrices. Using equations (4.40) and (4.41) in the Liapunov equation gives

$$\begin{aligned} \dot{Q}_{ss}(\mathbf{b}, t) &= \bar{A}Q_{ss}(\mathbf{b}, t) + Q_{ss}(\mathbf{b}, t)\bar{A}^T \\ &+ \sum_{n=1}^r \{A_n Q_{ss}(\mathbf{b}, t) + Q_{ss}(\mathbf{b}, t)A_n^T\} b_n \\ &+ 4\pi S_0 \theta^2(t) \left\{ \begin{array}{c} \mathbf{0} \\ M^{-1} \left( \bar{\mathbf{p}} + \sum_{n=1}^r \mathbf{p}_n b_n \right) \end{array} \right\} \left\langle \mathbf{0} M^{-1} \left( \bar{\mathbf{p}} + \sum_{n=1}^r \mathbf{p}_n b_n \right) \right\rangle. \end{aligned} \quad (4.42)$$

This last equation is a random first order ordinary differential equation for the evolution of the nonstationary covariance matrix with time. In order to solve it, let the covariance matrix  $Q_{ss}(\mathbf{b}, t)$  be expressed as

$$Q_{ss}(\mathbf{b}, t) = \sum_{0 \leq |\ell| \leq NP} Q_{ss\ell_1 \dots \ell_r}(t) \prod_{s=1}^r H_{\ell_s}^{b_s}(b_s), \quad (4.43)$$

where

$Q_{ss\ell_1 \dots \ell_r}(t)$  is an unknown deterministic matrix of time, and the remaining terms are as previously defined.

In addition to the first order recurrence relation for the orthogonal set of polynomials defined in Section 2.5, the following second order recurrence relation [29] will be also needed

$$\begin{aligned} b_n^2 H_{\ell_n}^{b_n}(b_n) &= \bar{a}_{\ell_n-2}^{b_n} H_{\ell_n-2}^{b_n}(b_n) + \bar{a}_{\ell_n-1}^{b_n} H_{\ell_n-1}^{b_n}(b_n) + \bar{a}_{\ell_n}^{b_n} H_{\ell_n}^{b_n}(b_n) \\ &+ \bar{a}_{\ell_n+1}^{b_n} H_{\ell_n+1}^{b_n}(b_n) + \bar{a}_{\ell_n+2}^{b_n} H_{\ell_n+2}^{b_n}(b_n) \end{aligned} \quad \begin{array}{l} n = 1, \dots, r \\ \ell_n = 0, 1, \dots, \end{array} \quad (4.44)$$

where the coefficients  $\bar{a}_{\ell_n}^{b_n}$  depend on the probability density function of the random variable  $b_n$ .

The set of differential equations for the coefficients  $Q_{\mathbf{s}\mathbf{s}\ell_1\dots\ell_r}(t)$  will be derived using the weighted residual method. Multiplying equation (4.42) by the weighting function  $\prod_{s=1}^r H_{\ell_s}^{b_s}(b_s)$ , then taking expectation with respect to spatial uncertainties, and finally considering the recurrence relations (2.40) and (4.44) of the orthogonal set of polynomials gives

$$\begin{aligned}
 \dot{Q}_{\mathbf{s}\mathbf{s}\ell_1\dots\ell_r}(t) &= \bar{A}Q_{\mathbf{s}\mathbf{s}\ell_1\dots\ell_r}(t) + Q_{\mathbf{s}\mathbf{s}\ell_1\dots\ell_r}(t)\bar{A}^T \\
 &+ \sum_{n=1}^r \left\{ A_n \left[ a_{\ell_n-1}^{b_n} Q_{\mathbf{s}\mathbf{s}\ell_1\dots\ell_n-1\dots\ell_r}(t) + a_{\ell_n}^{b_n} Q_{\mathbf{s}\mathbf{s}\ell_1\dots\ell_n\dots\ell_r}(t) \right. \right. \\
 &+ \left. \left. a_{\ell_n+1}^{b_n} Q_{\mathbf{s}\mathbf{s}\ell_1\dots\ell_n+1\dots\ell_r}(t) \right] + \left[ a_{\ell_n-1}^{b_n} Q_{\mathbf{s}\mathbf{s}\ell_1\dots\ell_n-1\dots\ell_r}(t) \right. \right. \\
 &+ \left. \left. a_{\ell_n}^{b_n} Q_{\mathbf{s}\mathbf{s}\ell_1\dots\ell_n\dots\ell_r}(t) + a_{\ell_n+1}^{b_n} Q_{\mathbf{s}\mathbf{s}\ell_1\dots\ell_n+1\dots\ell_r}(t) \right] A_n^T \right\} \\
 &+ 4\pi S_0 \theta^2(t) \left\{ \left\{ \begin{matrix} \mathbf{0} \\ M^{-1}\bar{\mathbf{p}} \end{matrix} \right\} \langle \mathbf{0} M^{-1}\bar{\mathbf{p}} \rangle \prod_{s=1}^r \delta_{\ell_s,0} \right. \\
 &+ \left. \sum_{n=1}^r \left( a_0^{b_n} \prod_{s=1}^r \delta_{\ell_s,0} + a_1^{b_n} \prod_{\substack{s=1 \\ s \neq n}}^r \delta_{\ell_s,0} \delta_{\ell_n,1} \right) \left[ \left\{ \begin{matrix} \mathbf{0} \\ M^{-1}\mathbf{p}_n \end{matrix} \right\} \langle \mathbf{0} M^{-1}\bar{\mathbf{p}} \rangle \right. \right. \\
 &+ \left. \left. \left\{ \begin{matrix} \mathbf{0} \\ M^{-1}\bar{\mathbf{p}} \end{matrix} \right\} \langle \mathbf{0} M^{-1}\mathbf{p}_n \rangle \right] \right\}
 \end{aligned}$$

$$\begin{aligned}
& + \sum_{n=1}^r \left( \bar{a}_0^{b_n} \prod_{s=1}^r \delta_{\ell_s,0} + \bar{a}_1^{b_n} \prod_{\substack{s=1 \\ s \neq n}}^r \delta_{\ell_s,0} \delta_{\ell_n,1} \right. \\
& + \left. \bar{a}_2^{b_n} \prod_{\substack{s=1 \\ s \neq n}}^r \delta_{\ell_s,0} \delta_{\ell_s,2} \right) \left\{ \begin{matrix} \mathbf{0} \\ M^{-1} \mathbf{p}_n \end{matrix} \right\} \langle \mathbf{0} M^{-1} \mathbf{p}_n \rangle \\
& + \sum_{\substack{n,m=1 \\ n \neq m}}^r \prod_{\substack{s=1 \\ s \neq n,m}}^r \delta_{\ell_s,0} \left( \bar{a}_0^{b_n} \bar{a}_0^{b_m} \delta_{\ell_n,0} \delta_{\ell_m,0} + \bar{a}_0^{b_n} \bar{a}_1^{b_m} \delta_{\ell_n,0} \delta_{\ell_m,1} \right. \\
& \left. + \bar{a}_1^{b_n} \bar{a}_0^{b_m} \delta_{\ell_n,1} \delta_{\ell_m,0} + \bar{a}_1^{b_n} \bar{a}_1^{b_m} \delta_{\ell_n,1} \delta_{\ell_m,1} \right) \left\{ \begin{matrix} \mathbf{0} \\ M^{-1} \mathbf{p}_n \end{matrix} \right\} \langle \mathbf{0} M^{-1} \mathbf{p}_n \rangle \}.
\end{aligned} \tag{4.45}$$

$$\begin{aligned}
\ell_s &= 0, 1, \dots \\
s &= 1, \dots, r.
\end{aligned}$$

#### 4.4.3 Response Uncertainty and Statistics

Equation (4.45) can be integrated in time using the modified Euler algorithm described in Section 2.7. Once the equation for the coefficients  $Q_{\mathbf{ss}\ell_1 \dots \ell_r}(t)$  has been solved, the second moment representation for the Gaussian response process can be defined. In particular, using equation (4.43), it follows that the expected value and the variance for the  $(i, j)$  component of the covariance matrix are given by

$$E\left((Q_{\mathbf{ss}}(\mathbf{b}, t))_{i,j}\right) = (Q_{\mathbf{ss}0 \dots 0}(t))_{i,j} \tag{4.46}$$

$$V_{ar}\left((Q_{\mathbf{ss}}(\mathbf{b}, t))_{i,j}\right) = \sum_{1 \leq |\ell| \leq NP} (Q_{\mathbf{ss}\ell_1 \dots \ell_r}(t))_{i,j}^2. \tag{4.47}$$

Finally, using equations (4.23), (4.46) and (4.47) gives the second moment characterization for the element response process as

$$E\left(E_t(u^{e^2}(\mathbf{x}, \mathbf{b}, t))\right) = \sum_{i=1}^{NEN} \sum_{j=1}^{NEN} (Q_{\mathbf{ss}0\dots 0}(t))_{i,j} \phi_j^e(\mathbf{x}) \phi_i^e(\mathbf{x}), \quad (4.48)$$

$$e = 1, \dots, NEL$$

$$V_{ar}\left(E_t(u^{e^2}(\mathbf{x}, \mathbf{b}, t))\right) = \sum_{i=1}^{NEN} \sum_{j=1}^{NEN} \sum_{k=1}^{NEN} \sum_{s=1}^{NEN} \sum_{1 \leq |\mathbf{l}| \leq NP} (Q_{\mathbf{ss}\mathbf{l}_1\dots\mathbf{l}_r}(t))_{i,j}$$

$$(Q_{\mathbf{ss}\mathbf{l}_1\dots\mathbf{l}_r}(t))_{k,s} \phi_i^e(\mathbf{x}) \phi_j^e(\mathbf{x}) \phi_k^e(\mathbf{x}) \phi_s^e(\mathbf{x}), \quad (4.49)$$

$$e = 1, \dots, NEL.$$

Equations (4.48) and (4.49) express the expected value and the variance, respectively, of the Gaussian response process variance, due to randomness in spatial properties.

Note that this characterization of the response is completely defined by the components of the covariance matrix, unlike the previous formulation. Also note that, using the analytical approximation for the covariance matrix, given by equation (4.43), a more complete probabilistic description for the Gaussian response process can be defined. For example, higher statistical moments can be computed as well as the probability function. These higher statistical moments can be computed using higher order recurrence relations for the orthogonal set of polynomials, while the probability function can be computed by numerical integration.

## Chapter 5

### Application to Primary-Secondary Systems

#### 5.1 Introduction

This chapter describes the application of the solution method presented in Chapter 4 to the dynamic response of primary-secondary systems. These systems consist of a primary structure supporting a secondary system. The secondary system may be a piece of equipment or a substructure which is distinguished from the primary structure. Secondary systems are usually characterized by a mass which is small in comparison with the mass of the structure by which they are supported. Frequently, such substructures are essential for the safety of the occupants of the primary structure and may have even greater importance. This is true especially in the design of crucial facilities such as a nuclear reactor. Therefore, the survival of such subsystems in an earthquake is often essential, and a dynamic analysis is called for.

Additional examples of structural systems consisting of light, secondary components supported on heavier primary structures, which are frequently encountered in engineering practice are: piping in industrial structures, drilling and exploration equipment on offshore platforms, communications and control devices on space vehicles, etc.

The objective of the numerical illustrations described in this chapter is to obtain insight concerning the sensitivity of the response of a secondary system by taking into account the statistical uncertainties of the parameters describing the load and structural properties.

In the next section, a particular problem chosen for study is discussed in detail.

## 5.2 Description of the Physical System

A simple five degree-of-freedom model representing a shear building is chosen as the primary system. A diagram of the finite element model is shown in Figure 5.1. The displacement relative to the base of the  $i$ -th degree-of-freedom at time  $t$  is denoted by  $u_i(t)$ . A nonuniform distribution of mass and stiffness along the height of the building is assumed. The floor masses are:  $m_1 = m$ ,  $m_2 = m$ ,  $m_3 = 0.7m$ ,  $m_4 = 0.7m$ ,  $m_5 = 0.6m$ , and the interstorey stiffnesses are:  $k_1 = k$ ,  $k_2 = k$ ,  $k_3 = 0.8k$ ,  $k_4 = 0.8k$ ,  $k_5 = 0.7k$ . The specification of the parameters  $m$  and  $k$  is discussed in Section 5.5. The primary system is assumed to be classically damped with 5% of critical damping in the first two modes. The secondary system is idealized as a single-degree-of-freedom oscillator of frequency  $\omega_s$ , damping ratio  $\beta_s$  and mass  $m_s$ , which is attached to the  $k$ -th d.o.f. of the primary system. Finally, the base acceleration  $\ddot{q}(t)$  is taken to be a random process.

The equation of motion of the combined primary-secondary system can be written as

$$M\ddot{\mathbf{d}} + C\dot{\mathbf{d}} + K\mathbf{d} = -M\mathbf{1}\ddot{q}(t) \quad (5.1)$$

in which

$$M = \begin{bmatrix} M_p & \mathbf{0} \\ \mathbf{0}^T & m_s \end{bmatrix}, \quad (5.2)$$

$$C = \begin{bmatrix} C_p & \mathbf{0} \\ \mathbf{0}^T & 0 \end{bmatrix} + C_s, \quad (5.3)$$

$$K = \begin{bmatrix} K_p & \mathbf{0} \\ \mathbf{0}^T & 0 \end{bmatrix} + K_s, \quad (5.4)$$

$$\mathbf{d} = \begin{Bmatrix} \mathbf{u}_p \\ u_s \end{Bmatrix}, \quad (5.5)$$

where

$M_p$  is the mass matrix associated with the primary structure,

$C_p$  is the damping matrix associated with the primary structure,

$K_p$  is the stiffness matrix associated with the primary structure,

$C_s$  is the damping coupling matrix associated with the secondary system,

$K_s$  is the stiffness coupling matrix associated with the secondary system,

$\mathbf{1}$  is the unitary vector,

$\mathbf{u}_p$  is the unknown displacement vector of the primary system, and

$u_s$  is the unknown displacement of the secondary system relative to the base of the primary system.

The matrices previously defined are of size  $\ell \times \ell$  where  $\ell = n + 1$  with  $n$  being the number of degrees-of-freedom of the primary structure. For this example  $n = 5$ . Note that in general, the combined primary-secondary system is nonclassically damped.

As mentioned before, the system is subjected to a random base excitation  $\ddot{q}(t)$ . The particular model for the stochastic seismic excitation to be used in this example is described in the following section.

### 5.3 Ground Motion Model

Theoretically, the class of possible ground motion could be determined if information were available regarding the local conditions, material properties, neighboring fault systems and the nature of expected fault rupture processes. However, the lack of such information and the complexity of the analytical problem that must be solved make this approach impractical for the present example. Defining the excitation as belonging to a general class of signals with prescribed time and/or frequency domain properties, such as duration, peak acceleration, total energy distribution over the frequency range, etc., appears to be a more suitable approach. Stochastic models of the seismic excitation are an example of such an approach, and often have been used in examining the seismic response of structural systems. It is reiterated that the actual earthquake process is understood to be deterministic, but it is replaced by a stochastic process in order to reflect the uncertainty of our knowledge in the process.

Most of the stochastic models for seismic excitation that have been proposed fall into one of two subclasses: stationary or nonstationary models. Stationary models have often been used for the representation of the frequency content of long duration seismic ground motion. Clearly, such models can only be used to represent the central high-intensity part of a strong-motion record. It cannot be expected to model short-duration earthquakes, or the buildup or tail of the ground motion. This type of model allows complete freedom in specification of the frequency content of

the earthquake. However, this frequency content must be consistent throughout the earthquake. Also, the duration of the ground motion is not explicitly included in the model, and must be artificially accounted for. This has often been done by considering a finite portion of the stationary process. For long-duration earthquakes, the beginning and ending phases may be expected to be unimportant. The effect of ignoring these phases is not clear, however, especially in the case of medium- and short-duration earthquakes.

The transient nature of the earthquake process may be modeled explicitly by modulating a stationary process with a deterministic function of time. Several forms of envelopes have been proposed [36,37]. In general, envelopes are chosen with only a few parameters to be estimated, such as intensity, duration, and buildup time. Note that stationary models are actually a special case of modulated stationary processes. A finite segment of stationary ground motion may be produced by an envelope which has a "boxcar" shape.

The parameters of the modulated stationary model are the stationary frequency content and the modulating function. This type of model is able to represent the major features of strong-motion (average frequency content, intensity, and duration), however it is unable to reproduce time-varying frequency content. To represent such cases, Saragoni and Hart [38] introduced an excitation model defined by three distinct, modulated stationary processes accounting for the arrival of longitudinal, shear and surface waves.

One drawback of modulated stationary processes is the lack of physical significance of the envelope. A model which has a more physically solid basis is the filtered, modulated white noise process. This process is obtained by passing a deterministic modulated Gaussian white noise signal through a filter with prescribed

transfer function. This model visualizes the earthquake process as a white noise source which is deterministically modulated, and then filtered by a transmission path. The envelope in this case is associated with the source mechanism, and the filter characteristics are determined in part by source properties as well as the transmission path. As in the case of a modulated stationary process, the parameters available are the modulating function and the frequency characteristics of the filter.

The artificial records produced by this model exhibit a slight frequency shift with time due to transient behavior of the filter, but it is unlikely that this is related to the actual phenomenon observed in strong-motion records, that is, a shift from higher frequencies to lower frequencies toward the end of the record. However, it is believed that the filtered modulated white noise process remains the best compromise between physical authenticity and computational or mathematical convenience.

Mathematically, the filter modulated white noise process can be defined as follows. Consider the excitation,  $\tilde{q}(t)$ , defined as

$$\tilde{q}(t) = M_{n_1}(x_g(t)) , \quad (5.6)$$

where  $x_g(t)$  is the solution of the following equation

$$L_{n_2}(x_g(t)) = \theta(t)n(t) , \quad (5.7)$$

where  $\theta(t)$  is a deterministic modulating time function,  $n(t)$  is a zero mean Gaussian white noise excitation with constant power spectral density  $S_0$ , and  $M_{n_1}$  and  $L_{n_2}$  are  $n_1$  and  $n_2$  order linear operators with  $n_1 < n_2$ .

The particular model for the earthquake ground motion acceleration,  $\ddot{q}(t)$ , to be used in this application, is defined as

$$\ddot{q}(t) = -2\xi_g \omega_g \dot{x}_g - \omega_g^2 x_g , \quad (5.8)$$

where

$$\ddot{x}_g + 2\xi_g \omega_g \dot{x}_g + \omega_g^2 x_g = \theta(t)n(t) , \quad (5.9)$$

and  $\xi_g, \omega_g$  are model parameters reflecting the local conditions. A boxcar type envelope function,  $\theta(t)$ , of duration  $T_0$ , is employed, where

$$\theta(t) = \begin{cases} 1 & \text{if } t \in [0, T_0] \\ 0 & \text{otherwise} \end{cases} \quad (5.10)$$

Note that this is a special case of the model described by the equations (5.6) and (5.7), corresponding to  $n_1 = 1, n_2 = 2$  and

$$M_{n_1}(x_g) = -2\xi_g \omega_g \dot{x}_g - \omega_g^2 x_g \quad (5.11)$$

$$L_{n_2}(x_g) = \ddot{x}_g + 2\xi_g \omega_g \dot{x}_g + \omega_g^2 x_g . \quad (5.12)$$

This model corresponds in frequency content to the Kanai-Tajimi model [39,40], which is frequently used in earthquake engineering. Physically, the Kanai-Tajimi model may be interpreted as corresponding to an ideal white noise excitation at bedrock level filtered through the overlaying soil deposit, which is modeled as a second-order linear filter. Within this context, the Kanai-Tajimi parameters are interpreted as the soil overburden effective damping coefficient  $\xi_g$  and natural frequency  $\omega_g$ . Although of a very simple form, this model is capable of defining the basic features of earthquake ground motion, such as duration, strength and frequency content.

#### 5.4 Formulation of the Covariance Equation

In this section, the general formulation of the covariance equation, described in Chapter 4, is specialized for the particular problem under consideration.

Using the particular model for the earthquake ground motion acceleration  $\ddot{q}(t)$ , described in the previous section, the equation of motion of the combined primary-secondary system becomes

$$M\ddot{\mathbf{d}} + C\dot{\mathbf{d}} + K\mathbf{d} = -M\mathbf{1}\ddot{q}(t) \quad (5.13)$$

$$\ddot{q}(t) = -2\xi_g \omega_g \dot{x}_g - \omega_g^2 x_g, \quad (5.14)$$

where  $x_g(t)$  is the solution of the equation

$$\ddot{x}_g + 2\xi_g \omega_g \dot{x}_g + \omega_g^2 x_g = \theta(t)n(t), \quad (5.15)$$

and all other terms are as previously defined.

The first-order state space equation corresponding to equations (5.13) through (5.15) takes the form

$$\dot{\mathbf{s}} = A\mathbf{s} + \mathbf{F}, \quad (5.16)$$

where the system state vector,  $\mathbf{s}$ , is

$$\mathbf{s} = \begin{Bmatrix} \mathbf{u}_p \\ x_g \\ \dot{\mathbf{u}}_p \\ \dot{x}_g \end{Bmatrix}, \quad (5.17)$$

the system matrix,  $A$ , is given by

$$A = \begin{bmatrix} 0 & 0 & I & 0 \\ 0^T & 0 & 0^T & 1 \\ -M^{-1}K & \omega_g^2 \mathbf{1} & -M^{-1}C & 2\xi_g \omega_g \mathbf{1} \\ 0^T & -\omega_g^2 & 0^T & -2\xi_g \omega_g \end{bmatrix}, \quad (5.18)$$

and the state space load vector,  $\mathbf{F}$ , is

$$\mathbf{F} = \begin{Bmatrix} 0 \\ 0 \\ 0 \\ \theta(t)n(t) \end{Bmatrix}. \quad (5.19)$$

As indicated in Chapter 4, the damping matrix and the stiffness matrix can be represented by

$$C(\mathbf{b}) = \bar{C} + \sum_{n=1}^r C_n b_n, \quad (5.20)$$

$$K(\mathbf{b}) = \bar{K} + \sum_{n=1}^r K_n b_n, \quad (5.21)$$

where  $\bar{C}$ ,  $\bar{K}$ ,  $C_n$  and  $K_n$  are deterministic matrices and  $b_n$  are independent random variables with zero mean.

In addition to uncertainties in the material properties of the combined primary-secondary system, the randomness in the transmission path of the ground motion model is considered. To allow uncertainties in the path, the model parameters  $\xi_g$  and  $\omega_g$  are modeled as random variables and represented by

$$\xi_g = \bar{\xi}_g + \xi_{g1} b_{r+1}, \quad (5.22)$$

$$\omega_g = \bar{\omega}_g + \omega_{g1} b_{r+2}, \quad (5.23)$$

where  $\bar{\xi}_g$  and  $\bar{\omega}_g$  denote the expected value of the filter damping coefficient and filter natural frequency, respectively,  $\xi_{g1}$  and  $\omega_{g1}$  are deterministic coefficients, and  $b_{r+1}$  and  $b_{r+2}$  are random variables with zero mean and unit variance.

The differential equation for the evolution of the nonstationary covariance matrix with time, may be defined as in Chapter 4, and takes the form

$$\dot{Q}_{\mathbf{ss}}(\mathbf{b}, t) = A(\mathbf{b})Q_{\mathbf{ss}}(\mathbf{b}, t) + Q_{\mathbf{ss}}(\mathbf{b}, t)A^T(\mathbf{b}) + 4\pi S_0 \theta^2(t) \begin{Bmatrix} 0 \\ 0 \\ 0 \\ 1 \end{Bmatrix} \langle 0001 \rangle, \quad (5.24)$$

where

$A(\mathbf{b})$  is the random system matrix,

$Q_{\mathbf{ss}}(\mathbf{b}, t)$  is the random state space covariance matrix, and

$\mathbf{b}$  is the vector of random variables, with components  $b_i$ ,  $i = 1, \dots, r + 2$ .

It follows from equations (5.20) through (5.23) that the system matrix may now be expressed as:

$$A(\mathbf{b}) = \bar{A} + \sum_{n=1}^{r+2} A_n b_n + A_{r+3} b_{r+1} b_{r+2} + A_{r+4} b_{r+2}^2, \quad (5.25)$$

where  $\bar{A}$  and  $A_n$ ,  $n = 1, \dots, r + 4$  are deterministic matrices.

Using equation (5.25) in the Liapunov equation (equation (5.24)), gives

$$\begin{aligned} \dot{Q}_{\mathbf{ss}}(\mathbf{b}, t) &= \bar{A} Q_{\mathbf{ss}}(\mathbf{b}, t) + Q_{\mathbf{ss}}(\mathbf{b}, t) \bar{A}^T \\ &+ \sum_{n=1}^{r+2} \left\{ A_n Q_{\mathbf{ss}}(\mathbf{b}, t) + Q_{\mathbf{ss}}(\mathbf{b}, t) A_n^T \right\} b_n \\ &+ \left\{ A_{r+3} Q_{\mathbf{ss}}(\mathbf{b}, t) + Q_{\mathbf{ss}}(\mathbf{b}, t) A_{r+3}^T \right\} b_{r+1} b_{r+2} \\ &+ \left\{ A_{r+4} Q_{\mathbf{ss}}(\mathbf{b}, t) + Q_{\mathbf{ss}}(\mathbf{b}, t) A_{r+4}^T \right\} b_{r+2}^2 \\ &+ 4\pi S_0 \theta^2(t) \begin{Bmatrix} 0 \\ 0 \\ 0 \\ 1 \end{Bmatrix} \langle 0001 \rangle. \end{aligned} \quad (5.26)$$

This last equation is a random first-order ordinary differential equation for the covariance matrix. As before, in order to solve this equation, let the covariance matrix  $Q_{\mathbf{ss}}(\mathbf{b}, t)$  be expressed as

$$Q_{\mathbf{ss}}(\mathbf{b}, t) = \sum_{0 \leq |\ell| \leq NP} Q_{\mathbf{ss}\ell_1 \dots \ell_{r+2}}(t) \prod_{s=1}^{r+2} H_{\ell_s}^{b_s}(b_s), \quad (5.27)$$

where

$Q_{ss\ell_1\dots\ell_{r+2}}(t)$  is an unknown deterministic matrix of time, and the remaining terms are as previously defined.

Finally, the set of differential equations for the coefficients  $Q_{ss\ell_1\dots\ell_{r+2}}(t)$  can be derived as in Chapter 4, and takes the form

$$\begin{aligned}
 \dot{Q}_{ss\ell_1\dots\ell_{r+2}}(t) &= \bar{A}Q_{ss\ell_1\dots\ell_{r+2}}(t) + Q_{ss\ell_1\dots\ell_{r+2}}(t)\bar{A}^T \\
 &+ \sum_{n=1}^{r+2} \left\{ A_n \left[ a_{\ell_n-1}^{b_n} Q_{ss\ell_1\dots\ell_{n-1}\dots\ell_{r+2}}(t) + a_{\ell_n}^{b_n} Q_{ss\ell_1\dots\ell_n\dots\ell_{r+2}}(t) \right. \right. \\
 &a_{\ell_n+1}^{b_n} Q_{ss\ell_1\dots\ell_{n+1}\dots\ell_{r+2}}(t) \left. \right] + \left[ a_{\ell_n-1}^{b_n} Q_{ss\ell_1\dots\ell_{n-1}\dots\ell_{r+2}}(t) \right. \\
 &\left. \left. + a_{\ell_n}^{b_n} Q_{ss\ell_1\dots\ell_n\dots\ell_{r+2}}(t) + a_{\ell_n+1}^{b_n} Q_{ss\ell_1\dots\ell_{n+1}\dots\ell_{r+2}}(t) \right] A_n^T \right\} \quad (5.28) \\
 &+ A_{r+3}Q_{r+1,r+2}(t) + Q_{r+1,r+2}(t)A_{r+3}^T + A_{r+4}Q_{r+2}(t) + Q_{r+2}(t)A_{r+4}^T \\
 &+ 4\pi S_0\theta^2(t) \begin{Bmatrix} 0 \\ 0 \\ 0 \\ 1 \end{Bmatrix} \langle 0 \ 0 \ 0 \ 1 \rangle \prod_{s=1}^{r+2} \delta_{\ell_s,0} ,
 \end{aligned}$$

where

$$\begin{aligned}
 Q_{r+1,r+2}(t) &= a_{\ell_{r+1}-1}^{b_{r+1}} a_{\ell_{r+2}-1}^{b_{r+2}} Q_{\mathbf{ss}\ell_1 \dots \ell_{r+1}-1, \ell_{r+2}-1}(t) \\
 &+ a_{\ell_{r+1}-1}^{b_{r+1}} a_{\ell_{r+2}}^{b_{r+2}} Q_{\mathbf{ss}\ell_1 \dots \ell_{r+1}-1, \ell_{r+2}}(t) + a_{\ell_{r+1}-1}^{b_{r+1}} a_{\ell_{r+2}+1}^{b_{r+2}} Q_{\mathbf{ss}\ell_1 \dots \ell_{r+1}-1, \ell_{r+2}+1}(t) \\
 &+ a_{\ell_{r+1}}^{b_{r+1}} a_{\ell_{r+2}-1}^{b_{r+2}} Q_{\mathbf{ss}\ell_1 \dots \ell_{r+1}, \ell_{r+2}-1}(t) + a_{\ell_{r+1}}^{b_{r+1}} a_{\ell_{r+2}}^{b_{r+2}} Q_{\mathbf{ss}\ell_1 \dots \ell_{r+1}, \ell_{r+2}}(t) \\
 &+ a_{\ell_{r+1}}^{b_{r+1}} a_{\ell_{r+2}+1}^{b_{r+2}} Q_{\mathbf{ss}\ell_1 \dots \ell_{r+1}, \ell_{r+2}+1}(t) + a_{\ell_{r+1}+1}^{b_{r+1}} a_{\ell_{r+2}-1}^{b_{r+2}} Q_{\mathbf{ss}\ell_1 \dots \ell_{r+1}+1, \ell_{r+2}-1}(t) \\
 &+ a_{\ell_{r+1}+1}^{b_{r+1}} a_{\ell_{r+2}}^{b_{r+2}} Q_{\mathbf{ss}\ell_1 \dots \ell_{r+1}+1, \ell_{r+2}}(t) + a_{\ell_{r+1}+1}^{b_{r+1}} a_{\ell_{r+2}+1}^{b_{r+2}} Q_{\mathbf{ss}\ell_1 \dots \ell_{r+1}+1, \ell_{r+2}+1}(t) ,
 \end{aligned} \tag{5.29}$$

$$\begin{aligned}
 Q_{r+2}(t) &= \bar{a}_{\ell_{r+2}-2}^{b_{r+2}} Q_{\mathbf{ss}\ell_1 \dots \ell_{r+2}-2}(t) + \bar{a}_{\ell_{r+2}-1}^{b_{r+2}} Q_{\mathbf{ss}\ell_1 \dots \ell_{r+2}-1}(t) \\
 &+ \bar{a}_{\ell_{r+2}}^{b_{r+2}} Q_{\mathbf{ss}\ell_1 \dots \ell_{r+2}}(t) + \bar{a}_{\ell_{r+2}+1}^{b_{r+2}} Q_{\mathbf{ss}\ell_1 \dots \ell_{r+2}+1}(t) \\
 &+ \bar{a}_{\ell_{r+2}+2}^{b_{r+2}} Q_{\mathbf{ss}\ell_1 \dots \ell_{r+2}+2}(t) ,
 \end{aligned} \tag{5.30}$$

and all other terms are as previously defined.

## 5.5 Description of the Example Problem

In Section 5.2, the physical system chosen for study was described. In what follows, the nominal properties of the primary-secondary system as well as the mean value properties of the filter parameters are presented.

The mass parameter  $m$  and stiffness parameters  $k$  of the primary system, previously defined, are chosen in such a way that the nominal natural frequencies of the primary system are as given in Table 5.1. It is noted that the fundamental

period of the system is 0.5 sec. A Rayleigh damping is considered with a 5% of critical damping in the first two modes.

mode	frequencies (Hz)
1	2.0
2	5.1
3	8.3
4	10.1
5	12.1

**Table 5.1** Natural frequencies of the primary system.

As noted previously, the secondary system is idealized as a single-degree of freedom oscillator, which is attached to the  $k$ -th d.o.f. of the primary system. In this particular example, the point of attachment is at the top of the primary system. The secondary system is assumed to have 2% of critical damping.

Due to their composite nature, primary-secondary systems possess some dynamics characteristics which significantly affect their response [41,42,43]. Among these are: (1) Tuning – which is the coincidence of the natural frequency of the secondary system with one or more natural frequencies of the primary system; and (2) Interaction – which is the feedback between the motions of the secondary system and the primary structure and results from the coupled nature of their equations of motion. Tuning gives rise to closely spaced modes in the composite primary-secondary system, and interaction reduces the response of the secondary system, particularly when the system is tuned and the ratio of secondary system to primary structure masses is sufficiently large.

In order to consider the effect of tuning on the response variability of the secondary system, four different ratios between the natural frequency of the secondary system  $\omega_s$  and the fundamental frequency of the primary system  $\omega_1$  are chosen. These are:  $\omega_s/\omega_1 = 0.5, 0.75, 1.25,$  and  $1.5$ . The cases  $\omega_s/\omega_1 = 0.75$  and  $1.25$  correspond to a nearly tuned condition for the secondary system. The effect of interaction on the response variability of the secondary system is taken into account by considering two different secondary system-to-floor mass ratio values  $\gamma$ . The selected values are  $\gamma = 0.01$  and  $\gamma = 0.1$ .

The filter parameters of the ground motion model are selected to be  $\omega_g = 4.0$  Hz and  $\xi_g = 0.3$  to represent a narrow banded excitation with high-frequency content, and  $\omega_g = 1.0$  Hz and  $\xi_g = 0.3$  to represent a narrow banded excitation with low-frequency content.

This completes the specification of the mean value properties of the system under consideration. The description of the uncertainties in the primary-secondary system, as well as in the filter parameters, is now discussed in detail.

In order to compare the relative importance of uncertainties in the system parameters on the response variability of the secondary system, three types of uncertainty are considered: uncertain ground motion parameters,  $\xi_g$  and  $\omega_g$ ; uncertain primary system interstory shear stiffness and damping; and uncertain secondary system support stiffness and damping ratio. In each type of uncertainty, only one parameter is treated as being random at a time. Furthermore, possible correlation between two different parameters is not taken into account. The representation of the uncertainties in the system parameters, under these assumptions, is presented in appendix A.

The probability density function for the system parameters is assumed to be of ultraspherical type, with a coefficient of variation of 40% for the damping coefficients, 30% for the stiffnesses, and 15% for the filter natural frequency  $\omega_g$ . These degrees of variability of the system parameters have been used elsewhere, and they are believed to be adequate to model the uncertainty of such parameters [44,45,46]. Figure 5.2 shows ultraspherical probability density functions with coefficients of variation of 15%, 30% and 40%.

As stated previously, the objective of this chapter is to investigate the influence of uncertainties in the system parameters and applied loads on the response variability of the secondary system. The response quantities to be considered in this example are the absolute acceleration of the secondary system and its displacement relative to the primary system. Then, the response processes are given by

$$\ddot{u}_s \text{ absolute} = \frac{1}{m_s} \{ (\dot{u}_5 - \dot{u}_s) c_s + (u_5 - u_s) k_s \}, \quad (5.31)$$

$$u_s \text{ relative} = u_s - u_5, \quad (5.32)$$

where

$m_s$  is the mass of the secondary system,

$c_s$  is the damping coefficient of the secondary system,

$k_s$  is the stiffness of the secondary system support,

$u_5$  is the displacement relative to the base of the fifth degree-of-freedom of the primary system, and

$u_s$  is the displacement of the secondary system relative to the base of the primary system.

Recall that, for a given set of deterministic system parameters, the response process described by equations (5.31) and (5.32) is a Gaussian process with zero mean. Due to the uncertainties in the system parameters, the standard deviation of this process is itself random, and it is completely defined by the components of the random covariance matrix  $Q_{ss}(\mathbf{b}, t)$ .

The effects of the statistical uncertainties in the system parameters on the response processes, previously defined, are presented in the following section.

## 5.6 Results of the Example Problem

Figures 5.3 through 5.6 show the influence of uncertainties in the filter parameters on the absolute acceleration response of the secondary system for the case of an excitation with high-frequency content ( $\omega_g = 4.0$  Hz). The duration of the excitation is equal to  $T_0 = 15T_1$ , where  $T_1$  is the fundamental period of the primary system. For each of these plots, the transient R.M.S. value of absolute acceleration of the secondary system is normalized by the stationary standard deviation response of the nominal system.

As these plots show, there is very little influence of the uncertainties in the filter parameters on the acceleration response of the secondary system. It is also noted that the effect of interaction is negligible. That is, the effect of the uncertainties in the filter parameters is nearly the same for both mass ratios. Thus, the uncertainties in the filter parameters has little influence on the response variability of the secondary system.

The influence of uncertainties in the primary system parameters are shown in Figures 5.7 through 5.10. Small influence is observed on the variability of the

absolute acceleration response by the uncertainty in the damping coefficient. At the same time, it is noted that the effect of interaction is almost negligible.

On the contrary, the uncertainty in the shear stiffness shows an important influence on the acceleration response variability of the secondary system. For the case  $\omega_s/\omega_1 = 1.25$  (Figure 5.8a) the mean plus one standard deviation value of the stationary solutions is more than twice the nominal stationary solution. Thus, the uncertainty of this parameter is of the same order of importance as the uncertainty in the input excitation. It is also noted that the effect of the uncertainty in the shear stiffness is strongly dependent of the mass ratio. The interaction effect reduces the response variability of the secondary system in more than 50% for the cases  $\omega_s/\omega_1 = 0.75$  and  $\omega_s/\omega_1 = 1.25$  (nearly tuned cases). For the other two cases, the feedback effect is less significant.

From these results, it is clear that uncertainty in the shear stiffness is much more significant than uncertainty in the damping parameter, even though the coefficient of variation of the stiffness (30%) is smaller than that of the damping (40%). This is due to the strong influence of tuning on the secondary response, particularly for small mass ratios, and the likelihood of such tuning when the stiffness is uncertain.

Finally, Figures 5.11 through 5.14 show the influence of uncertainties in the secondary system parameters on the absolute acceleration response process. Once again, it is clear that the uncertainty in stiffness is more significant than the uncertainty in damping. For all cases, the mean plus one standard deviation value of the stationary solution is less than 20% larger than the nominal stationary solution, when the damping coefficient is uncertain. The effect of uncertainty in this parameter is nearly the same for both mass ratios.

The uncertainty in stiffness has significant influence on the response process of the secondary system. For the case  $\omega_s/\omega_1 = 0.75$  (Figure 5.11b), the mean plus one standard deviation value of the stationary solution is more than twice the nominal stationary solution. Therefore, uncertainty in the stiffness parameter is again of the same order of importance as uncertainty in the stochastic input. It is also noted that the feedback effect on the response variability of the secondary system is quite significant. For example, the response variability is reduced in more than 45% for the cases  $\omega_s/\omega_1 = 0.75$  and  $\omega_s/\omega_1 = 1.25$  (nearly tuned cases).

The effects of the statistical uncertainties in the system parameters on the relative displacement response of the secondary system are qualitatively similar to those reported for the absolute acceleration response. That is, the high sensitivity of the response to uncertainty in the stiffness of the primary and secondary system, and the relatively low sensitivity of the response to uncertainty in the filter parameters.

For the case of the excitation with low-frequency content ( $\omega_g = 1.0$  Hz), similar results are obtained concerning the sensitivity of the response process of the secondary system when the primary and secondary system parameters were kept uncertain. However, the uncertainty in the filter natural frequency is more significant than in the case of the excitation with high-frequency content. This is reasonable, since the natural frequency of the filter is closer to the fundamental frequency of the primary system. To illustrate this result, Figure 5.15 shows the influence of uncertainties in the filter parameter on the absolute acceleration response of the secondary system for the case  $\omega_s/\omega_1 = 0.75$ . It is noted that the mean plus one standard deviation value of the stationary solution is about 40% higher than the nominal one, when the filter natural frequency is uncertain. Small influence is observed on the response variability by the uncertainty in the damping coefficient.

It is also noted that the effect of uncertainties in the filter parameters is nearly uniform for both mass ratios.

In summary, this analysis has shown that uncertainty in the stiffness parameters of the primary-secondary system may have equal or greater influence on the response variability of the secondary system than uncertainty in the input. As previously pointed out, the stiffness parameters determine the fundamental frequencies of the two systems which strongly influence the system response due to the effect of tuning. Also, uncertainty in the filter natural frequency may have some influence on the response variability of the secondary system, in particular, when the nominal ground motion model is nearly tuned with the primary system.

Finally, it is noted that the following orders of approximation in the probability space are used throughout this example. A fourth order approximation is used when the stiffness of the primary and secondary system are uncertain, and a second order approximation is used for the rest of the uncertainties. The influence of higher order approximation is found to have negligible influence on the response.

## 5.7 Application of the Results to Reliability Analysis

In the study of the response of dynamical systems to random excitation, a classical problem is to determine the probability that the value of some response variable will remain below a given threshold throughout a specified time interval. The probability distribution of the time required for the variable to first exceed the threshold is referred to as the first passage probability distribution. Knowledge of this distribution is of great practical importance in many engineering problems. Since first passage probabilities are often associated with failure probabilities, it is appropriate to use the term "safe" or "unsafe" to refer to the domain where the

random process is respectively below or above the threshold. The first passage problem consists of determining the probability distribution of the time when the trajectory of the response first leaves the safe region and enters the unsafe region.

Let  $W(T)$  be the probability that the magnitude of the relative displacement of the secondary system  $u_{s, \text{relative}}$  does not exceed a level  $\eta$  throughout the interval  $[0, T]$ . Hence,

$$W(T) = P_r \left[ |u_{s, \text{relative}}(t)|_{\max} < \eta ; 0 \leq t \leq T \right], \quad (5.33)$$

where  $P_r[\cdot]$  denotes the probability that the bracketed expression is true.  $W(T)$  is called the reliability function and is related to the first passage probability density through

$$P(T) = -\frac{dW}{dT}, \quad (5.34)$$

where  $P(T)dT$  is the probability that the first passage occurs on the interval  $[T, T + dT]$ .

Although the first passage problem for a linear oscillator may be precisely formulated [47], no closed-form solution for this problem has yet been presented. In the absence of an exact analytical solution, numerous approximate solutions have been proposed [48,49,50,51]. For the purpose of this example, the reliability function is evaluated using the analytical approach of Mason and Iwan [51]. It has been observed that the results of this method show generally good agreement with simulation results.

In this approach, the reliability function for the nonstationary response is given by

$$W(T) = \exp \left( - \int_0^T \alpha(t) dt \right), \quad (5.35)$$

where  $\alpha(t)$  is the limiting decay rate of the first crossing density or the average crossing rate. The approximation of this parameter is given by

$$\alpha(t) = \frac{-2\nu(\eta, t) \text{Ln}(P^*(t))}{\left[1 + q_{11}^2(t)/\sigma_s^4(t)\right] \left[1 - \nu(\eta, t)/\nu(0, t)\right]}, \quad (5.36)$$

where  $\nu(\eta, t)$  is the expected frequency of up-crossing of a level  $\eta$  and defined by

$$\nu(\eta, t) = \frac{\sqrt{\det Q}}{2\pi q_{11}} \left[ \exp\left(-\frac{\phi_{11}\eta^2}{2}\right) - \eta\phi_{12} \sqrt{\frac{\pi}{2\phi_{22}}} \exp\left(-\frac{\eta^2}{2q_{11}}\right) \text{erfc}\left(\frac{\eta\phi_{12}}{\sqrt{2\phi_{22}}}\right) \right] \quad (5.37)$$

for which  $\text{erfc}(\cdot)$  is the complementary error function,

$$\Phi = [\phi_{ij}(t)] = Q^{-1}(t) = [q_{ij}(t)]^{-1}, \quad (5.38)$$

and  $Q(t)$  is the covariance matrix of the joint probability density of  $u_s$  relative and  $\dot{u}_s$  relative at time  $t$ ,

$\nu(0, t)$  is the expected frequency of zero crossings with positive slope and defined by

$$\nu(0, t) = \frac{\sqrt{\det Q}}{2\pi q_{11}}, \quad (5.39)$$

$P^*(t)$  is a function of time and defined by

$$P^*(t) = \frac{1}{\text{erfc}\left(\frac{\eta}{\sqrt{2q_{11}}}\right)} \left\{ \frac{1}{2} \left[ 1 - \frac{\eta\sqrt{2/q_{11}}}{\sqrt{\pi(1-c^2)}} \right] [\text{erf}(y_1) - \text{erf}(y_2)] + \frac{c}{\pi\sqrt{1-c^2}} \left( e^{-y_2^2} - e^{-y_1^2} \right) + \text{erfc}(y_1) \right\} \quad (5.40)$$

for which  $\text{erf}(\cdot)$  is the error function,

$$c = \exp\left(\frac{-\pi\xi}{\sqrt{1-\xi^2}}\right), \quad (5.41)$$

$$y_1 = \frac{1}{c} \left( \frac{\eta}{\sqrt{2q_{11}}} + \frac{1}{2} \sqrt{\pi(1-c^2)} \right), \quad (5.42)$$

$$y_2 = \max \left[ \frac{\eta}{\sqrt{2q_{11}}}, \frac{1}{c} \left( \frac{\eta}{\sqrt{2q_{11}}} - \frac{1}{2} \sqrt{\pi(1-c^2)} \right) \right], \quad (5.43)$$

where  $\xi$  is the fraction of critical damping of the secondary system, and

$\sigma_s^2(t)$  is the stationary response variance of the secondary system associated with the instantaneous value of the excitation.

Note that the solution of the covariance matrix equation (equation 5.26) allows one to arrive at the response statistics necessary to compute the reliability function of the secondary system (equation 5.35). Also note that the randomness of the covariance matrix, due to the uncertainties in the system parameters, implies the randomness of the reliability function.

As it was shown in the previous section, the response of the secondary system is highly sensitive to uncertainties in the stiffness parameters of the system, particularly when the secondary system is nearly tuned and the mass ratio is small. The effects of the statistical uncertainties in the stiffness parameters on the reliability of the secondary system are shown in Figures 5.16 and 5.17.

These figures depict the probability of exceedancy  $P_E(T)$  versus time for the most sensitive cases presented in the previous section, that is, the system with uncertainty in the stiffness parameter of the primary system with  $\omega_s/\omega_1 = 1.25$ , and the system with uncertainty in the stiffness parameter of the secondary system with  $\omega_s/\omega_1 = 0.75$ . In these cases, the probability of exceedance is computed using

the mean plus one standard deviation value for the components of the covariance matrix. The time is normalized by the natural period of the secondary system and the duration of the excitation approaches infinity. Two threshold levels  $\eta$  are considered:  $\eta = \sigma_n$  and  $\eta = 2\sigma_n$ , where  $\sigma_n$  is the stationary standard deviation of the nominal system. Finally, note that  $P_E(T)$  is defined in terms of the reliability function as

$$P_E(T) = 1 - W(T) . \quad (5.44)$$

From these results, it is clear that uncertainty in the stiffness parameter has very significant influence on the reliability of the secondary system. The nominal case may considerably underestimate the probability of exceedance. The higher the threshold level, the more significant is the effect of stiffness uncertainty.

Finally, it is interesting to note that it is normally assumed that uncertainties in the parameters of a structural system, such as stiffness, have negligible effects on the response of the system to stochastic input. However, as it has been shown in this example, uncertainty in the stiffness parameters of a primary-secondary system, may have a strong influence on the reliability of the system. Therefore, these uncertainties should be properly accounted for in the reliability analysis of such systems.

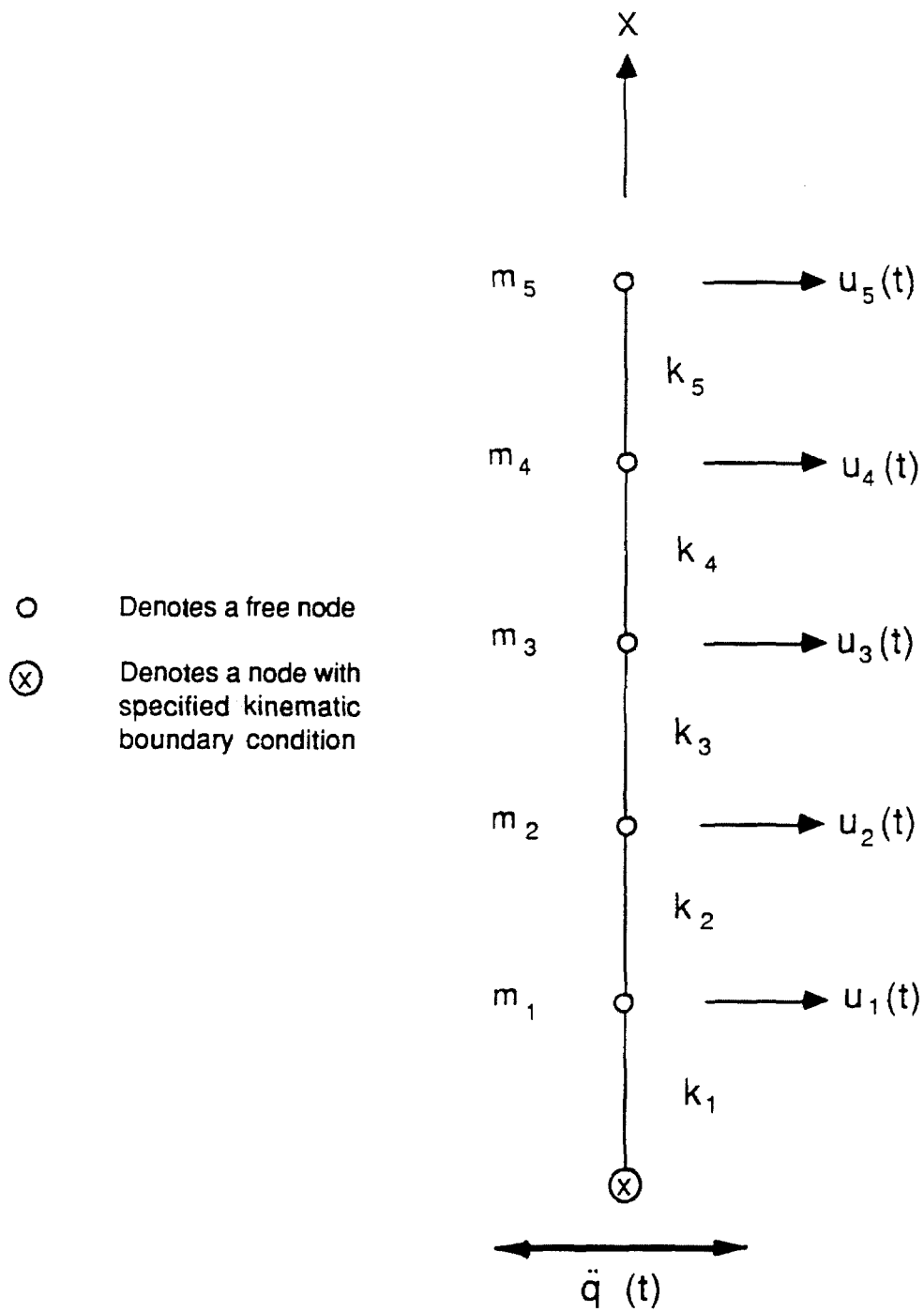
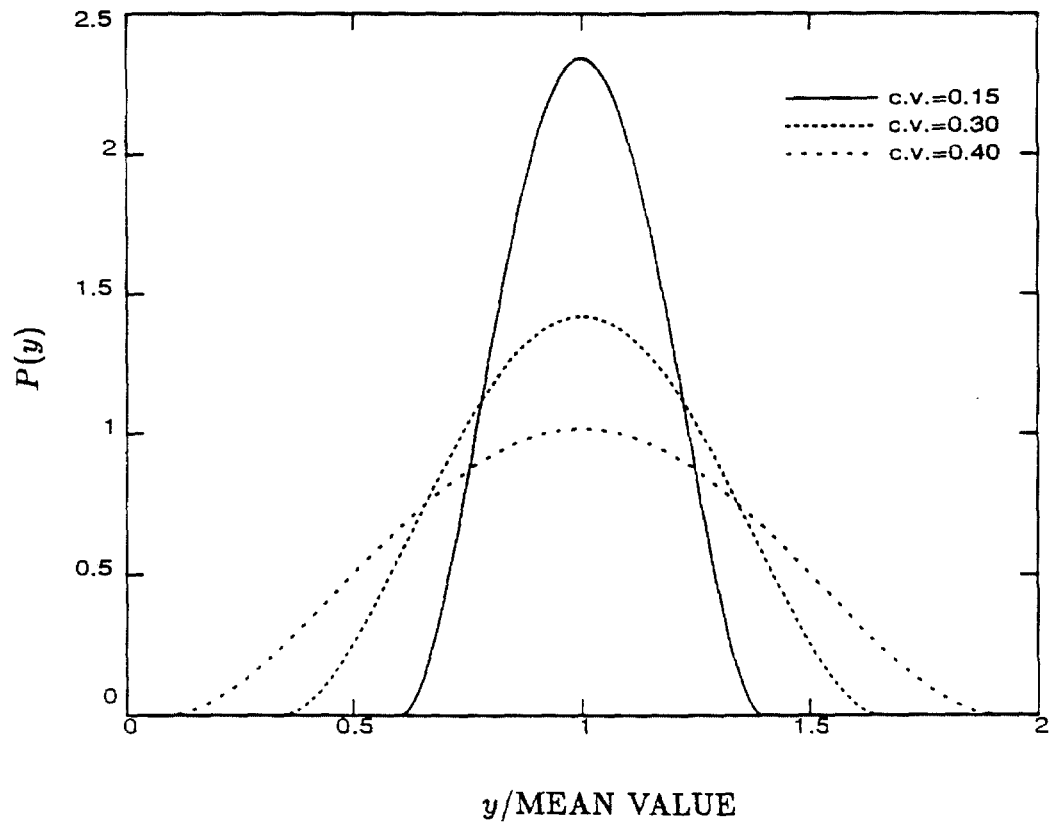
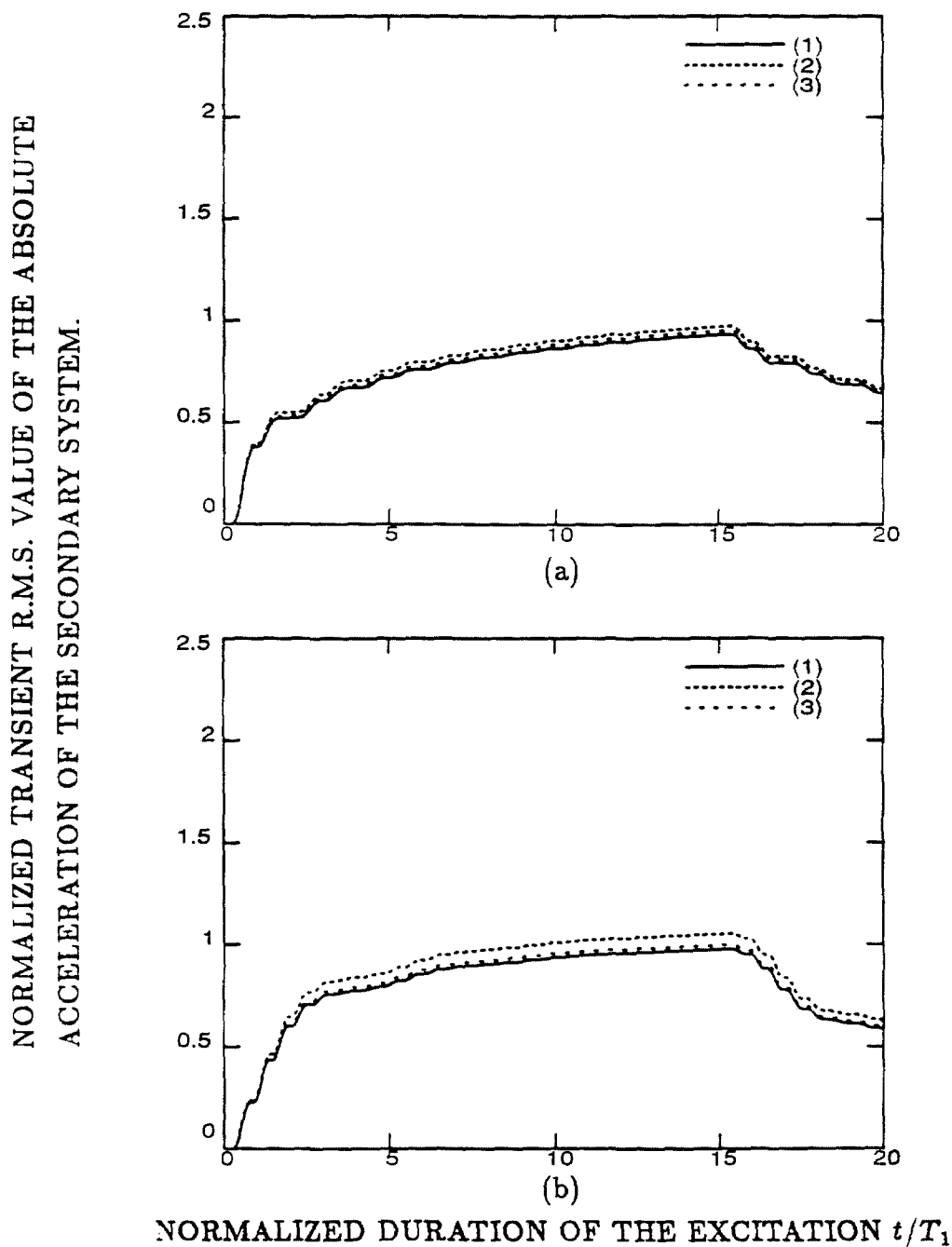


Figure 5.1: Finite element model for the primary system.

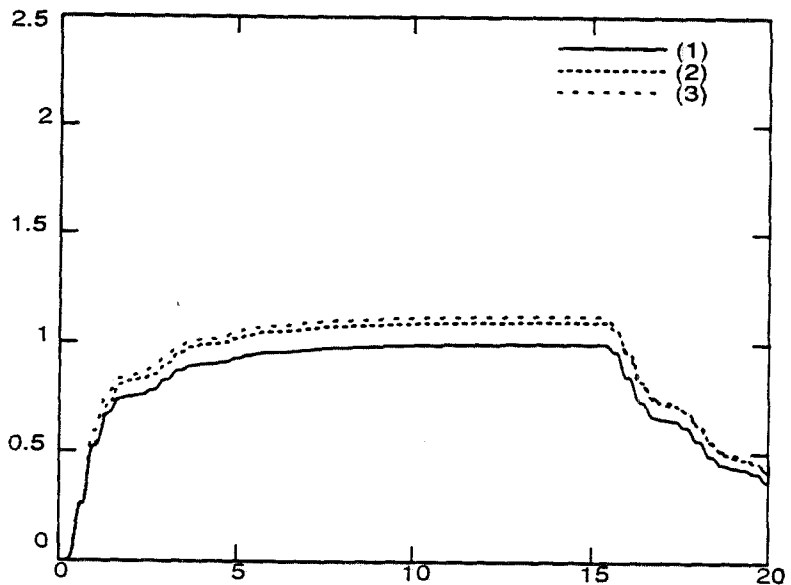
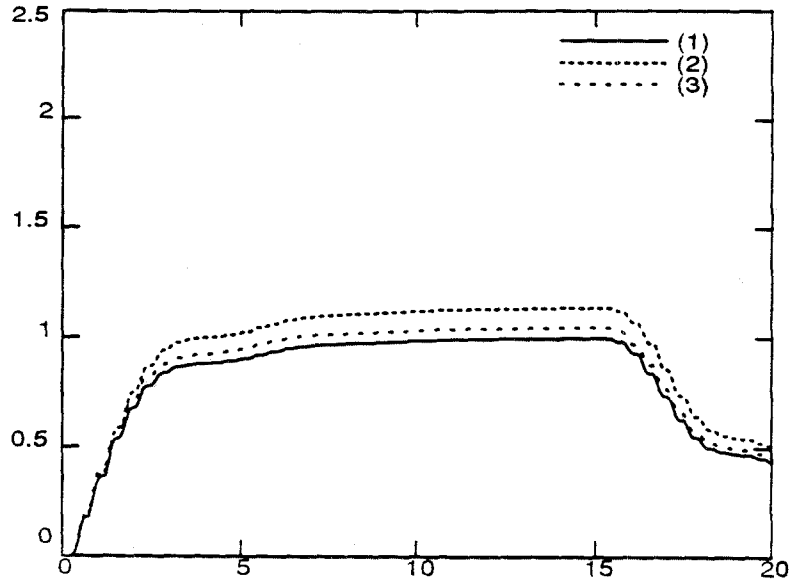


**Figure 5.2:** Ultraspherical probability density functions with coefficients of variation(c.v.) of 15%, 30% and 40%.



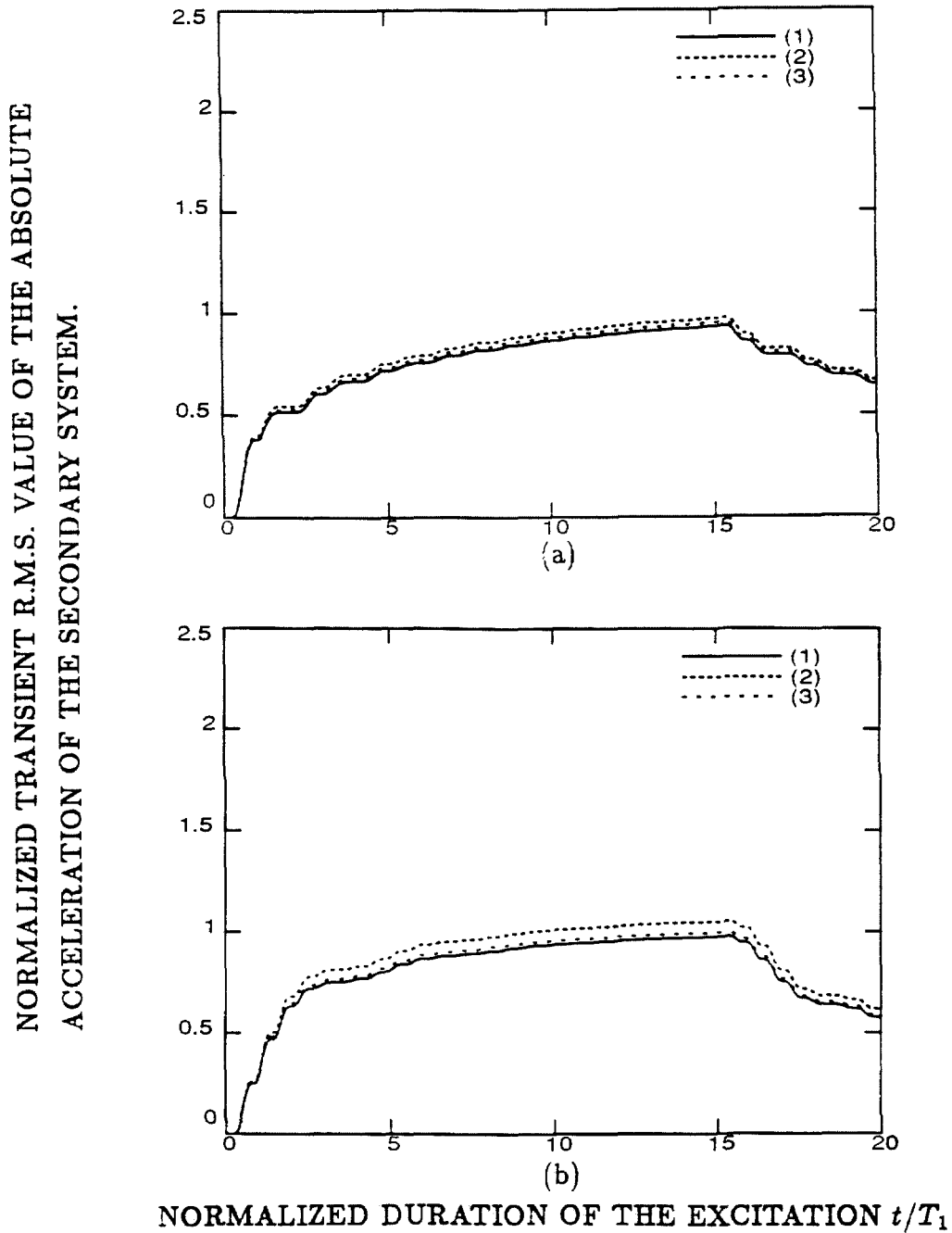
**Figure 5.3:** Effect of the uncertainties in the filter parameters on the response variability of the secondary system. Nominal filter parameters:  $\omega_g = 4.0$  Hz,  $\xi_g = 0.3$ . (1) Normalized nominal solution. (2) Normalized mean plus one standard deviation value of the solution when the frequency is uncertain. (3) Normalized mean plus one standard deviation value of the solution when the damping is uncertain. (a)  $\omega_s/\omega_1 = 0.50, \gamma = 0.01$ . (b)  $\omega_s/\omega_1 = 0.75, \gamma = 0.01$ .

NORMALIZED TRANSIENT R.M.S. VALUE OF THE ABSOLUTE  
ACCELERATION OF THE SECONDARY SYSTEM.



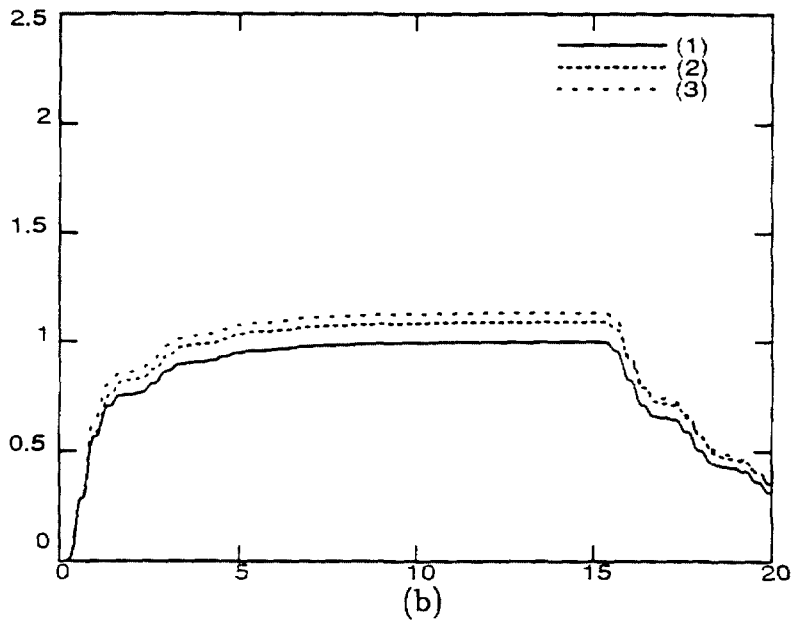
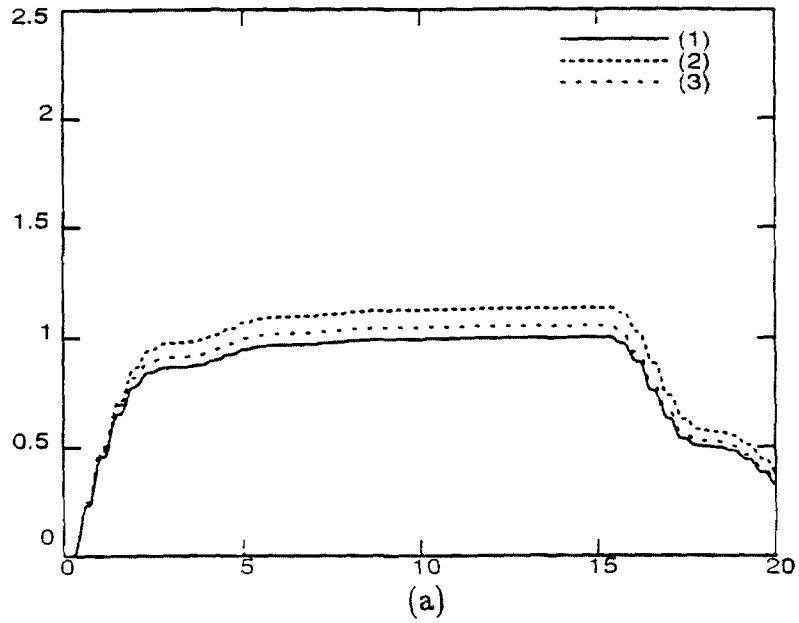
NORMALIZED DURATION OF THE EXCITATION  $t/T_1$

Figure 5.4: Effect of the uncertainties in the filter parameters on the response variability of the secondary system. Nominal filter parameters:  $\omega_g = 4.0$  Hz,  $\xi_g = 0.3$ . (1) Normalized nominal solution. (2) Normalized mean plus one standard deviation value of the solution when the frequency is uncertain. (3) Normalized mean plus one standard deviation value of the solution when the damping is uncertain. (a)  $\omega_s/\omega_1 = 1.25, \gamma = 0.01$ . (b)  $\omega_s/\omega_1 = 1.50, \gamma = 0.01$ .



**Figure 5.5:** Effect of the uncertainties in the filter parameters on the response variability of the secondary system. Nominal filter parameters:  $\omega_g = 4.0$  Hz,  $\xi_g = 0.3$ . (1) Normalized nominal solution. (2) Normalized mean plus one standard deviation value of the solution when the frequency is uncertain. (3) Normalized mean plus one standard deviation value of the solution when the damping is uncertain. (a)  $\omega_s/\omega_1 = 0.50, \gamma = 0.1$ . (b)  $\omega_s/\omega_1 = 0.75, \gamma = 0.1$ .

NORMALIZED TRANSIENT R.M.S. VALUE OF THE ABSOLUTE  
ACCELERATION OF THE SECONDARY SYSTEM.



NORMALIZED DURATION OF THE EXCITATION  $t/T_1$

**Figure 5.6:** Effect of the uncertainties in the filter parameters on the response variability of the secondary system. Nominal filter parameters:  $\omega_g = 4.0$  Hz,  $\xi_g = 0.3$ . (1) Normalized nominal solution. (2) Normalized mean plus one standard deviation value of the solution when the frequency is uncertain. (3) Normalized mean plus one standard deviation value of the solution when the damping is uncertain. (a)  $\omega_s/\omega_1 = 1.25, \gamma = 0.1$ . (b)  $\omega_s/\omega_1 = 1.50, \gamma = 0.1$ .

NORMALIZED TRANSIENT R.M.S. VALUE OF THE ABSOLUTE  
 ACCELERATION OF THE SECONDARY SYSTEM.

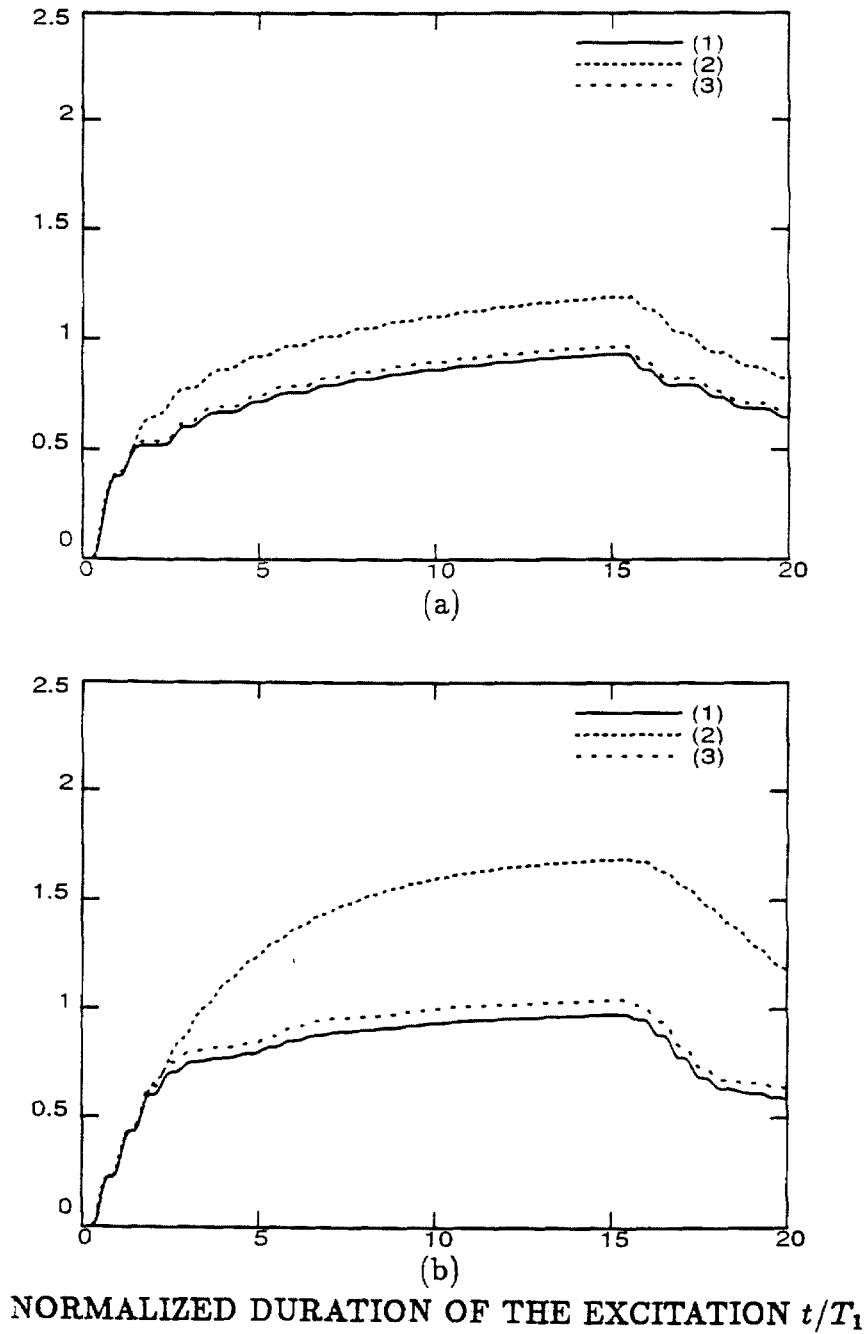
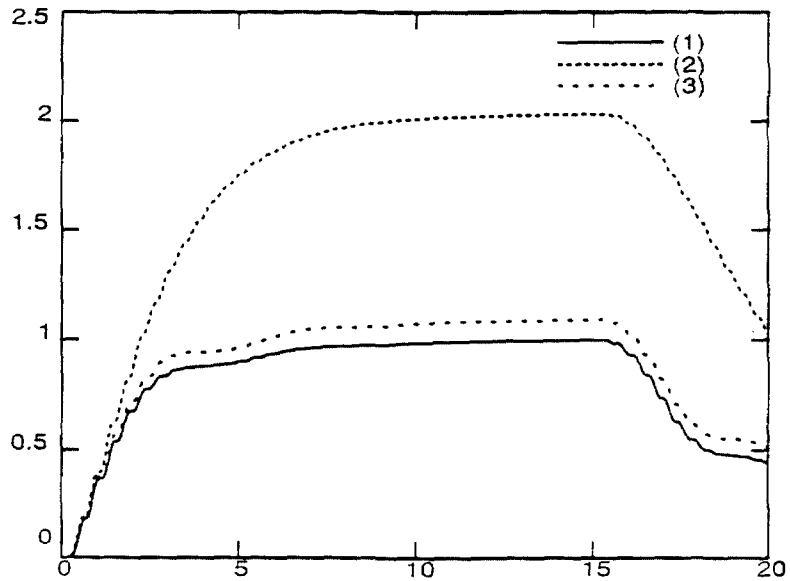
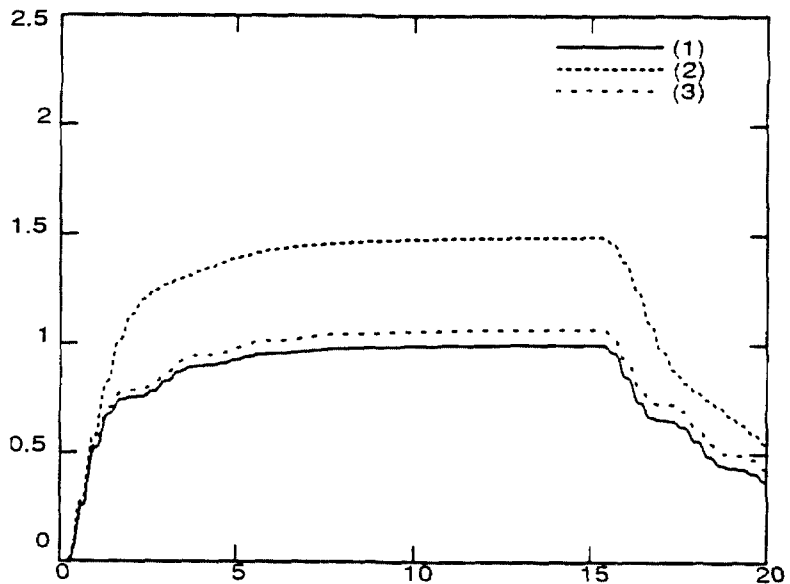


**Figure 5.7:** Effect of the uncertainties in the primary system parameters on the response variability of the secondary system. Nominal filter parameters:  $\omega_g = 4.0$  Hz,  $\xi_g = 0.3$ . (1) Normalized nominal solution. (2) Normalized mean plus one standard deviation value of the solution when the stiffness is uncertain. (3) Normalized mean plus one standard deviation value of the solution when the damping is uncertain. (a)  $\omega_s/\omega_1 = 0.50, \gamma = 0.01$ . (b)  $\omega_s/\omega_1 = 0.75, \gamma = 0.01$ .

NORMALIZED TRANSIENT R.M.S. VALUE OF THE ABSOLUTE  
ACCELERATION OF THE SECONDARY SYSTEM.



(a)



(b)

NORMALIZED DURATION OF THE EXCITATION  $t/T_1$

**Figure 5.8:** Effect of the uncertainties in the primary system parameters on the response variability of the secondary system. Nominal filter parameters:  $\omega_g = 4.0$  Hz,  $\xi_g = 0.3$ . (1) Normalized nominal solution. (2) Normalized mean plus one standard deviation value of the solution when the stiffness is uncertain. (3) Normalized mean plus one standard deviation value of the solution when the damping is uncertain. (a)  $\omega_s/\omega_1 = 1.25, \gamma = 0.01$ . (b)  $\omega_s/\omega_1 = 1.50, \gamma = 0.01$ .

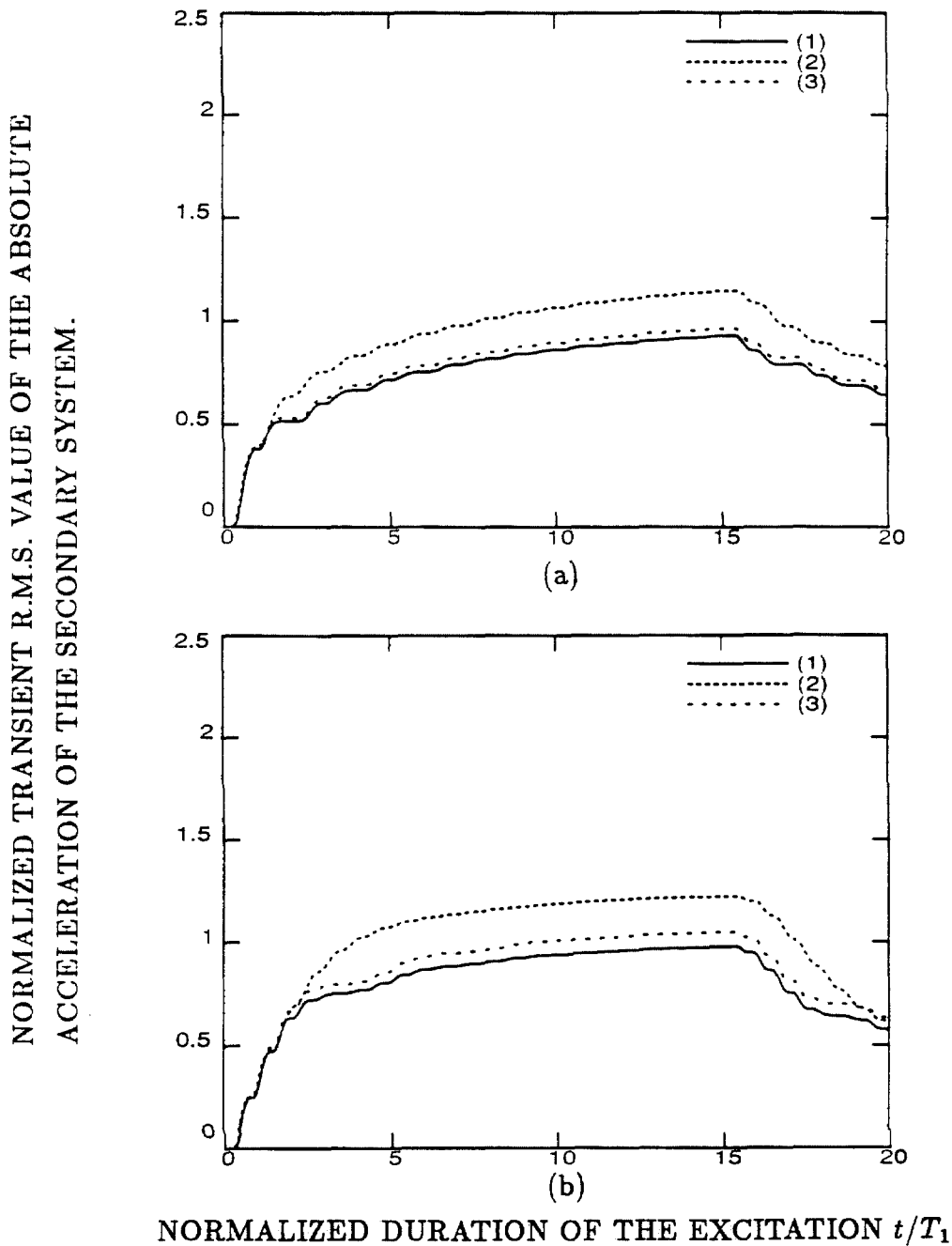


**Figure 5.9:** Effect of the uncertainties in the primary system parameters on the response variability of the secondary system. Nominal filter parameters:  $\omega_g = 4.0$  Hz,  $\xi_g = 0.3$ . (1) Normalized nominal solution. (2) Normalized mean plus one standard deviation value of the solution when the stiffness is uncertain. (3) Normalized mean plus one standard deviation value of the solution when the damping is uncertain. (a)  $\omega_s/\omega_1 = 0.50, \gamma = 0.1$ . (b)  $\omega_s/\omega_1 = 0.75, \gamma = 0.1$ .

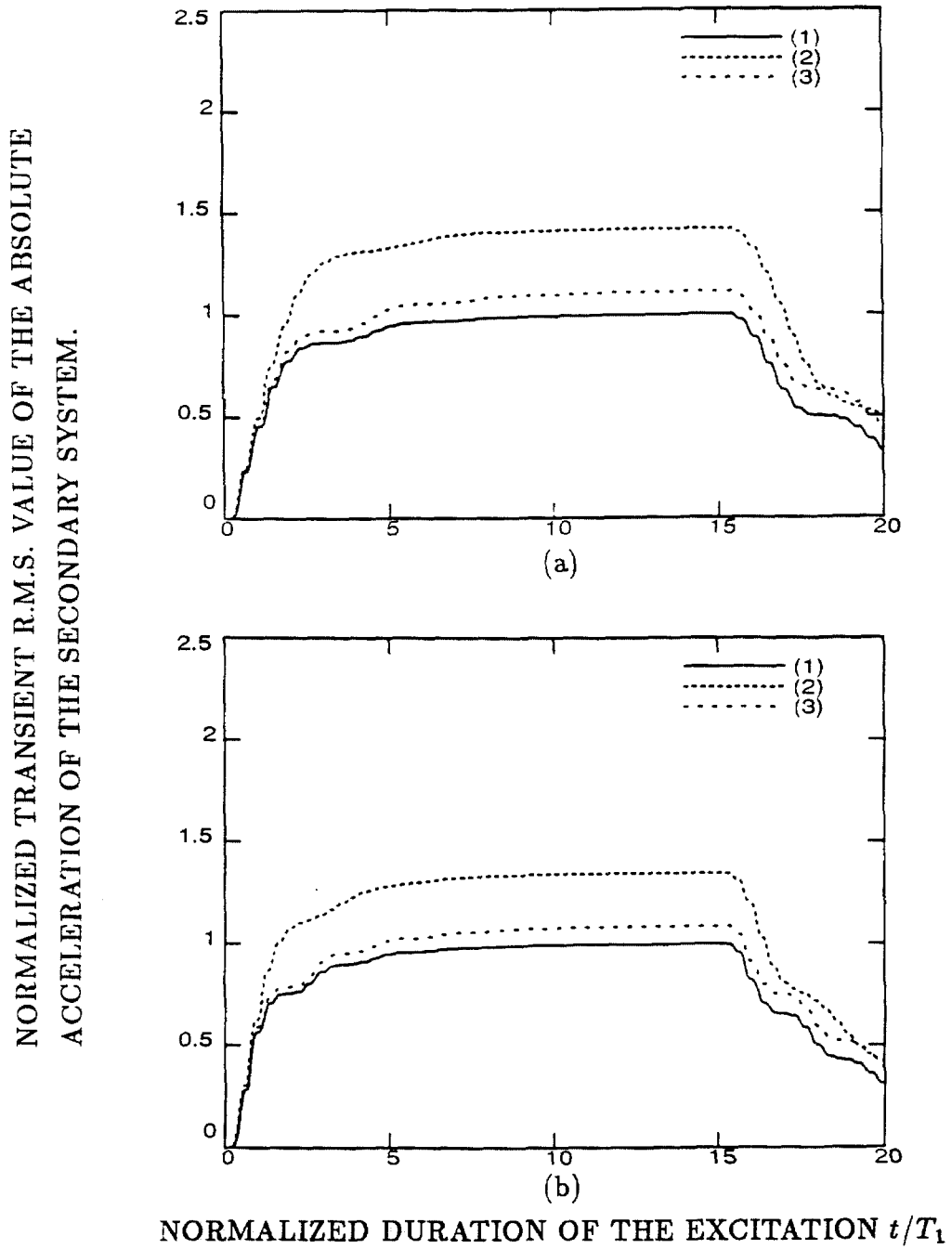
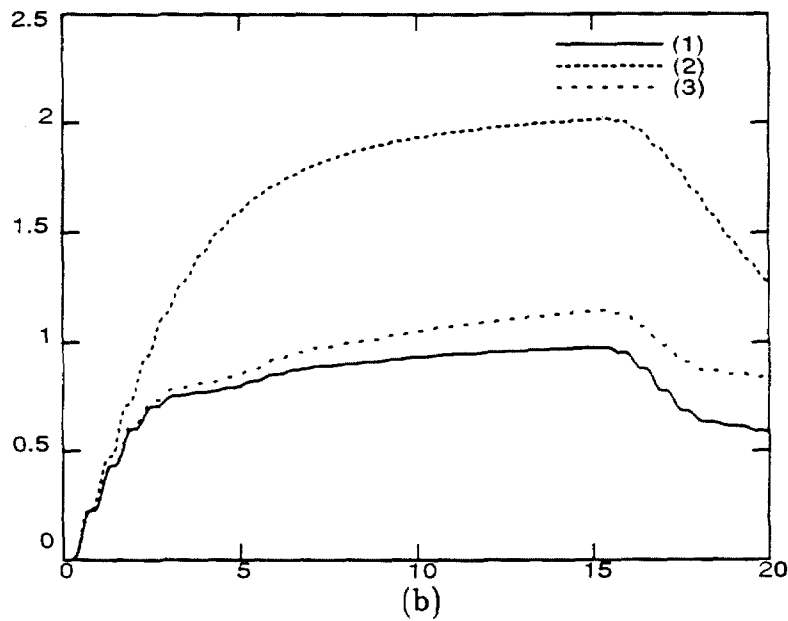
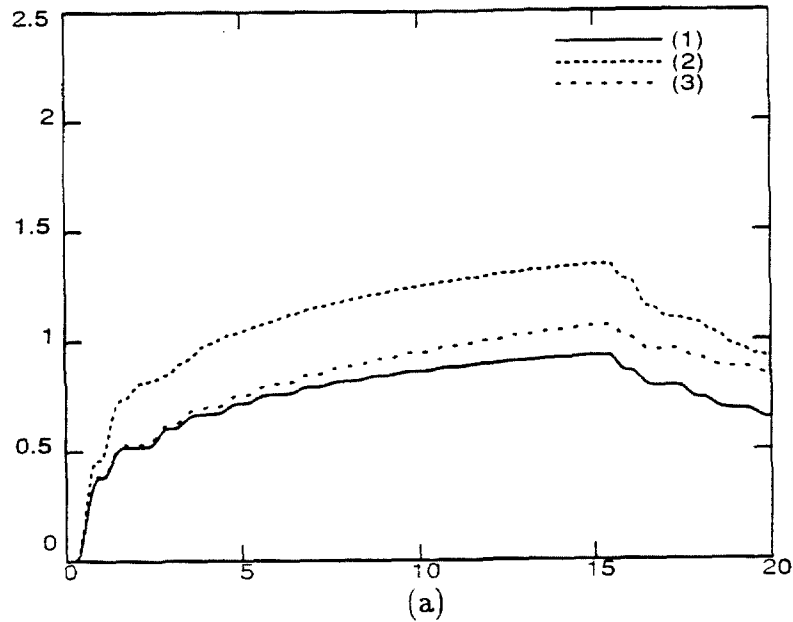


**Figure 5.10:** Effect of the uncertainties in the primary system parameters on the response variability of the secondary system. Nominal filter parameters:  $\omega_g = 4.0$  Hz,  $\xi_g = 0.3$ . (1) Normalized nominal solution. (2) Normalized mean plus one standard deviation value of the solution when the stiffness is uncertain. (3) Normalized mean plus one standard deviation value of the solution when the damping is uncertain. (a)  $\omega_s/\omega_1 = 1.25, \gamma = 0.1$ . (b)  $\omega_s/\omega_1 = 1.50, \gamma = 0.1$ .

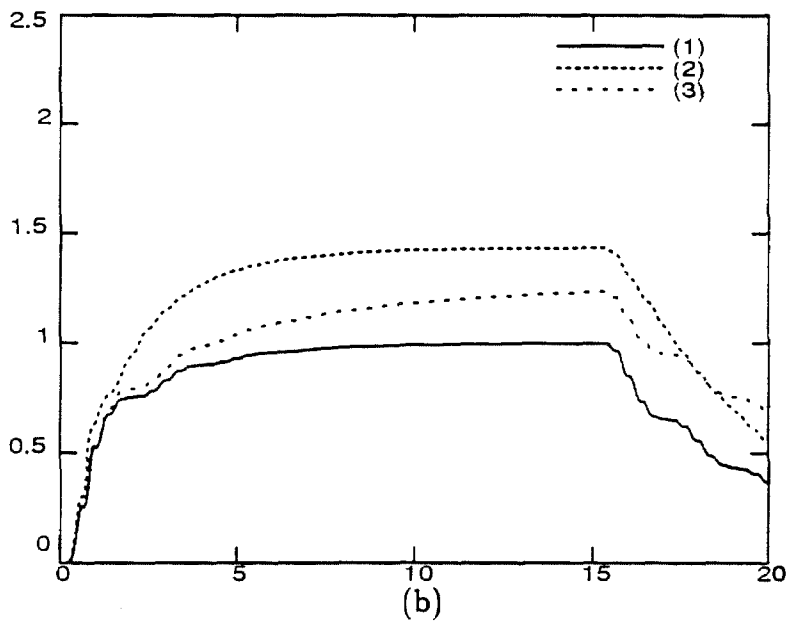
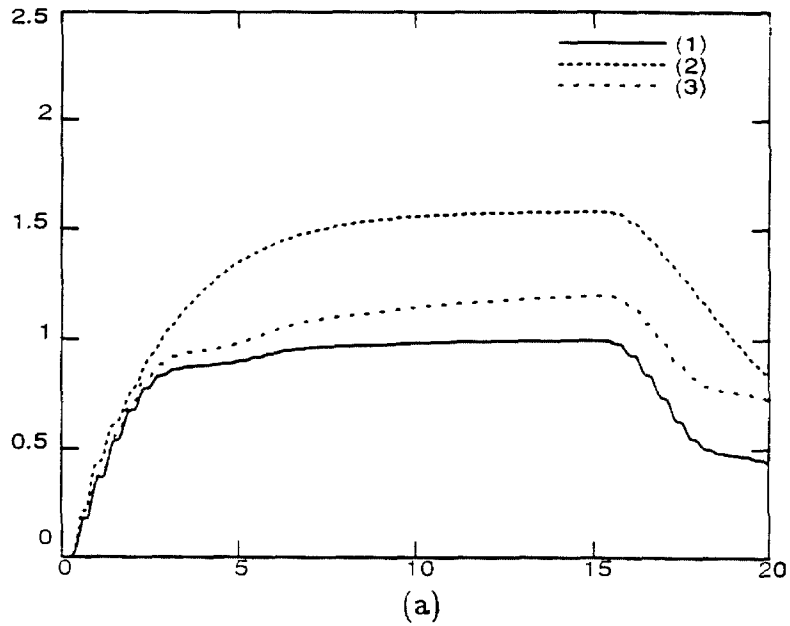
NORMALIZED TRANSIENT R.M.S. VALUE OF THE ABSOLUTE  
 ACCELERATION OF THE SECONDARY SYSTEM.



NORMALIZED DURATION OF THE EXCITATION  $t/T_1$

**Figure 5.11:** Effect of the uncertainties in the secondary system parameters on the response variability of the secondary system. Nominal filter parameters:  $\omega_g = 4.0$  Hz,  $\xi_g = 0.3$ . (1) Normalized nominal solution. (2) Normalized mean plus one standard deviation value of the solution when the stiffness is uncertain. (3) Normalized mean plus one standard deviation value of the solution when the damping is uncertain. (a)  $\omega_s/\omega_1 = 0.50, \gamma = 0.01$ . (b)  $\omega_s/\omega_1 = 0.75, \gamma = 0.01$ .

NORMALIZED TRANSIENT R.M.S. VALUE OF THE ABSOLUTE  
 ACCELERATION OF THE SECONDARY SYSTEM.



NORMALIZED DURATION OF THE EXCITATION  $t/T_1$

**Figure 5.12:** Effect of the uncertainties in the secondary system parameters on the response variability of the secondary system. Nominal filter parameters:  $\omega_g = 4.0$  Hz,  $\xi_g = 0.3$ . (1) Normalized nominal solution. (2) Normalized mean plus one standard deviation value of the solution when the stiffness is uncertain. (3) Normalized mean plus one standard deviation value of the solution when the damping is uncertain. (a)  $\omega_s/\omega_1 = 1.25, \gamma = 0.01$ . (b)  $\omega_s/\omega_1 = 1.50, \gamma = 0.01$ .

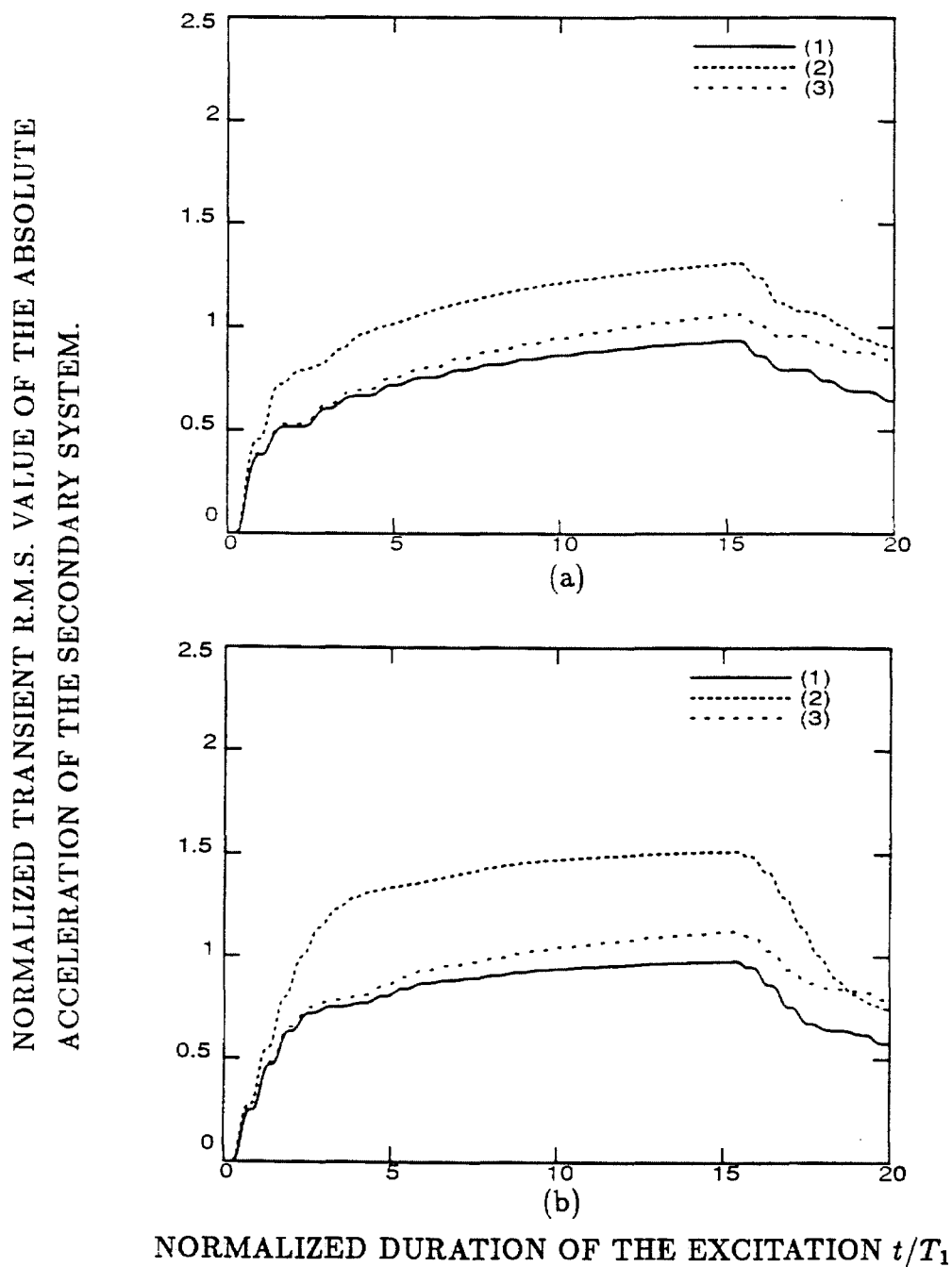


**Figure 5.13:** Effect of the uncertainties in the secondary system parameters on the response variability of the secondary system. Nominal filter parameters:  $\omega_g = 4.0$  Hz,  $\xi_g = 0.3$ . (1) Normalized nominal solution. (2) Normalized mean plus one standard deviation value of the solution when the stiffness is uncertain. (3) Normalized mean plus one standard deviation value of the solution when the damping is uncertain. (a)  $\omega_s/\omega_1 = 0.50, \gamma = 0.1$ . (b)  $\omega_s/\omega_1 = 0.75, \gamma = 0.1$ .

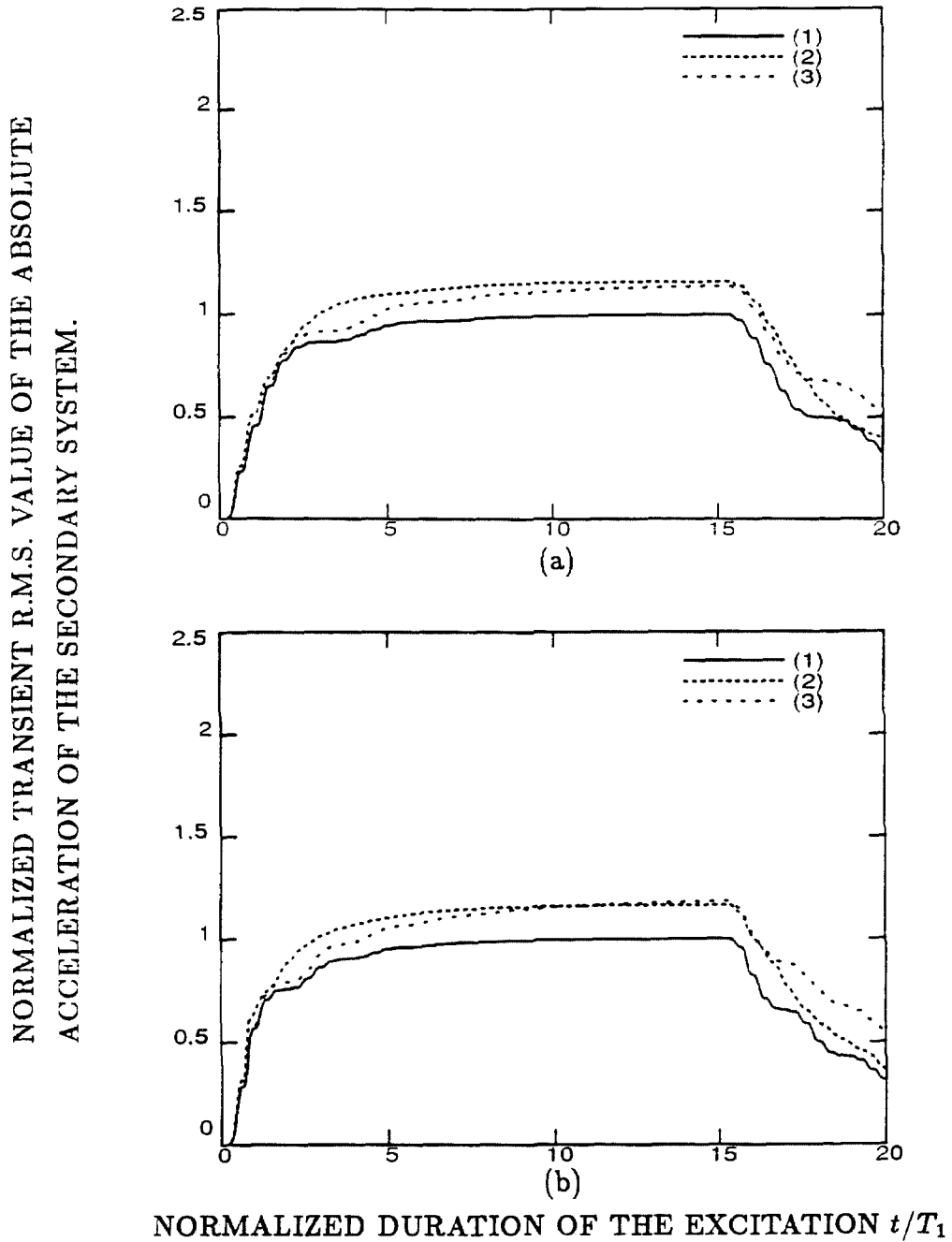
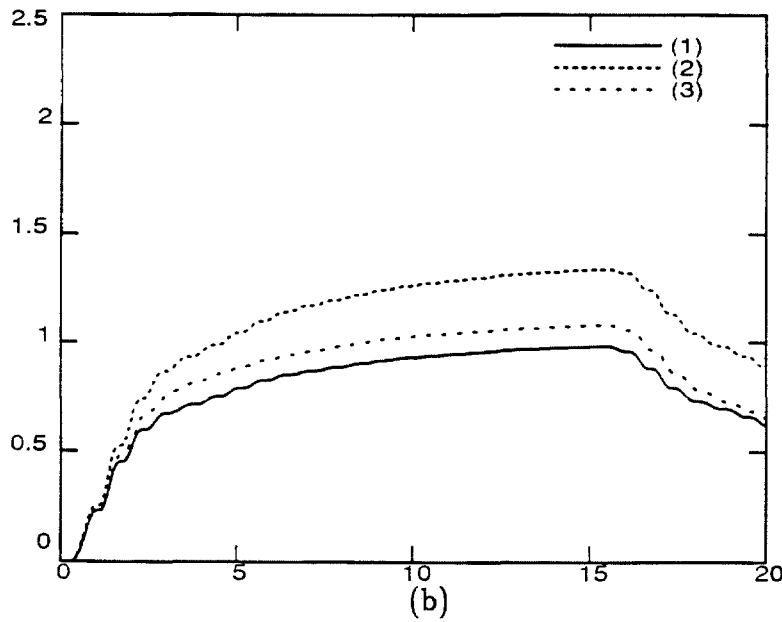
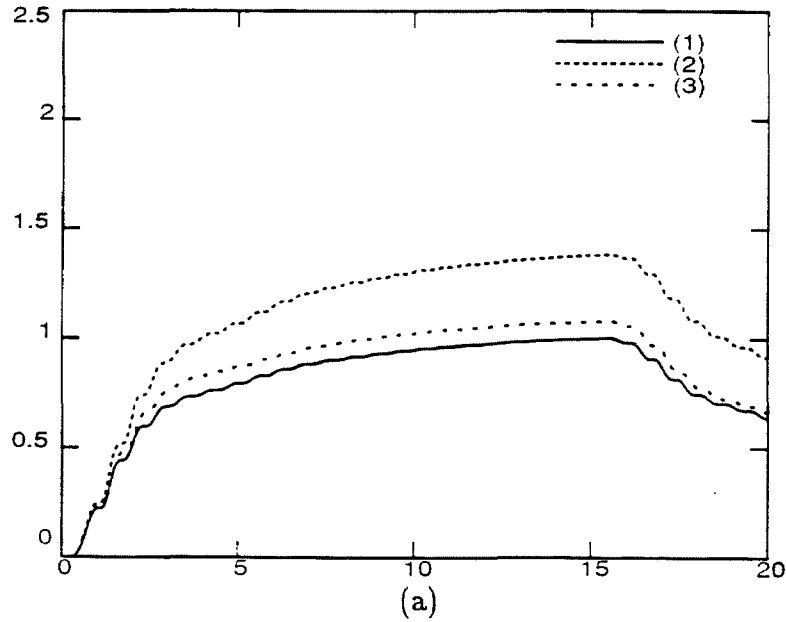


**Figure 5.14:** Effect of the uncertainties in the secondary system parameters on the response variability of the secondary system. Nominal filter parameters:  $\omega_g = 4.0$  Hz,  $\xi_g = 0.3$ . (1) Normalized nominal solution. (2) Normalized mean plus one standard deviation value of the solution when the stiffness is uncertain. (3) Normalized mean plus one standard deviation value of the solution when the damping is uncertain. (a)  $\omega_s/\omega_1 = 1.25, \gamma = 0.1$ . (b)  $\omega_s/\omega_1 = 1.50, \gamma = 0.1$ .

NORMALIZED TRANSIENT R.M.S. VALUE OF THE ABSOLUTE  
ACCELERATION OF THE SECONDARY SYSTEM.



NORMALIZED DURATION OF THE EXCITATION  $t/T_1$

Figure 5.15: Effect of the uncertainties in the filter parameters on the response variability of the secondary system. Nominal filter parameters:  $\omega_g = 1.0$  Hz,  $\xi_g = 0.3$ . (1) Normalized nominal solution. (2) Normalized mean plus one standard deviation value of the solution when the frequency is uncertain. (3) Normalized mean plus one standard deviation value of the solution when the damping is uncertain. (a)  $\omega_s/\omega_1 = 0.75, \gamma = 0.01$ . (b)  $\omega_s/\omega_1 = 0.75, \gamma = 0.1$ .

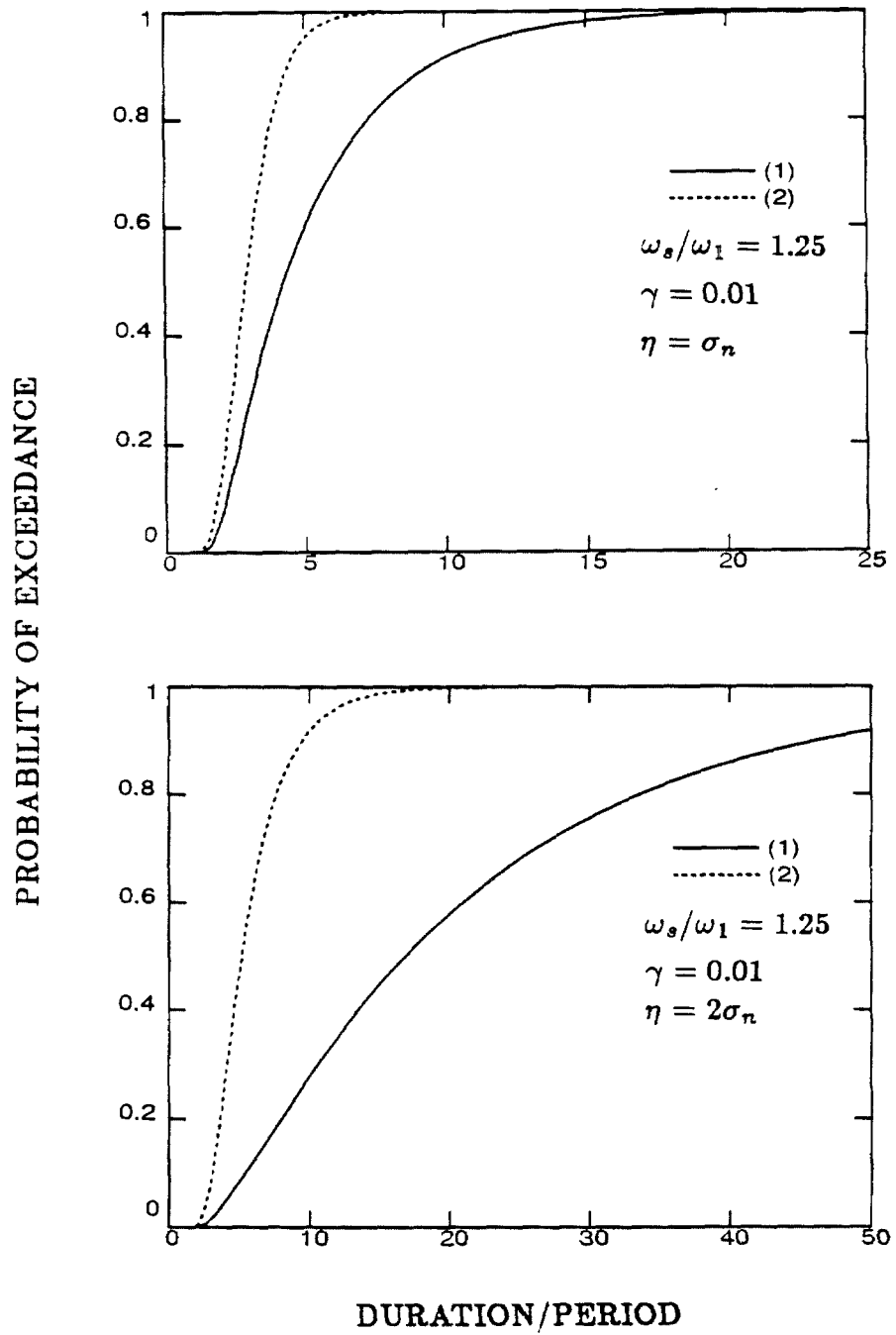


**Figure 5.16:** Probability of exceeding the threshold level  $\eta$  versus time for the relative displacement of the secondary system. Nominal filter parameters:  $\omega_g = 4.0$  Hz,  $\xi_g = 0.3$ . (1) Probability of exceedance for the nominal system. (2) Probability of exceedance for the system with uncertainty in the stiffness parameter of the primary system.

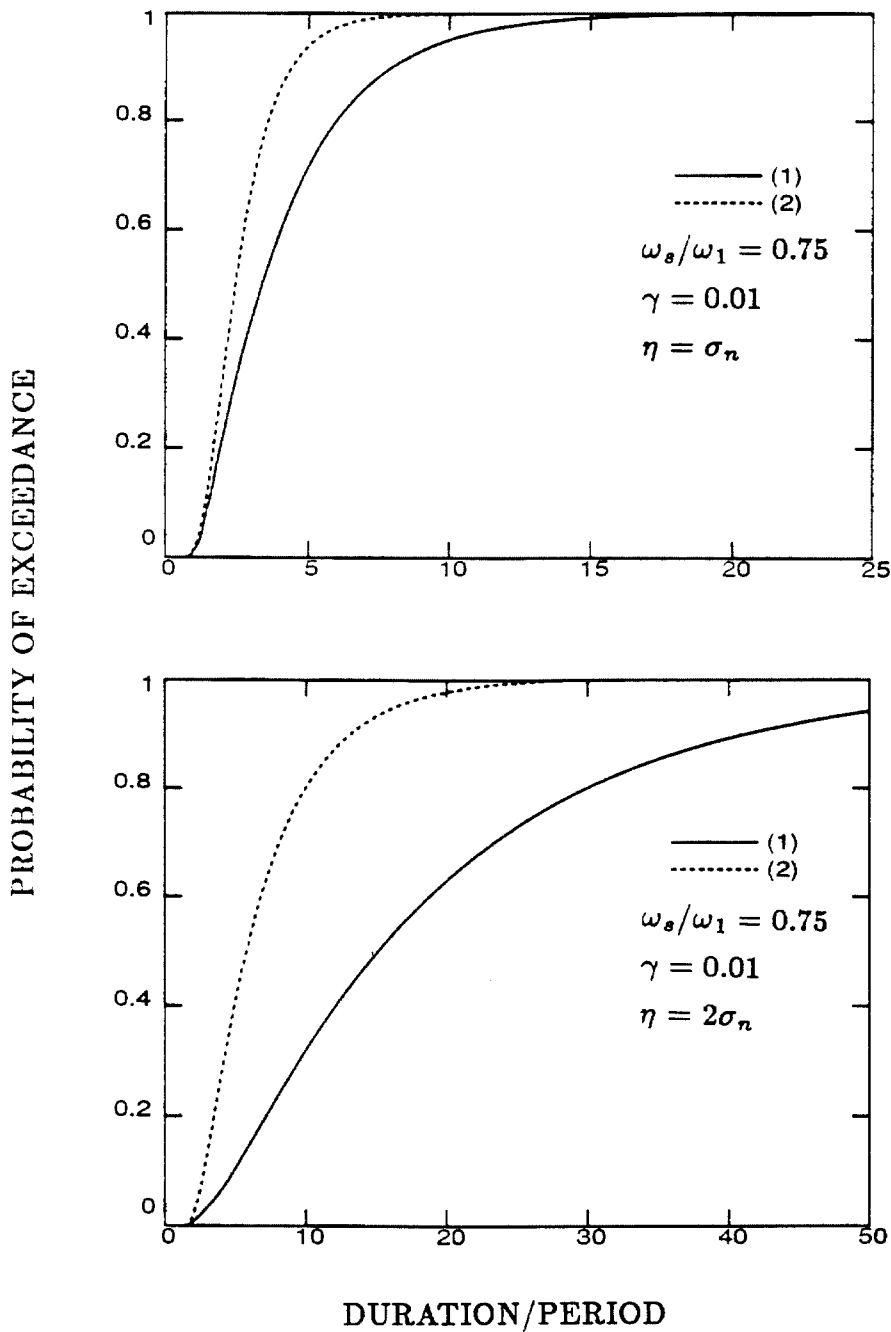


Figure 5.17: Probability of exceeding the threshold level  $\eta$  versus time for the relative displacement of the secondary system. Nominal filter parameters:  $\omega_g = 4.0$  Hz,  $\xi_g = 0.3$ . (1) Probability of exceedance for the nominal system. (2) Probability of exceedance for the system with uncertainty in the stiffness parameter of the secondary system.

## Chapter 6

### Summary and Conclusions

This thesis presents a new method for the dynamic analysis of linear structural systems with parameter uncertainties. The motivation of this investigation together with a brief description of existing analysis approaches are presented in Chapter 1.

In Chapter 2, the problem is specified and a general form of the governing partial differential equation with random coefficients is given. This is followed by the characterization for random fields which is used to represent the spatial variation of the material properties of the system and the spatial variation of the external loads. The strong form of the problem and its variational counterpart are then presented. The variational formulation of the problem is solved using Galerkin's method together with the finite element method for the spatial discretization. Random shape functions are introduced to approximate the solution in the spatial domain and in the probability space. A system of linear ordinary differential equations for the unknowns of the problem is then derived and integrated in time. Finally, the response variability is computed.

It is observed that the newly developed solution method represents an extension of the deterministic finite element method to problems involving parameter uncertainties. The application of this new method to the solution of one specific system of engineering interest is described in Chapter 3. The system chosen for study is

a one-dimensional continuum described by the wave equation in which the physical properties exhibit a one-dimensional spatial random variation. As a physical conceptualization of this equation, a base-excited shear beam whose rigidity varies randomly along its length is chosen for study. It is observed that the response variability of the absolute acceleration at the free end of the beam is relatively high.

Some engineering applications of these results are discussed in both an earthquake ground motion and a structural context. In an earthquake ground motion context, one might think of a shear beam as a column of soil excited by bedrock motions. Then, the surface motions are represented by the free end of the beam, and the uncertainty of such motions is represented by the response variability at the top of the beam. The computed surface motions from the soil column are used as a base excitation for a simple single-degree-of-freedom system, and the effects of the uncertainty of these surface motions on this simple system are discussed. It is observed that this uncertainty may cause significant changes in the dynamic characteristics of the simple system.

From a structural engineering point of view, one might consider the shear beam to be a shear structure, such a shear building. Then, the response uncertainty at the top of the beam represents the top floor response variability. The effects of this response variability on the response of a substructure located at the top of the building are discussed. The substructure, which may represent a piece of equipment or a secondary system, is idealized as a single-degree-of-freedom system. It is observed that the presence of uncertainties in the superstructure rigidity properties can markedly alter the substructure response characteristics.

The validation calculations presented in Chapter 3 show that the results from the new method agree well with those of Monte-Carlo simulation and numerical integration. It is observed that, for the test problems considered in these calculations, the new formulation is more economical than simulation. These validation calculations also show the inaccuracy of the perturbation method in dynamic problems, and the high nonlinearity of the response as a function of the uncertain system parameters.

The extension of the method described in Chapter 2 to cases where the excitation is random in time is developed in Chapter 4. The response uncertainty is now caused by the spatial randomness in material properties and external loads as well as the time history uncertainty of the forcing function. The forcing function is modeled as a modulated Gaussian white noise process. It follows that the response of the system given its properties is a Gaussian process which is characterized by its covariance matrix, but due to the uncertainties in spatial properties, this characterization is itself random, that is, the coefficients of the covariance matrix are random variables.

Two procedures to derive the random response covariance matrix are presented. In the first, the Liapunov equation for the response covariance matrix is derived directly from the system of linear ordinary differential equations for the unknowns defined in Chapter 2. Then, the Liapunov equation is integrated in time and the response statistics are computed. In the alternative procedure, a random first order differential equation for the evolution of the nonstationary covariance matrix with time is first derived. Next, a set of differential equations for the unknowns is obtained, and this set is integrated in time to find the response variability and statistics. One of the advantages of this alternative formulation is that the second

moment characterization of the Gaussian response process is completely defined by the components of the random covariance matrix defined herein, and does not require the solution of a multiple integral in the probability space, unlike the first procedure.

Chapter 5 describes the application of the solution method described in Chapter 4 to the random response of primary-secondary systems. A simple five degree-of-freedom model representing a shear building is chosen as the primary system while a single-degree-of-freedom oscillator is used to model the secondary system. The combined primary-secondary system is subjected to a random base excitation. Some stochastic models of ground motions are discussed and the particular model for the random base excitation used in this application is presented.

Later in Chapter 5, the general formulation of the covariance equation, described in Chapter 4, is specialized for the particular problem under consideration. This is followed by the description of the nominal properties of the system, and by the description of the uncertainties in the primary-secondary system as well as the uncertainties in the parameters of the ground motion model.

In the last part of Chapter 5, the effects of statistical uncertainties in the system parameters on the absolute acceleration response of the secondary system and on its displacement relative to the primary system are presented. It is found that uncertainty in the stiffness parameters of the primary-secondary system may have equal or greater influence on the response variability of the secondary system than uncertainty in the stochastic input. Finally, the application of these results to reliability analysis is presented. The reliability function of the secondary system is evaluated using the analytical approach given by Mason and Iwan, and the effects of statistical uncertainties in the system parameters on this reliability function are

discussed. It is found that the uncertainty in the stiffness parameters of the primary-secondary system has very significant influence on the reliability of the secondary system.

In conclusion, the newly developed method is seen to be a powerful tool for obtaining the random response of a linear continuous or discrete system in which the system parameters are permitted to have spatially random properties, and the external loads are permitted to have time history uncertainties as well as spatially random properties. It has been shown to perform well on two application problems. Although the numerical solution of problems involving parameter uncertainties is quite computationally intensive when compared with deterministic analysis, this method could handle complex engineering problems using present supercomputers. This capability is expected to grow rapidly in the coming years given the current rate of progress in supercomputing power.

Finally, the following paragraphs suggest some possible applications and extensions of the present work.

It is noted that the new formulation could be easily extended to consider partial differential equations of order higher than two. This class of equations allows the modeling of many structures of interest in mechanical and civil engineering. Among these are structures modeled with beam elements, plate elements, and shell elements. Therefore, the new method could be extended to the area of structural finite elements. This extension would allow random response solutions for a broad range of complex engineering problems.

As mentioned in Chapter 2, the response variability of structural quantities other than displacements and accelerations could also be computed. For example,

stresses, strains, and member forces could be computed. These quantities are obviously useful in assessing the structural response. Modifications in the formulation of the new method to permit randomness in the mass of the system, and randomness in boundary and initial conditions could also be considered. These would permit consideration of a wide variety of problems.

Additional areas of possible applications of the present work are those of sensitivity of structural performance to parameter variations, design optimization, and reliability analysis. Finally, an area for further work involves the extension of the method to systems exhibiting nonlinear behavior.

## References

- [1] Astill, C.J., Nosseir, S.B., and Shinozuka, M., "Impact Loading on Structures with Random Properties," *Journal of Structural Mechanics*, **1**(1), 1972, pp. 63-77.
- [2] Shinozuka, M., "Monte Carlo Solution of Structural Dynamics," *International Journal of Computers and Structures*, **2**, 1972, pp. 855-874.
- [3] Shinozuka, M. and Jan, C.M., "Digital Simulation of Random Processes and Its Applications," *Journal of Sound and Vibration*, **25**, 1972, pp. 111-128.
- [4] Caravani, P. and Thomson, W.T., "Frequency Response of a Dynamic System with Statistical Damping," *AIAA Journal*, **11**(2), 1973, pp. 170-173.
- [5] Shinozuka, M., *Stochastic Mechanics*, Vol. III, Department of Civil Engineering and Operations Research, Princeton University, 1988.
- [6] Chen, P.C. and Soroka, W.W., "Impulse Response of a Dynamic System with Statistical Properties," *Journal of Sound and Vibration*, **31**, 1973, pp. 309-314.
- [7] Chen, P.C. and Soroka, W.W., "Multi-Degree Dynamic Response of a System with Statistical Properties," *Journal of Sound and Vibration*, **37**(4), 1974, pp. 547-556.
- [8] Soong, T.T. and Cozzarelli, F.A., "Vibration of Disordered Structural Systems," *The Shock and Vibration Digest*, **8**(5), 1976, pp. 21-35.
- [9] Contreras, H., "The Stochastic Finite Element Method," *Computers and Structures*, **12**, 1980, pp. 341-348.
- [10] Hisada, T. and Nakagiri, S., "Stochastic Finite Element Method Developed for Structural Safety and Reliability," *3rd International Conference on Structural Safety and Reliability*, Trondheim, Norway, 1981.

- [11] Hisada, T. and Nakagiri, S., "Stochastic Finite Element Analysis of Uncertain Structural Systems," *4th International Conference on Finite Element Methods*, Melbourne, Australia, 1982.
- [12] Vanmarcke, E. and Grigoriu, M., "Stochastic Finite Element Analysis of Simple Beams," *Journal of Engineering Mechanics*, **109**(5), 1983, pp. 1203-1214.
- [13] Branstetter, L. and Paez, T., "Dynamic Response Moments of Random Parametered Structures with Random Excitation," *Proceedings 3rd Conference on the Dynamic Response of Structures*, Los Angeles, ASCE, New York, 1986.
- [14] Liu, W.K., Mani, and Belytschko, T., "Finite Element Methods in Probabilistic Mechanics," *Probabilistic Engineering Mechanics*, **2**(4), 1987, pp. 201-213.
- [15] Der Keureghian, A. and Ke, J.B., "The Stochastic Finite Element Method in Structural Reliability," *Probabilistic Engineering Mechanics*, **3**(2), 1988, pp. 83-91.
- [16] Zeitoun, D.I., Baker, R., and Uzan, J., "Application of Random Elasticity to Soil Engineering," *Structural Safety*, **5**, 1988, pp. 79-93.
- [17] Liu, W.K., Besterfield, G.H., and Belytschko, T., "Variational Approach to Probabilistic Finite Elements," *Journal of Engineering Mechanics*, **114**(12), 1988, pp. 2115-2133.
- [18] Shinozuka, M., "Probabilistic Modeling of Concrete Structures," *Journal of the Engineering Mechanics Division*, ASCE, **98**(6), 1972, pp. 1433-1451.
- [19] Vanmarcke, E., Shinozuka, M., Nakagiri, S., Shueller, G.I., and Grigoriu, M., "Random Fields and Stochastic Finite Elements," *Structural Safety*, **3**, 1986, pp. 143-166.
- [20] Shinozuka, M., "Structural Response Variability," *Journal of Engineering Mechanics*, **113**(6), 1987, pp. 825-842.

- [21] Shinozuka, M. and Deodatis, G., "Response Variability of Stochastic Finite Element Systems," *Journal of Engineering Mechanics*, **114**(3), 1988, pp. 499-519.
- [22] Yamazaki, F., Shinozuka, M., and Dasgupta, G., "Neumann Expansion for Stochastic Finite Element Analysis," *Journal of Engineering Mechanics*, **114**(8), 1988, pp. 1335-1354.
- [23] Vanmarcke, E., "Probabilistic Modeling of Soil Profiles," *Journal of the Geotechnical Engineering Division*, **103**(GT11), 1977, pp. 1227-1246.
- [24] Vanmarcke, E., "On the Reliability of Earth Slopes," *Journal of the Geotechnical Engineering Division*, ASCE, **103**(GT11), 1977, pp. 1247-1265.
- [25] Benaroya, H. and Rehak, M., "Finite Element Methods in Probabilistic Structural Analysis: A Selective Review," *Applied Mechanics Reviews*, **41**(5), 1988, pp. 201-213.
- [26] Liu, W.K., Belytschko, T., Mani, A., and Besterfield, G.A., "A Variational Formulation for Probabilistic Mechanics," *Finite Element Methods for Plate and Shell Structures, Vol. 2: Formulations and Algorithms*, T. Hughes and E. Hinton, Eds., Pineridge, U.K., 1988.
- [27] Spanos, P.D. and Ghanem, R., "Stochastic Finite Element Expansion for Random Media," *Journal of Engineering Mechanics*, **115**(5), 1989, pp. 1035-1053.
- [28] Beck, J.L. and Katafygiotis, L., "Treating Model Uncertainties in Structural Dynamics," *Proceedings of Ninth World Conference on Earthquake Engineering*, **5**, Tokyo-Kyoto, Japan, 1989.
- [29] Abramowitz, M. and Stegun, I.A., *Handbook of Mathematical Functions*, Dover Publications, Inc., New York, 1964.
- [30] Hughes, T.J.R., *The Finite Element Method: Linear Static and Dynamic Finite Element Analysis*, Prentice-Hall, 1987.

- [31] Press, W.H., Flannery, B.P., Tenkolsky, S.A., and Vetterling, W.T., *Numerical Recipes: The Art of Scientific Computing*, Cambridge University Press, 1986.
- [32] Vanmarcke, E., *Random Fields: Analysis and Synthesis*, MIT Press, Cambridge, Mass., 1983.
- [33] Burnside, O.H., "Probabilistic Structural Analysis for Space Propulsion System Components," *Symposium on Probabilistic Structural Analysis and Design*, ASME, Winter Annual Meeting, Miami, 1985.
- [34] Dias, J.B. and Nagtegaal, J.C., "Efficient Algorithms for Use in Probabilistic Finite Element Analysis," *Symposium on Probabilistic Structural Analysis and Design*, ASME, Winter Annual Meeting, Miami, 1985.
- [35] Ruiz, P. and Penzien, J., "Probabilistic Study of the Behavior of Structures During Earthquakes," Report No. EERC 69-3, College of Engineering, University of California, Berkeley, CA, 1969.
- [36] Shinozuka, M. and Sato, Y., "Simulation of Nonstationary Random Process," *Journal of the Engineering Mechanics Division*, **93**(EM1), 1967, pp. 11-40.
- [37] Jennings, P.C., Housner, G.W., and Tsai, C., "Simulated Earthquake Motions," Earthquake Engineering Research Laboratory, California Institute of Technology, Pasadena, CA, 1968.
- [38] Saragoni, G.R. and Hart, G.C., "Simulation of Artificial Earthquakes," *Earthquake Engineering and Structural Dynamics*, **2**, 1974, pp. 249-267.
- [39] Tajimi, H., "A Statistical Method of Determining the Maximum Response of a Building Structure During an Earthquake," *Proceedings of the 2nd World Conference on Earthquake Engineering*, **11**, Tokyo, Japan, 1960.
- [40] Kanai, K., "An Empirical Formula for the Spectrum of Strong Earthquake Motions," *Bulletin of the Earthquake Research Institute*, University of Tokyo, **39**, 1961.

- [41] Sackman, J.L., Der Kiureghian, A., and Nour-Omid, B., "Dynamic Analysis of Light Equipment in Structures: Modal Properties of the Combined System," *Journal of Engineering Mechanics*, **109**(1), 1983, pp. 73-89.
- [42] Igusa, T. and Der Kiureghian, A., "Dynamic Characterization of Two-Degree-of-Freedom Equipment-Structure Systems," *Journal of Engineering Mechanics*, **111**(1), 1985, pp. 1-19.
- [43] Igusa, T. and Der Kiureghian, A., "Dynamic Response of Multiply Supported Secondary Systems," *Journal of Engineering Mechanics*, **111**(1), 1985, pp. 20-41.
- [44] Lai, S.P., "Statistical Characterization of Strong Ground Motions Using Power Spectral Density Function," *Bulletin of the Seismological Society of America*, **72**(1), 1982, pp. 259-274.
- [45] Igusa, T. and Der Kiureghian, A., "Response of Uncertain Systems to Stochastic Excitation," *Journal of Engineering Mechanics*, **114**(5), 1988, pp. 812-832.
- [46] Wall, F.J. and Bucher, C.G., "Sensitivity of Expected Exceedance Rate of SDOF-System Response to Statistical Uncertainties of Loading and System Parameters," *Probabilistic Engineering Mechanics*, **2**(3), 1987, pp. 138-146.
- [47] Crandall, S.H., "First Crossing Probabilities of a Linear Oscillator," *Journal of Sound and Vibration*, **12**, 1970, pp. 285-299.
- [48] Mark, W.D., "On False Alarm Probabilities of Filtered Noise," *Proc. IEEE*, **54**, 1966, p. 316.
- [49] Corotis, R.B., Vanmarcke, E.H., and Cornell, C.A., "Power Spectra and First Passage of Nonstationary Processes," *Journal of Engineering Mechanics*, **98**(EM2), 1972, pp. 401-414.

- [50] Vanmarcke, E.H., "On the Distribution of the First Passage Time for Normal Stationary Random Processes," *ASME Journal of Applied Mechanics*, **42**, 1975, pp. 215-220.
- [51] Mason, Jr., A.B. and Iwan, W.D., "An Approach to the First Passage Problem in Random Vibration," *Journal of Applied Mechanics*, **50**, 1983, pp. 641-646.

## Appendix A

### Representation of the Uncertainties in the Primary-Secondary System Example Problem

As it was stated in Section 5.5, three types of uncertainty are considered to compare the relative importance of uncertainties in the system parameters on the response variability of the secondary system. These are: uncertain filter parameters, uncertain primary system parameters and uncertain secondary system parameters.

The representation of the uncertainties in the filter parameters is given directly by equations (5.22) and (5.23).

The uncertain parameters of the primary system are the interstory shear stiffness and damping. The uncertainty in the interstory shear stiffness is defined by the uncertainty in the shear stiffness parameter  $k$ . Defining this parameter in terms of a mean value plus a deviatoric component, it is easily shown that equation (5.21) becomes

$$K(\mathbf{b}) = \bar{K} + K_1 b_1 , \quad (A.1)$$

where  $\bar{K}$  is the mean value of the stiffness matrix, and  $K_1$  is the deviatoric component of the stiffness matrix due to the uncertainty in  $k$ .

The uncertainty in the damping matrix of the primary system is characterized by the uncertainty in the parameters that reflect the participation of damping proportional to the stiffness matrix and damping proportional to the mass matrix

(Rayleigh damping). Defining these parameters in terms of a mean value plus a deviatoric component, it can be shown that equation (5.20) becomes

$$C(\mathbf{b}) = \bar{C} + C_1 b_1 , \quad (A.2)$$

where  $\bar{C}$  is the mean value of the damping matrix, and  $C_1$  is the deviatoric component of the damping matrix due to the uncertainty in the parameters mentioned above.

Finally, the uncertain parameters of the secondary system are the support stiffness and damping ratio. The uncertainty in the support stiffness is defined by the uncertainty in the stiffness parameter of the secondary system  $k_s$ . As before, it can be shown that equation (5.21) becomes

$$K(\mathbf{b}) = \bar{K} + K_1 b_1 , \quad (A.3)$$

where  $\bar{K}$  is the mean value of the stiffness matrix, and  $K_1$  is the deviatoric component of the stiffness matrix due to the uncertainty in  $k_s$ . In the same manner, the uncertainty in the damping ratio is defined by the uncertainty in the damping coefficient of the secondary system  $c_s$ . Once again, equation (5.20) becomes

$$C(\mathbf{b}) = \bar{C} + C_1 b_1 , \quad (A.4)$$

where  $\bar{C}$  is the mean value of the damping matrix, and  $C_1$  is the deviatoric component of the damping matrix due to the uncertainty in  $c_s$ .

# CALIFORNIA INSTITUTE OF TECHNOLOGY

Reports Published

by

Earthquake Engineering Research Laboratory\*

Dynamic Laboratory

Disaster Research Center

*Note:* Numbers in parenthesis are Accession Numbers assigned by the National Technical Information Service; these reports may be ordered from the National Technical Information Service, 5285 Port Royal Road, Springfield, Virginia, 22161. Accession Numbers should be quoted on orders for reports (PB — —). Reports without this information either have not been submitted to NTIS or the information was not available at the time of printing. An N/A in parenthesis indicates that the report is no longer available at Caltech.

1. Alford, J.L., G.W. Housner and R.R. Martel, "Spectrum Analysis of Strong-Motion Earthquake," 1951. (Revised August 1964). (N/A)
2. Housner, G.W., "Intensity of Ground Motion During Strong Earthquakes," 1952. (N/A)
3. Hudson, D.E., J.L. Alford and G.W. Housner, "Response of a Structure to an Explosive Generated Ground Shock," 1952. (N/A)
4. Housner, G.W., "Analysis of the Taft Accelerogram of the Earthquake of 21 July 1952." (N/A)
5. Housner, G.W., "A Dislocation Theory of Earthquakes," 1953. (N/A)
6. Caughey, T.K. and D.E. Hudson, "An Electric Analog Type Response Spectrum," 1954. (N/A)
7. Hudson, D.E. and G.W. Housner, "Vibration Tests of a Steel-Frame Building," 1954. (N/A)
8. Housner, G.W., "Earthquake Pressures on Fluid Containers," 1954. (N/A)
9. Hudson, D.E., "The Wilmot Survey Type Strong-Motion Earthquake Recorder," 1958. (N/A)

---

\* To order directly by phone, the number is (703) 487-4650.

10. Hudson, D.E. and W.D. Iwan, "The Wilmot Survey Type Strong-Motion Earthquake Recorder, Part II," 1960. (N/A)
11. Caughey, T.K., D.E. Hudson and R.V. Powell, "The CIT Mark II Electric Analog Type-Response Spectrum Analyzer for Earthquake Excitation Studies," 1960. (N/A)
12. Keightley, W.O., G.W. Housner and D.E. Hudson, "Vibration Tests of the Encino Dam Intake Tower," 1961. (N/A)
13. Merchant, H.C., "Mode Superposition Methods Applied to Linear Mechanical Systems Under Earthquake Type Excitation," 1961. (N/A)
14. Iwan, W.D., "The Dynamic Response of Bilinear Hysteretic Systems," 1961. (N/A)
15. Hudson, D.E., "A New Vibration Exciter for Dynamic Test of Full-Scale Structures," 1961. (N/A)
16. Hudson, D.E., "Synchronized Vibration Generators for Dynamic Tests of Full-Scale Structures," 1962. (N/A)
17. Jennings, P.C., "Velocity Spectra of the Mexican Earthquakes of 11 May and 19 May 1962," 1962. (N/A)
18. Jennings, P.C., "Response of Simple Yielding Structures to Earthquake Excitation," 1963. (N/A)
19. Keightley, W.O., "Vibration Tests of Structures," 1963. (N/A)
20. Caughey, T.K. and M.E.J. O'Kelly, "General Theory of Vibration of Damped Linear Dynamic Systems," 1963. (N/A)
21. O'Kelly, M.E.J., "Vibration of Viscously Damped Linear Dynamic Systems," 1964. (N/A)
22. Nielsen, N.N., "Dynamic Response of Multistory Buildings," 1964. (N/A)
23. Tso, W.K., "Dynamics of Thin-Walled Beams of Open Section," 1964. (N/A)
24. Keightley, W.O., "A Dynamic Investigation of Bouquet Canyon Dam," 1964. (N/A)
25. Malhotra, R.K., "Free and Forced Oscillations of a Class of Self-Excited Oscillators," 1964.
26. Hanson, R.D., "Post-Elastic Response of Mild Steel Structures," 1965.
27. Masri, S.F., "Analytical and Experimental Studies of Impact Dampers," 1965.

28. Hanson, R.D., "Static and Dynamic Tests of a Full-Scale Steel-Frame Structures," 1965.
29. Cronin, D.L., "Response of Linear, Viscous Damped Systems to Excitations Having Time-Varying Frequency," 1965.
30. Hu, P.Y.-F., "Analytical and Experimental Studies of Random Vibration," 1965.
31. Crede, C.E., "Research on Failure of Equipment when Subject to Vibration," 1965.
32. Lutes, L.D., "Numerical Response Characteristics of a Uniform Beam Carrying One Discrete Load," 1965. (N/A)
33. Rocke, R.D., "Transmission Matrices and Lumped Parameter Models for Continuous Systems," 1966. (N/A)
34. Brady, A.G., "Studies of Response to Earthquake Ground Motion," 1966. (N/A)
35. Atkinson, J.D., "Spectral Density of First Order Piecewise Linear Systems Excited by White Noise," 1967. (N/A)
36. Dickerson, J.R., "Stability of Parametrically Excited Differential Equations," 1967. (N/A)
37. Giberson, M.F., "The Response of Nonlinear Multi-Story Structures Subjected to Earthquake Excitation," 1967. (N/A)
38. Hallanger, L.W., "The Dynamic Stability of an Unbalanced Mass Exciter," 1967.
39. Husid, R., "Gravity Effects on the Earthquake Response of Yielding Structures," 1967. (N/A)
40. Kuroiwa, J.H., "Vibration Test of a Multistory Building," 1967. (N/A)
41. Lutes, L.D., "Stationary Random Response of Bilinear Hysteretic Systems," 1967.
42. Nigam, N.C., "Inelastic Interactions in the Dynamic Response of Structures," 1967.
43. Nigam, N.C. and P.C. Jennings, "Digital Calculation of Response Spectra from Strong-Motion Earthquake Records," 1968.
44. Spencer, R.A., "The Nonlinear Response of Some Multistory Reinforced and Prestressed Concrete Structures Subjected to Earthquake Excitation," 1968. (N/A)
45. Jennings, P.C., G.W. Housner and N.C. Tsai, "Simulated Earthquake Motions," 1968.

46. "Strong-Motion Instrumental Data on the Borrego Mountain Earthquake of 9 April 1968," (USGS and EERL Joint Report), 1968.
47. Peters, R.B., "Strong Motion Accelerograph Evaluation," 1969.
48. Heitner, K.L., "A Mathematical Model for Calculation of the Run-Up of Tsunamis," 1969.
49. Trifunac, M.D., "Investigation of Strong Earthquake Ground Motion," 1969. (N/A)
50. Tsai, N.C., "Influence of Local Geology on Earthquake Ground Motion," 1969. (N/A)
51. Trifunac, M.D., "Wind and Microtremor Induced Vibrations of a Twenty-Two Steel Frame Building," EERL 70-01, 1970.
52. Yang, I-M., "Stationary Random Response of Multidegree-of-Freedom Systems," DYNL-100, June 1970. (N/A)
53. Patula, E.J., "Equivalent Differential Equations for Non-linear Dynamic Systems," DYNL-101, June 1970.
54. Prelewicz, D.A., "Range of Validity of the Method of Averaging," DYNL-102, 1970.
55. Trifunac, M.D., "On the Statistics and Possible Triggering Mechanism of Earthquakes in Southern California," EERL 70-03, July 1970.
56. Heitner, K.L., "Additional Investigations on a Mathematical Model for Calculation of Run-Up of Tsunamis," July 1970.
57. Trifunac, M.D., "Ambient Vibration Tests of a Thirty-Nine Story Steel Frame Building," EERL 70-02, July 1970.
58. Trifunac, M.D. and D.E. Hudson, "Laboratory Evaluations and Instrument Corrections of Strong-Motion Accelerographs," EERL 70-04, August 1970. (N/A)
59. Trifunac, M.D., "Response Envelope Spectrum and Interpretation of Strong Earthquake Ground Motion," EERL 70-06, August 1970.
60. Keightley, W.O., "A Strong-Motion Accelerograph Array with Telephone Line Interconnections," EERL 70-05, September 1970.
61. Trifunac, M.D., "Low Frequency Digitization Errors and a New Method for Zero Baseline Correction of Strong-Motion Accelerograms," EERL 70-07, September 1970.
62. Vijayaraghavan, A., "Free and Forced Oscillations in a Class of Piecewise-Linear Dynamic Systems," DYNL-103, January 1971.

63. Jennings, P.C., R.B. Mathiesen and J.B. Hoerner, "Forced Vibrations of a 22-Story Steel Frame Building," EERL 71-01, February 1971. (N/A) (PB 205 161)
64. Jennings, P.C., "Engineering Features of the San Fernando Earthquake of February 9, 1971," EERL 71-02, June 1971. (PB 202 550)
65. Bielak, J., "Earthquake Response of Building-Foundation Systems," EERL 71-04, June 1971. (N/A) (PB 205 305)
66. Adu, R.A., "Response and Failure of Structures Under Stationary Random Excitation," EERL 71-03, June 1971. (N/A) (PB 205 304)
67. Skattum, K.S., "Dynamic Analysis of Coupled Shear Walls and Sandwich Beams," EERL 71-06, June 1971. (N/A) (PB 205 267)
68. Hoerner, J.B., "Model Coupling and Earthquake Response of Tall Buildings," EERL 71-07, June 1971. (N/A) (PB 207 635)
69. Stahl, K.J., "Dynamic Response of Circular Plates Subjected to Moving Massive Loads," DYNL-104, June 1971. (N/A)
70. Trifunac, M.D., F.E. Udawadia and A.G. Brady, "High Frequency Errors and Instrument Corrections of Strong-Motion Accelerograms," EERL 71-05, 1971. (PB 205 369)
71. Furuike, D.M., "Dynamic Response of Hysteretic Systems With Application to a System Containing Limited Slip," DYNL-105, September 1971. (N/A)
72. Hudson, D.E. (Editor), "Strong-Motion Instrumental Data on the San Fernando Earthquake of February 9, 1971," (Seismological Field Survey, NOAA, C.I.T. Joint Report), September 1971. (PB 204 198)
73. Jennings, P.C. and J. Bielak, "Dynamics of Building-Soil Interaction," EERL 72-01, April 1972. (PB 209 666)
74. Kim, B.-K., "Piecewise Linear Dynamic Systems with Time Delays," DYNL-106, April 1972.
75. Viano, D.C., "Wave Propagation in a Symmetrically Layered Elastic Plate," DYNL-107, May 1972.
76. Whitney, A.W., "On Insurance Settlements Incident to the 1906 San Francisco Fire," DRC 72-01, August 1972. (PB 213 256)
77. Udawadia, F.E., "Investigation of Earthquake and Microtremor Ground Motions," EERL 72-02, September 1972. (PB 212 853)

78. Wood, J.H., "Analysis of the Earthquake Response of a Nine-Story Steel Frame Building During the San Fernando Earthquake," EERL 72-04, October 1972. (PB 215 823)
79. Jennings, P.C., "Rapid Calculation of Selected Fourier Spectrum Ordinates," EERL 72-05, November 1972.
80. "Research Papers Submitted to Fifth World Conference on Earthquake Engineering, Rome, Italy, 25-29 June 1973," EERL 73-02, March 1973. (PB 220 431)
81. Udawadia, F.E. and M.D. Trifunac, "The Fourier Transform, Response Spectra and Their Relationship Through the Statistics of Oscillator Response," EERL 73-01, April 1973. (PB 220 458)
82. Housner, G.W., "Earthquake-Resistant Design of High-Rise Buildings," DRC 73-01, July 1973. (N/A)
83. "Earthquake and Insurance," Earthquake Research Affiliates Conference, 2-3 April, 1973, DRC 73-02, July 1973. (PB 223 033)
84. Wood, J.H., "Earthquake-Induced Soil Pressures on Structures," EERL 73-05, August 1973. (N/A)
85. Crouse, C.B., "Engineering Studies of the San Fernando Earthquake," EERL 73-04, March 1973. (N/A)
86. Irvine, H.M., "The Veracruz Earthquake of 28 August 1973," EERL 73-06, October 1973.
87. Iemura, H. and P.C. Jennings, "Hysteretic Response of a Nine-Story Reinforced Concrete Building During the San Fernando Earthquake," EERL 73-07, October 1973.
88. Trifunac, M.D. and V. Lee, "Routine Computer Processing of Strong-Motion Accelerograms," EERL 73-03, October 1973. (N/A) (PB 226 047/AS)
89. Moeller, T.L., "The Dynamics of a Spinning Elastic Disk with Massive Load," DYNL 73-01, October 1973.
90. Blevins, R.D., "Flow Induced Vibration of Bluff Structures," DYNL 74-01, February 1974.
91. Irvine, H.M., "Studies in the Statics and Dynamics of Simple Cable Systems," DYNL-108, January 1974.
92. Jephcott, D.K. and D.E. Hudson, "The Performance of Public School Plants During the San Fernando Earthquake," EERL 74-01, September 1974. (PB 240 000/AS)

93. Wong, H.L., "Dynamic Soil-Structure Interaction," EERL 75-01, May 1975. (N/A) (PB 247 233/AS)
94. Foutch, D.A., G.W. Housner and P.C. Jennings, "Dynamic Responses of Six Multistory Buildings During the San Fernando Earthquake," EERL 75-02, October 1975. (PB 248 144/AS)
95. Miller, R.K., "The Steady-State Response of Multidegree-of-Freedom Systems with a Spatially Localized Nonlinearity," EERL 75-03, October 1975. (PB 252 459/AS)
96. Abdel-Ghaffar, A.M., "Dynamic Analyses of Suspension Bridge Structures," EERL 76-01, May 1976. (PB 258 744/AS)
97. Foutch, D.A., "A Study of the Vibrational Characteristics of Two Multistory Buildings," EERL 76-03, September 1976. (PB 260 874/AS)
98. "Strong Motion Earthquake Accelerograms Index Volume," Earthquake Engineering Research Laboratory, EERL 76-02, August 1976. (PB 260 929/AS)
99. Spanos, P-T.D., "Linearization Techniques for Non-Linear Dynamical Systems," EERL 76-04, September 1976. (PB 266 083/AS)
100. Edwards, D.B., "Time Domain Analysis of Switching Regulators," DYNL 77-01, March 1977.
101. Abdel-Ghaffar, A.M., "Studies of the Effect of Differential Motions of Two Foundations upon the Response of the Superstructure of a Bridge," EERL 77-02, January 1977. (PB 271 095/AS)
102. Gates, N.C., "The Earthquake Response of Deteriorating Systems," EERL 77-03, March 1977. (PB 271 090/AS)
103. Daly, W., W. Judd and R. Meade, "Evaluation of Seismicity at U.S. Reservoirs," USCOLD, Committee on Earthquakes, May 1. (PB 270 036/AS)
104. Abdel-Ghaffer, A.M. and G.W. Housner, "An Analysis of the Dynamic Characteristics of a Suspension Bridge by Ambient Vibration Measurements," EERL 77-01, January 1977. (PB 275 063/AS)
105. Housner, G.W. and P.C. Jennings, "Earthquake Design Criteria for Structures," EERL 77-06, November 1977 (PB 276 502/AS)
106. Morrison, P., R. Maley, G. Brady and R. Porcella, "Earthquake Recordings on or Near Dams," USCOLD, Committee on Earthquakes, November 1977. (PB 285 867/AS)
107. Abdel-Ghaffar, A.M., "Engineering Data and Analyses of the Whittier, California Earthquake of January 1, 1976," EERL 77-05, November 1977. (PB 283 750/AS)

108. Beck, J.L., "Determining Models of Structures from Earthquake Records," EERL 78-01, June 1978 (PB 288 806/AS)
109. Psycharis, I., "The Salonica (Thessaloniki) Earthquake of June 20, 1978," EERL 78-03, October 1978. (PB 290 120/AS)
110. Abdel-Ghaffar, A.M. and R.F. Scott, "An Investigation of the Dynamic Characteristics of an Earth Dam," EERL 78-02, August 1978. (PB 288 878/AS)
111. Mason, A.B., Jr., "Some Observations on the Random Response of Linear and Nonlinear Dynamical Systems," EERL 79-01, January 1979. (PB 290 808/AS)
112. Helmberger, D.V. and P.C. Jennings (Organizers), "Strong Ground Motion: N.S.F. Seminar-Workshop," SL-EERL 79-02, February 1978.
113. Lee, D.M., P.C. Jennings and G.W. Housner, "A Selection of Important Strong Motion Earthquake Records," EERL 80-01, January 1980. (PB 80 169196)
114. McVerry, G.H., "Frequency Domain Identification of Structural Models from Earthquake Records," EERL 79-02, October 1979. (PB-80-194301)
115. Abdel-Ghaffar A.M., R.F.Scott and M.J.Craig, "Full-Scale Experimental Investigation of a Modern Earth Dam," EERL 80-02, February 1980. (PB-81-123788)
116. Rutenberg, A., P.C. Jennings and G.W. Housner, "The Response of Veterans Hospital Building 41 in the San Fernando Earthquake," EERL 80-03, May 1980. (PB-82-201377)
117. Haroun, M.A., "Dynamic Analyses of Liquid Storage Tanks," EERL 80-04, February 1980. (PB-81-123275)
118. Liu, W.K., "Development of Finite Element Procedures for Fluid-Structure Interaction," EERL 80-06, August 1980. (PB 184078)
119. Yoder, P.J., "A Strain-Space Plasticity Theory and Numerical Implementation," EERL 80-07, August 1980. (PB-82-201682)
120. Krousgrill, C.M., Jr., "A Linearization Technique for the Dynamic Response of Nonlinear Continua," EERL 80-08, September 1980. (PB-82-201823)
121. Cohen, M., "Silent Boundary Methods for Transient Wave Analysis," EERL 80-09, September 1980. (PB-82-201831)
122. Hall, S.A., "Vortex-Induced Vibrations of Structures," EERL 81-01, January 1981. (PB-82-201849)

123. Psycharis, I.N., "Dynamic Behavior of Rocking Structures Allowed to Uplift," EERL 81-02, August 1981. (PB-82-212945)
124. Shih, C.-F., "Failure of Liquid Storage Tanks Due to Earthquake Excitation," EERL 81-04, May 1981. (PB-82-215013)
125. Lin, A.N., "Experimental Observations of the Effect of Foundation Embedment on Structural Response," EERL 82-01, May 1982. (PB-84-163252)
126. Botelho, D.L.R., "An Empirical Model for Vortex-Induced Vibrations," EERL 82-02, August 1982. (PB-84-161157)
127. Ortiz, L.A., "Dynamic Centrifuge Testing of Cantilever Retaining Walls," SML 82-02, August 1982. (PB-84-162312)
128. Iwan, W.D. (Editor) "Proceedings of the U.S. National Workshop on Strong-Motion Earthquake Instrumentation, April 12-14, 1981, Santa Barbara, California," California Institute of Technology, Pasadena, California, 1981.
129. Rashed, A., "Dynamic Analysis of Fluid-Structure Systems," EERL 82-03, July 1982. (PB-84-162916)
130. National Academy Press, "Earthquake Engineering Research—1982."
131. National Academy Press, "Earthquake Engineering Research—1982, Overview and Recommendations."
132. Jain, S.K., "Analytical Models for the Dynamics of Buildings," EERL 83-02, May 1983. (PB-84-161009)
133. Huang, M.-J., "Investigation of Local Geology Effects on Strong Earthquake Ground Motions," EERL 83-03, July 1983. (PB-84-161488)
134. McVerry, G.H. and J.L. Beck, "Structural Identification of JPL Building 180 Using Optimally Synchronized Earthquake Records." EERL 83-01, August 1983. (PB-84-162833)
135. Bardet, J.P., "Application of Plasticity Theory to Soil Behavior: A New Sand Model," SML 83-01, September 1983. (PB-84-162304)
136. Wilson, J.C., "Analysis of the Observed Earthquake Response of a Multiple Span Bridge," EERL 84-01, May 1984. (PB-85-240505/AS)
137. Hushmand, B., "Experimental Studies of Dynamic Response of Foundations," SML 83-02, November 1983. (PB-86-115383/A)

138. Cifuentes, A.O., "System Identification of Hysteretic Structures," EERL 84-04, 1984. (PB-240489/AS14)
139. Smith, K.S., "Stochastic Analysis of the Seismic Response of Secondary Systems," EERL 85-01, November 1984. (PB-85-240497/AS)
140. Maragakis, E., "A Model for the Rigid Body Motions of Skew Bridges," EERL 85-02, December 1984. (PB-85-248433/AS)
141. Jeong, G.D., "Cumulative Damage of Structures Subjected to Response Spectrum Consistent Random Process," EERL 85-03, January 1985. (PB-86-100807)
142. Chelvakumar, K., "A Simple Strain-Space Plasticity Model for Clays," EERL 85-05, 1985. (PB-87-234308/CC)
143. Pak, R.Y.S., "Dynamic Response of a Partially Embedded Bar Under Transverse Excitations," EERL 85-04, May 1985. (PB-87-232856/A06)
144. Tan, T.-S., "Two Phase Soil Study: A. Finite Strain Consolidation, B. Centrifuge Scaling Considerations," SML 85-01, August 1985. (PB-87-232864/CC)
145. Iwan, W.D., M.A. Moser and C.-Y. Peng, "Strong-Motion Earthquake Measurement Using a Digital Accelerograph," EERL 84-02, April 1984.
146. Beck, R.T. and J.L. Beck, "Comparison Between Transfer Function and Modal Minimization Methods for System Identification," EERL 85-06, November 1985. (PB-87-234688/A04)
147. Jones, N.P., "Flow-Induced Vibration of Long Structures," DYNL 86-01, May 1986. (PB-88-106646/A08)
148. Peek, R., "Analysis of Unanchored Liquid Storage Tanks Under Seismic Loads," EERL 86-01, April 1986. (PB-87-232872/A12)
149. Papparizos, L.G., "Some Observations on the Random Response of Hysteretic Systems," EERL 86-02. 1986. (PB-88235668/CC)
150. Moser, M.A., "The Response of Stick-Slip Systems to Random Seismic Excitation," EERL 86-03, September 1986. (PB-89-194427/AS)
151. Burrige, P.B., "Failure of Slopes," SML 87-01, March 1987. (PB-89-194401/AS)
152. Jayakumar, P., "Modeling and Identification in Structural Dynamics," EERL 87-01, May 1987. (PB-89-194146/AS)
153. Dowling, M.J., "Nonlinear Seismic Analysis of Arch Dams," EERL 87-03, September 1987. (PB-89-194443/AS)

154. Duron, Z.H., "Experimental and Finite Element Studies of a Large Arch Dam," EERL 87-02, September 1987. (PB-89-194435/AS)
155. Whirley, R.G., "Random Response of Nonlinear Continuous Systems," EERL 87-04, September 1987. (PB-89-194153/AS)
156. Peng, C.-Y., "Generalized Model Identification of Linear and Nonlinear Dynamic Systems," EERL 87-05, September 1987. (PB-89-194419/AS)
157. Levine, M.B., J.L. Beck, W.D. Iwan, P.C. Jennings and R. Relles, "Accelerograms Recorded at Caltech During the Whittier Narrows Earthquakes of October 1 and 4, 1987: A Preliminary Report," EERL 88-01, August 1988. PB-
158. Nowak, P.S., "Effect of Nonuniform Seismic Input on Arch Dams," EERL 88-03, September 1988. (PB-89-194450/AS)
159. El-Aidi, B., "Nonlinear Earthquake Response of Concrete Gravity Dam Systems," EERL 88-02, August 1988. (PB-89-193124/AS)
160. Smith, P.W., Jr., "Considerations for the Design of Gas-Lubricated Slider Bearings," DYNL 89-01, January 1988. PB-
161. Donlon, W.P., Jr., "Experimental Investigation of the Nonlinear Seismic Response of Concrete Gravity Dams," EERL 89-01, January 1989. PB-

